



universität
wien

MASTERARBEIT

Titel der Masterarbeit

„Impacts of human LDLR overexpression on the production
of a VSVG-pseudotyped lentiviral vector“

verfasst von

Otahal Alexander, BSc

angestrebter akademischer Grad

Master of Science (MSc)

Wien, 2015

Studienkennzahl lt. Studienblatt:

A 066 834

Studienrichtung lt. Studienblatt:

Masterstudium Molekulare Biologie

Betreut von:

ao. Univ.-Prof. Dipl.-Ing. Dr. Dieter Blaas

Table of contents

1 Introduction	1
1.1 Familial Hypercholesterolaemia.....	1
1.2 Gene therapy.....	3
1.3 Designing lentiviral vectors.....	4
1.4 Producing a gene therapy vector for FH.....	6
2 Materials.....	9
2.1 Plasmids.....	9
2.2 Primers.....	9
2.3 Primary antibodies.....	10
2.4 Secondary antibodies.....	10
3 Methods.....	10
3.1 Cell culture.....	10
3.2 Preparation of transfection reagent.....	11
3.3 Production of pseudotyped lentiviral vector particles	11
3.4 Concentrating vector particles by ultracentrifugation.....	12
3.5 Titration of lentiviral vector particles via flow cytometry.....	12
3.6 Titration of lentiviral vector RNA copy number via RT-qPCR.....	13
3.7 Viral RNA fractionation from LDLR co-expressing cells.....	14
3.8 Cell lysis in buffer A (OGP lysis buffer).....	15
3.9 Cell lysis in buffer B (RIPA lysis buffer).....	15
3.10 Western blot.....	15
3.11 Site-directed mutagenesis.....	16
3.12 Electroporation of XL1-Blue cells.....	18
3.13 Indirect immunofluorescence microscopy.....	18
3.14 Quantification of Western Blots.....	19
4 Results	19
4.1 Transfection efficiency of TurboFect and PEI.....	19
4.2 Vector yield is independent of transmembrane protein presence.....	20
4.3 LDLR-expression correlates with released vector copy number.....	22
4.4 Partitioning of vector RNA in supernatant, cell surface and interior.....	24
4.5 Vector particles are not subject to degradation.....	28
4.6 Up- and downregulation of endogenous LDLR in HEK293 cells.....	30
4.7 Comparison of endogenous and ectopically expressed LDLR.....	33
4.8 LDLR deletion constructs.....	34
4.9 Syncytia formation correlates with released vector yield.....	36
4.10 VSVG mRNA levels are not a function of LDLR expression.....	40
4.11 VSVG and LDLR localize to a perinuclear compartment.....	41
4.12 LDLR prevents VSVG progression to the Golgi.....	44
4.13 VSVG colocalizes with the ERGIC and lysosomal compartments.....	45
5 Discussion.....	49
6 Acknowledgements.....	52
7 Abbreviations.....	53

1 Introduction

1.1 Familial Hypercholesterolaemia

Familial hypercholesterolaemia (FH) is a genetically inherited disease leading to high blood serum low-density lipoprotein cholesterol (LDL-C) levels (Marais, 2004). Patients suffer from early-onset pathological conditions such as coronary artery disease (CAD) (Brown and Goldstein, 1986) or tendon xanthomas caused by LDL containing plaque deposits in arteries (Uchida et al., 2013) and tendons (van den Bosch and Vos, 1998; Koul et al., 2007). As a result, atherosclerosis starts early in childhood, causing CAD early in adulthood (Wiegman et al., 2004).

Mutations of the low-density lipoprotein receptor (*LDLR*) gene are the main cause of FH (Brown and Goldstein, 1986), however, a spectrum of FH phenotypes exist that result from different types of mutations and their extent of biochemical consequences as well as whether one or more factors are mutated that are involved in recognition and uptake of low-density lipoprotein (LDL) particles (Burnett and Hooper, 2008). More than 1,000 distinct genetic alterations of *LDLR* were described (Leigh et al., 2008). The functional classification of *LDLR* mutations (Burnett and Hooper, 2008) encompasses five groups including synthesis (Mozas et al., 2002), transport through the secretory pathway (Esser and Russel, 1988), ligand binding, internalisation from the plasma membrane (Kingsley and Krieger, 1984) or recycling.

The *LDLR* pathway is a complex interplay between biosynthesis, transport processes and turnover. *LDLR* is synthesized at the rough endoplasmic reticulum as a precursor with an apparent mass of 120kD which is *N*- and *O*-glycosylated in the Golgi *en route* to the plasma membrane yielding a mature 160kD glycoprotein (Tolleshaug et al., 1982). The extent of *LDLR* expression is target of sterol-mediated feedback regulation (Russel et al., 1983). The receptor engages in receptor-ligand interactions with LDL particles at the plasma membrane which triggers ligand-mediated internalisation (Goldstein et al., 1985). Acidification of endosomes releases LDL from *LDLR* via a conformational change (Rudenko et al., 2002), released LDL is then metabolized in lysosomes (Schneede et al., 2011). The receptor is recycled back to the plasma membrane (Brown and Goldstein, 1986) or is subjected to proteolytic degradation mediated by the protease PCSK9 (Maxwell and Breslow, 2004; Leren, 2014).

The mature *LDLR* molecule is composed of five functional domains. The extracellular part consists of the N-terminal ligand binding domain with seven cysteine-rich repeats (Südhof et al., 1985), the epidermal growth factor (EGF) precursor homology domain with three EGF-like repeats and a β -propeller motif (Russell et al., 1984), a highly glycosylated serine- and threonine-rich domain (Davis

et al., 1986), a transmembrane domain and a cytoplasmic domain containing a juxtamembraneous NPxY internalisation signal (Chen et al., 1990). The EGF precursor domain is engaged in conformational stabilization of the receptor molecule to provide an accessible binding interface for LDL and acid-dependent ligand release upon internalization (Davis et al., 1987). The ligand-binding capability of LDLR and its conformation is achieved by cysteine-rich Ca^{2+} -binding modules (Fass et al., 1997; Arias-Moreno et al., 2008). These structural features are required for proper function of the receptor, low calcium concentration decreases, reducing agents or mutations abolish ligand binding (Goldstein and Brown, 1974; Goldstein et al., 1985; Blacklow and Kim, 1996). The various functional aspects constitute plenty of opportunities to disrupt the complex architecture of LDLR via mutations.

Besides defects in *LDLR* causing classical FH (OMIM #143890), mutations in *APOB* encoding apolipoprotein B-100 (apoB-100), one of the physiological ligands for LDLR found in LDL particles, give rise to similar phenotypes known as familial defective apo B-100 (FDB, OMIM #144010). A single aminoacid substitution (R3500Q) in apoB-100 decreases the affinity to the receptor (Soria et al., 1989). Defective apo B-100 leads to elevated LDL-C plasma levels due to inefficient clearance from the serum caused by a reduced receptor-ligand interaction (Brown and Goldstein, 1983; Innerarty et al., 1987; Burnett and Hooper, 2008).

Other factors involved in the LDL-C uptake pathway such as proprotein convertase subtilisin/kexin type 9 (*PCSK9*) were also found mutated in different types of FH, although less frequently (Damgaard et al., 2004). *PCSK9* mediates intracellular degradation of internalized LDLR (reviewed in Leren, 2014). In contrast to the loss-of-function mutations in *LDLR* or *APOB*, *PCSK9* mutations also include gain-of-function variants such as D374Y, that were found in subjects with particularly high LDL-C serum levels (Naoumova et al., 2005). Defective *PCSK9* is unable to degrade internalized LDLR, which leads to increased expression level LDLR that is clearing larger amounts of LDL-C from the serum than in normal subjects. This opposite extreme condition is called hypocholesterolaemia, which does not require medical treatment, but is considered to constitute a congenital protection against atherosclerosis and CAD (Cohen et al., 2006), in case fully functional LDLR is expressed. Otherwise, elevated turnover of LDLR without proper recycling leads to FH-like symptoms, which are addressed by state-of-the art *PCSK9*-targeted therapies (Milionis et al., 2015).

In addition, a distinction has to be made between mild heterozygous and severe homozygous FH (Bown and Goldstein, 1986; Marais, 2004). Heterozygous patients express functional LDLR receptor from only one of their two *LDLR* copies, resulting in moderately elevated LDL-C levels. (Soutar and Naoumova, 2007) The prevalence of heterozygous FH caused by LDLR is estimated to be one in 500 individuals irrespective of ethnic background, whereas homozygous FH is relatively

rare (1:1,000,000) (reviewed in Cuchel et al., 2014)

1.2 Gene therapy

In contrast to infectious diseases, genetically inherited diseases are based upon a person's inherent genetic nature. Therefore, only symptoms can be treated, as long as the genetic cause persists. For example, administration of statins in case for FH has rendered the disease treatable (Scandinavian Simvastatin Group, 1994; Shepherd, 1998). Alternative means to reduce LDL-C in FH patients include LDL apheresis (reviewed in Stefanutti and Thompson, 2015) or liver transplantation (Page et al., 2014), which both impose substantial constraints on a patient's quality of life in terms of regular recurrence at health care facilities or life-long immunosuppression, respectively.

The effective cure of the disease can only be achieved, if a physician gains an opportunity to permanently modify a patient's genome, which is not trivial, but could be addressed by gene therapeutic methods. Promising trials to permanently reduce LDL-C levels were already done in mice (Ishibashi et al., 1993) and rabbits (Kankkonen et al., 2004) with different types of gene therapeutic vectors.

Gene therapy is a means of introducing transgenes into the genome of a living organism. It is a way to administer a functional allele of a mutated gene to a patient, persistently integrate it into the genome of specific cells and revert physical manifestations of a genetically inherited disease such as FH. A physiological way of inserting genetic material into a genome is the use of viruses, which insert their genetic material into a host genome during their normal life cycle. In the past decades, several approaches were developed that make use of genetically modified viruses for the production of viral vectors suitable for gene therapy. Among these viruses are adenoviruses, adeno-associated viruses, retro- and lentiviruses (reviewed in Al-Allaf et al., 2010).

Lentiviruses are a subgroup of *retroviridae*, a family of enveloped viruses with positive single stranded RNA genome replicating through reverse transcription, insertion into the host genome and transcription of viral RNA genomes from the integrated provirus in the host cell. Members include HIV-1 (*human immunodeficiency virus 1*), HIV-2 or EIAV (*equine infectious anaemia virus*). They are characterized by the unique ability of integrating their viral genome into the host genome in dividing and non-dividing cells. All other known integrating viruses require a full cycle of host cell division to gain access to the host genome. Lentiviruses encode and contain accessory proteins in the virion such as integrase, which facilitates active nuclear import, the main barrier to integration and replication for other retroviruses (De Rijck et al., 2007).

Therefore, lentiviral vectors put themselves forward for potent agents for in vivo gene delivery in gene therapy as they employ the lentiviral infection mechanism allowing the long-term expression of transduced genes (reviewed in Naldini, 1998). This circumstance has already been used for gene

delivery in basic research (Naldini et al., 1996) and enjoys increasing popularity in the production of vectors for gene therapy (Kankkonen et al., 2004; Al-Allaf et al., 2010).

Lentiviruses are notoriously potent pathogens, so turning them into potent cures is a challenging endeavor. Farreaching safety precautions not only during the therapeutic application but also the production of virus-derived transduction systems have to be adopted to limit adverse effects for scientists, patients and medical personnel. For this reason, several types of genetic modifications were introduced into the sequences of wildtype viruses. This led to the development of a series of vector packaging systems, termed generations, of vector production systems based on primate and non-primate lentiviruses (Durand and Cimarelli, 2011). In short, first generation packaging systems were composed of three plasmids, which were transiently cotransfected into producer cells. One plasmid, called *vector construct*, encoded the viral RNA derived from HIV1, containing *cis*-regulatory sequences and the transgene to be transduced, but no viral proteins. A second plasmid termed *packaging construct*, that lacked the viral packaging signal ψ , was used to express viral proteins for assembly and budding of vector particles, with the exception of an envelope glycoprotein, which was provided on the third plasmid, the *envelope construct* (Naldini et al., 1996). In second generation systems, viral accessory protein-encoding sequences were removed from the packaging construct. In addition, a deletion in U3 of the 3'-LTR of the vector construct leads to self-inactivation (SIN) upon reverse transcription, which prevents the transcription of viral RNA by transduced cells (Miyoshi et al., 1998). Third generation packaging systems employ packaging constructs that are tat-independent and encode *gag* and *pol* only, without *rev*, which is provided in trans on a fourth plasmid for vector production (Dull et al., 1998). In the following, a fourth generation vector production system was published (Wu et al., 2000), that even includes two individual plasmids for the *gag* and *pol* coding sequences, respectively.

The goal of these genetic modifications is making recombination between viral sequences virtually impossible to prevent the appearance of replication competent lentiviruses (RCL). However, an appropriate risk assessment for RCL in vector products intended for clinical application is inevitable in spite of the many genetically implemented safety precautions (Cornetta et al., 2011).

1.3 Designing lentiviral vectors

The aforementioned vector production systems allow specific designs of vector particles in a plug and play manner which enables the combination a viral core with surface glycoproteins of different viruses to generate gene delivery vectors, which is called pseudotyping.

The surface glycoprotein of vesicular stomatitis virus (VSVG) is mainly used to pseudotype HIV1-derived vector particles (Cronin et al., 2005). VSVG-pseudotyped vectors have very broad host tropism (Hastie et al., 2013) and can even transduce non-mammalian species (Lu et al., 1996).

Alternatives to the pantropic VSVG include retroviral surface glycoproteins such as from amphotropic murine leukaemia virus (MLV-A) (Spector et al., 1990; Page et al., 1990), human T cell leukaemia virus type 1 (HTLV1) (Landau et al., 1991), but also non-retroviral envelope proteins, for example from herpes simplex virus (Zhu et al., 1990). Cronin and colleagues (2005) provide a list of viral surface proteins which have been successfully used for pseudotyping. The pseudotype determines the host cell tropism of the produced vector and enables tissue- or celltype-specific gene delivery (Parveen et al., 2003; Höfig et al., 2014), so care has to be taken, that the respective host cell receptor is actually present at the target cells, in case the used pseudotype is selective.

Some pseudotypes are incompatible with specific cores such as gibbon ape leukaemia virus (GALV) surface glycoprotein fails at enveloping a HIV1-derived core (Lucas et al., 2010). However, packaging a vector with structural proteins from MLV pseudotyped with GALV generates infectious virions (Ghani et al., 2009).

The pseudotype has influence on the stability of the vector *in vitro* and *in vivo*. VSVG-pseudotyped vectors can yield high titers and are resistant to concentration by ultracentrifugation (Burns et al., 1993), however, they are inactivated upon contact with human serum resulting in nearly complete complement-mediated loss of infectivity (DePolo et al., 2000). Other pseudotypes such as a fusion construct of the envelope protein of feline endogenous retrovirus (RD114) and MLV-A surface-glycoprotein termed RD114A proved to withstand inactivation by serum (Sandrin et al., 2002).

Transduction efficiency depends on the type of vector (HIV- or EIAV-based), the target species and a combination thereof (Ikeda et al., 2002). HIV- and EIAV-based vectors are transducing target cells from different species, however, transgene expression works best from HIV1-based vectors infecting human or even non-human cells (O'Rourke et al., 2002). Alternatively, MLV-based vector productions systems are available (Naviaux et al., 1996; Cavazza et al., 2013). However, these vectors are limited to transducing dividing cells only, because MLV is a retro- and not a lentivirus.

Finally, after appropriate choices concerning pseudotype and core have been made, the used vector RNA has to contain a packaging signal, which needs to be compatible with the respective matrix proteins to become assembled into transduction-capable vector particles. Some retroviruses are capable of cross-packaging that is the incorporation of heterologous RNA from different phylogenetic groups. Spleen necrosis virus (SNV) structural proteins are capable of recognizing and packaging HIV1 RNA (Parveen et al., 2004), also successful cross-packaging of HIV1 RNA and by Mason-Pfizer monkey virus (MPMV) proteins were reported (Al Shamsi et al., 2011), while other combinations fail at packaging RNA, propagating it or both (reviewed in Al Shamsi et al., 2011).

1.4 Producing a gene therapy vector for FH

Previous attempts to produce an equine infectious anaemia virus (EIAV) based VSVG-pseudotyped lentiviral vector carrying cDNA encoding functional human *LDLR* under the control of CMV promoter resulted in a strong titer decrease upon increased LDLR expression. Similarly, the titer of a vector carrying *lacZ* instead of *LDLR* decreased upon providing a non-viral CMV-driven *LDLR* expression plasmid *in trans* during vector production, however, the vector titer was unaffected when the vector was packaged in presence of vector RNA encoding EGFP (Al-Allaf, unpublished).

In order to confirm this initial observation and determine the underlying mechanism, a modified human immunodeficiency virus 1 (HIV1) based packaging system was employed which has been used already for gene delivery *in vivo* (Naldini et al., 1996). It consists of the second generation self-inactivating (SIN) vector construct pHR-CMV-EGFP (Addgene #14858), the packaging construct psPAX2 (a gift from Didier Trono, Addgene #12260), and the envelope construct pMD2.G, encoding VSVG (a gift from Didier Trono, Addgene #12259). This type of three-plasmid packaging system is capable of producing high titer particles by transient transfection (Miyoshi et al., 1997). Table 1.1 summarizes the HIV1- and EIAV packaging components, figure 1.1 provides a schematic overview of the HIV1-based packaging system used in this work.

	EIAV-based system	HIV1-based system
Vector construct	pEIAV-LDLR	pHR-CMV-EGFP
Packaging construct	pONY 3.1	psPAX2
Envelope construct	pRV67	pMD2.G

Table 1.1. Overview of components of the EIAV-based used by Al-Allaf (unpublished) and the HIV1-based vector production system applied in this work.

The HIV-based vector particles packaged in this system contain viral RNA transcribed from pHR-CMV-EGFP carrying an EGFP coding sequence under control of CMV immediate early enhancer / CMV promoter element driving strong transgene expression (Gruh et al., 2008). Therefore, after infection of and genome integration in recipient cells (HeLa), EGFP is expressed allowing flowcytometric determination of vector titer. As a byproduct, EGFP is expressed from pHR-CMV-EGFP during vector production in HEK293 cells, which allows an estimation of transfection efficiency.

The vector capsid produced in the used HIV1-based packaging system consists of HIV1 Gag rather than EIAV structural proteins. This difference might have lead to failure in replicating the initial observation, as EIAV structural protein expression might not be compatible with LDLR expression, but with HIV1 Gag expression. In addition, the specific infectivity and/or packaging efficiency of EIAV-based vectors was found to be lower than of HIV1-based vectors, although the same

pseudotype was used (Ikeda et al., 2002). Nevertheless, there is no focus on maximum titer yield in this work, so both systems are considered comparable in case concentration-dependent effects of *LDLR* provided *in trans* show similar trends.

The HIV1-based vector particles as well as the EIAV-based vector particles are pseudotyped with VSVG, so both types of particles share the same universal tissue tropism (Hastie et al., 2013). This is particularly important as different pseudotypes could confer different infection efficiencies and might have led to uncomparable results during titer determination via flow cytometry.

The construction of a gene therapy vector in HEK293 packaging cells exploits host cell components and mimics the assembly of wildtype viruses. The structural proteins for the vector capsid in this work are expressed from plasmid psPAX2 as Gag (Pr55gag) and Gag-Pro-Pol precursors. Wildtype HIV1 myristoylated Gag forms membrane associated patches called assembly sites at the plasma membrane. Two copies of viral RNA are packaged into the capsid via interaction of Gag with their packaging signal (ψ) alongside with the viral enzymes reverse transcriptase (RT), integrase (IN) and protease (PR). The latter is activated by the packaging process and proteolytically processes immature Gag precursor molecules. The release of virions is mediated by the host cell endosomal complexes required for transport (ESCRT) machinery (reviewed in Sundquist and Kräusslich, 2012). The assembly and budding of a single HIV1 virus particle was shown to take around 10 min (Ivanchenko et al., 2009). Ectopically expressed Gag mediates release of virus-like particles independently from RNA packaging (Gheysen et al., 1989).

In parallel, the surface protein VSVG is transcribed from pMD2.G plasmid and translated at the rough ER, where it trimerizes (Doms et al., 1988). The protein is glycosylated in the Golgi apparatus *en route* through the secretory pathway to the plasma membrane (Fries and Rothman, 1980), where VSVG microdomains assemble autonomously (Brown and Lyles, 2003). VSVG microdomains and Gag assembly sites encounter by an unknown mechanism and the cellular ESCRT machinery presumably facilitates the release of nascent vector particles in analogy to wildtype HIV1 (Sundquist and Kräusslich, 2012). The requirements for a given surface protein to being accepted by a distinct capsid is still under debate.

The aim of this work consists in the identification of the steps in vector production which are interfered by *LDLR* over-expression. A number of molecular biological methods including RNA profiling or production and screening of *LDLR* deletion mutants as well as protein biochemistry and fluorescence microscopy analyses will shed light on cellular processes ranging from RNA transcription to intracellular protein sorting that are vitally important to successfully package an infectious viral vector. The results will provide insights into how to circumvent limitations of the production system and how to generate a gene therapy vector expressing human *LDLR* under the control of a constitutive promoter at applicable titers for the treatment of FH.

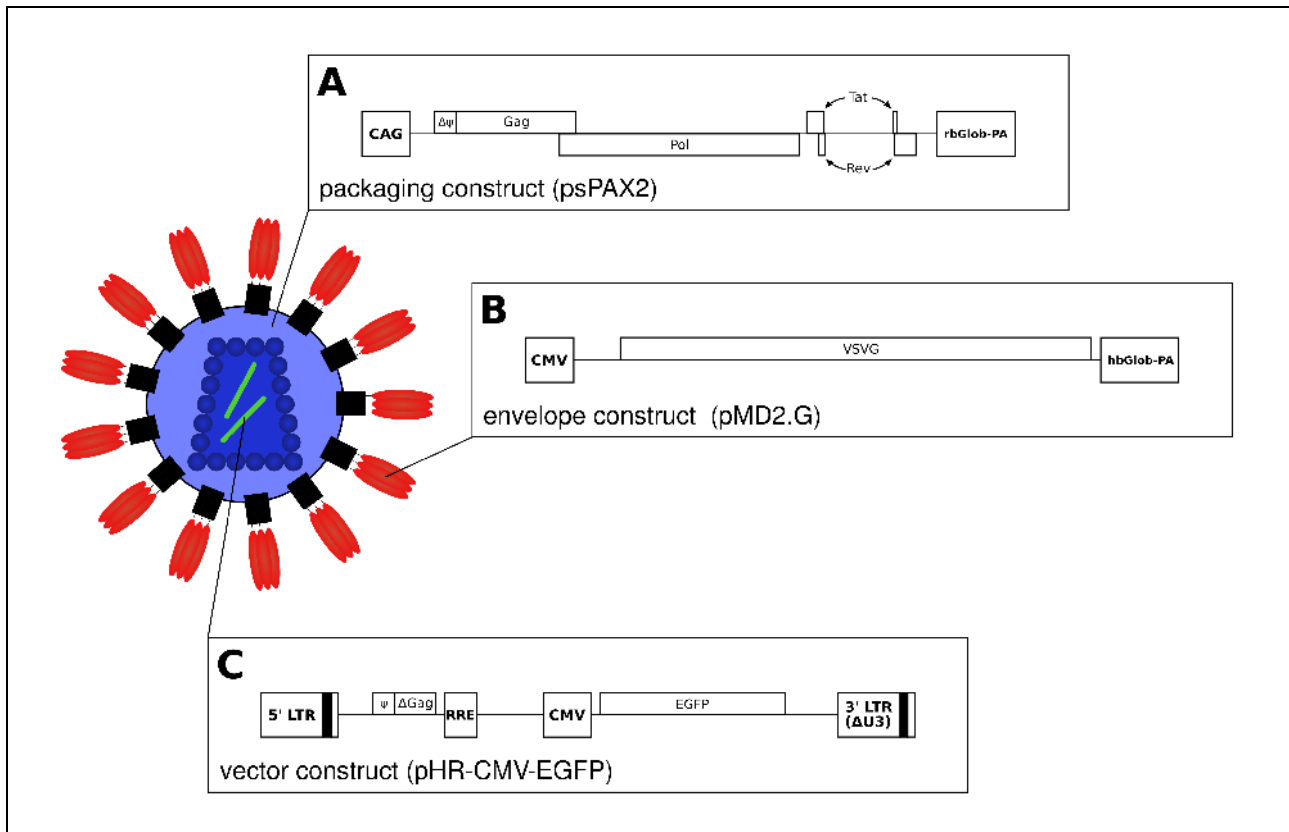


Figure 1.1. Schematic overview of the 2nd generation HIV1-based vector packaging system used in this work. Only relevant features are depicted and not drawn to scale. **A)** Packaging construct psPAX2. HIV1 *gag* and *pol* as well the accessory genes *tat* and *rev* are included under the control of a human cytomegal virus (CMV) promoter. The transcript is terminated by rabbit β -globulin polyadenylation signal (rbGlob-PA). The HIV1-packaging signal is deleted ($\Delta\psi$). **B)** Envelope construct pMD2.G encoding vesicular stomatitis virus glycoprotein (VSVG) under control of CMV promoter and human β -globulin polyadenylation signal (hbGlob-PA). **C)** Viral vector construct pHR-CMV-EGFP contains EGFP under the CMV promoter, a packaging signal (ψ), *rev*-responsive element (RRE) as well as a 399bp deletion in U3 of the 3' LTR.

2 Materials

2.1 Plasmids

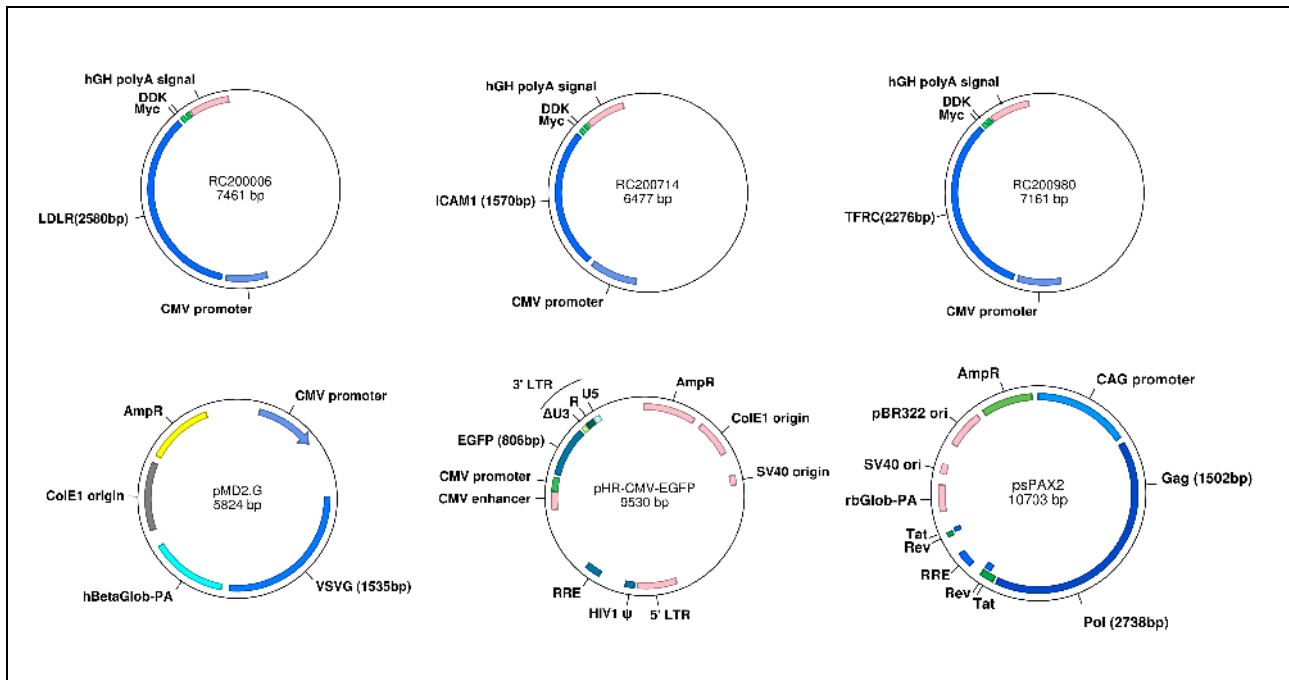


Figure 2.1. Maps of the plasmids used in this work. The upper row shows the expression plasmids of LDLR (Origene #RC200006), ICAM1 (Origene #RC200714) and TfR1 (Origene #200980). The virus production constructs pMD2.G (Addgene #12259), pHR-CMV-EGFP (Addgene #14858) and psPAX2 (Addgene #12260) are shown in the lower row.

2.2 Primers

name	sequence	length [nt]	%GC	Tm [°C]
EGFP_for	5' - TGAACCGCATCGAGCTGAAG - 3'	20	55	59
EGFP_rev	5' - TAGACGTTGTGGCTGTTGTAGTTG - 3'	24	45	59
psi_for	5' - GGACTCGGCTTGCTGAAGC - 3'	19	63	59
psi_rev	5' - CACCCATCTCTCTCCTTCTAGC - 3'	22	55	57
W6STOP_for	5' - CCTGGGGCTGaAAATTGCG - 3'	19	58	58
W6STOP_rev	5' - CGCAATTTtCAGCCCCAGG - 3'	19	58	58
signal_for	5' - GACAGATGTGAAAGAAACGAGTTCCAGTGCCAAGACGG - 3'	38	50	69
signal_rev	5' - CATGGCGATCGCGGCGGCAGATCTC - 3'	25	68	69
LBD_for	5' - GGGACCAACGAATGCTTGACAACAACGGC - 3'	30	57	69
LBD_rev	5' - GCCCACTGCAGTCCCCGCCG - 3'	20	80	69
NPVY_for	5' - CAGAAGACCACAGAGGATGAGGTCC - 3'	25	56	62
NPVY_rev	5' - GTCAAAGTTGATGCTGTTGATGTTC - 3'	25	40	66
RC200006_for	5' - CCACTCGCCCAAGTTTACC - 3'	19	58	57
CMV-for	5' - CGCAAATGGGCGGTAGGCGTG - 3'	21	65	67

Table 2.1. Primers used in this work. Melting temperatures were determined with ApE software. Primers were ordered at Microsynth. Mutagenic positions are indicated by bold lowercase letters.

2.3 Primary antibodies

host	target	supplier	dilution	application
mouse	DDK tag (DYKDDDDK)	Origene (#TA50011-100)	1:1000	WB
mouse	DDK tag (DYKDDDDK)	Origene (#TA50011-100)	1:200	IF
rabbit	VSVG	ThermoScientific (#PA1-30138)	1:5000	WB
mouse	γ -Tubulin	Sigma (#T5326)	1:5000	WB
chicken	LDLR (1-292)	<i>produced in-house</i>	1:250	WB
mouse	EEA1	BD Transduction Laboratories™ (#610456)	1:400	IF
mouse	GM130	BD Transduction Laboratories™ (#610822)	1:200	IF
mouse	ERGIC53	Alexis Biochemicals (#ALX-804-602)	1:200	IF
mouse	LAMP2	BD Pharmingen™ (#555803)	1:400	IF
mouse	Calnexin	BD Transduction Laboratories™ (#610524)	1:100	IF
rabbit	PDI	Stressgen (#SPA-890)	1:200	IF

Table 2.2. Primary antibodies used in this work.

2.4 Secondary antibodies

host	target	supplier	conjugate	dilution	application
goat	mouse IgG	Jackson ImmunoResearch (#115-035-062)	HRP	1:10000	WB
goat	rabbit IgG	Jackson ImmunoResearch (#111-035-003)	HRP	1:10000	WB
goat	chicken IgY	Jackson ImmunoResearch (#103-035-155)	HRP	1:10000	WB
goat	mouse IgG	Lifetechnologies (#A-11001)	Alexa488	1:1000	IF
goat	rabbit IgG	Lifetechnologies (#A-21428)	Alexa555	1:1000	IF
donkey	goat IgG	Lifetechnologies (#A-11055)	Alexa488	1:1000	IF

Table 2.3. Secondary antibodies used in this work.

3 Methods

3.1 Cell culture

HEK293 and HeLa Ohio Flow cells were kept in growth medium (Dulbecco's Modified Eagle's medium (DMEM) (GIBCO #41965-039) supplemented with 10% heat inactivated fetal calf serum (FCS) (Sigma, #F7524) and 1% antibiotics (100 U/ml penicillin and 100 U/ml streptomycin endconcentration, Lonza #DE17-602E) in T75 or T175 flasks for stock cultures. Cell passage was done by aspirating the growth medium, washing once with 10 ml PBS to remove residual serum components. Cells were detached by adding 2ml trypsin (GIBCO #25300-054) for 1-3 min, followed by adding 8 ml growth medium to inactivate trypsin and resuspension by gentle pipetting. HEK293 and HeLa were usually split 1:10 twice a week. Discarded volumes were then filled up with fresh growth medium before returning the flasks to the incubator.

3.2 Preparation of transfection reagent

Adjust the pH of sterile, endotoxin-free PBS to pH 4.5 with HCl. Add 200 mg Polyethyleneimine (PEI) powder (Polysciences #23966-2; M_w 25,000 Da) to 180 ml PBS. Heat up the suspension to 50°C until the solution is completely clear. Cool down to room temperature and fill up with PBS to 200ml to yield a stock solution of 1 mg/ml. After filter sterilization (0.22 μ m) in the cell culture hood, aliquot to 2 ml and store at -20°C, keep the rest in 50 ml tubes at -20°C. Working stocks can be repeatedly frozen and thawed, or kept at 4°C, and were used up after 2 months maximum. Do not use aliquot where precipitates have formed.

3.3 Production of pseudotyped lentiviral vector particles

HEK293 cells were seeded in 10 cm² plates (2.5*10⁶ cells each) or in 6-well plates (1*10⁶ cells per well) and incubated at 37°C and 5% CO₂. After 24 h cells were transiently transfected either using TurboFect transfection reagent (ThermoScientific, #R0531) following the manufacturer's recommendations or using polyethyleneimine (1 μ g/ μ l) in a 3:1 ratio (PEI:DNA) according to a suggestion from Guijs Versteeg. The transfection mixes included packaging and envelope constructs (psPAX2, pMD2.G) without a viral vector construct (pHR-CMV-EGFP) as negative control (NC) or with packaging and envelope constructs plus vector construct as positive control (PC). In the latter case virus production can occur successfully, whereas in the negative control only virus-like particles can form that lack packaged viral RNA (Doan et al., 2004). The DNA amount of pHR-CMV-EGFP, pSPAX2 and pMD2.G was kept constant throughout all experiments. In addition, expression vector plasmids encoding the transmembrane receptors human low-density lipoprotein receptor (LDLR, Origene #RC200006), human intercellular adhesion molecule 1 (ICAM1, Origene #RC200174), or human transferrin receptor (TFRC, Origene #RC200980) were co-transfected at distinct weight ratios to pHR-CMV-EGFP. A 1:2 ratio of LDLR:pHR-CMV-EGFP means that the amount of pHR-CMV-EGFP divided by two of #RC200006 were added, for example if 3 μ g pHR-CMV-EGFP were used, 1.5 μ g #RC200006 would have been added. Therefore, a ratio of 1:4, 1:8, or 1:16 inform that a quarter, an eighth or the sixteenth part of pHR-CMV-EGFP micrograms of #RC200006 were present in the corresponding transfection mix. The same rules apply for #RC200174 and #RC200980. In order to exclude potential effects elicited by unequal DNA concentrations in the transfection mixes, appropriate amounts of hering sperm DNA were added where necessary to maintain equal DNA concentrations. Table 3.1 summarizes the transfection scheme for 10 cm² plates, which were transfected with a total of 11.66 μ g DNA. Transfection mixes were prepared in 300 μ l serum-free DMEM without antibiotics. After adding DNA, the appropriate amount of PEI is added last. A third of the indicated DNA amounts and solute volume was used per well for six-well plates, accordingly. After adding DNA, the mixes were incubated at room

temperature for at least 20 min to allow the association of DNA with PEI. Then, they were added dropwise directly into the medium and plates were returned to the incubator. After 24 h, the medium was replaced with transfection medium that consists of growth medium (DMEM, 10% FCS) supplemented with 5mM sodium butyrate ($\geq 98.5\%$ (GC) (Sigma #B5887)), a histone deacetylase inhibitor (Turner, 1991; Wade et al., 1997), which is known to enable the production of high virus titers (Kafri et al., 1999) via inhibiting the epigenetic silencing of viral promoters (Choi et al., 2005). Incubation at 37° C / 5% CO₂ was continued for 24 h.

	NC	PC	LDLR 1:2	LDLR 1:4	LDLR 1:8	LDLR 1:16	ICAM1 1:2	ICAM1 1:8	TFRC 1:2	TFRC 1:2
pHR-CMV-EGFP [μ g]	-	3.33	3.33	3.33	3.33	3.33	3.33	3.33	3.33	3.33
psPAX2 [μ g]	5.00	5.00	5.00	5.00	5.00	5.00	5.00	5.00	5.00	5.00
pMD2.G [μ g]	1.66	1.66	1.66	1.66	1.66	1.66	1.66	1.66	1.66	1.66
RC200006 [μ g]	-	-	1.66	0.83	0.42	0.21	-	-	-	-
RC200174 [μ g]	-	-	-	-	-	-	1.66	0.42	-	-
RC200980 [μ g]	-	-	-	-	-	-	-	-	1.66	0.42
hering DNA [μ g]	5.00	1.66	-	0.83	1.24	1.45	-	1.24	-	1.24
PEI [μ g]	35.00	35.00	35.00	35.00	35.00	35.00	35.00	35.00	35.00	35.00
DMEM [μ l]	300.00	300.00	300.00	300.00	300.00	300.00	300.00	300.00	300.00	300.00

Table 3.1. Components of transfection mixes for virus production in 10cm² plates. The total DNA amount transfected was 11.66 μ g.

3.4 Concentrating vector particles by ultracentrifugation

Viral supernatants were put into 10 ml polycarbonate tubes 48 hours post transfection (hpt). Tubes were balanced with PBS. Ultracentrifugation was done in a Beckman T70.1 rotor at 4°C and 40.000 \times g for 90 min without rotor brake on a Beckman Optima L-80 XP ultracentrifuge. Medium was aspirated by removing half the volume at first and then carefully tilting the tube while aspirating the rest to avoid touching or approaching the invisible pellet with the pipette. The pellet was resuspended in 100 μ l PBS by pipetting 20 times up and down avoiding foaming and stored at -80°C.

3.5 Titration of lentiviral vector particles via flow cytometry

HeLa cells were plated either in 12-well plates at a density of 1×10^5 cells in 1.5 ml growth medium (DMEM / 10% FCS) per well or in 6-well plates at a density of 5×10^5 or 1×10^6 cells in 1.5 ml growth medium at least four hours before infection to allow attachment of the cells to the culture dish. This period is too short to allow a full cell cycle to finish and therefore prevents increase in cell number until inoculation with virus. As a result, a known cell number rather than an estimation can be used for calculating the vector titer via formula (1) according to White et al. (1999)

rendering the determined titer more accurate.

Growth medium was replaced by 0.5 ml infection medium (DMEM / 2% FCS). Then, as little as 5 µl concentrated viral supernatant or up to 100 µl unconcentrated viral supernatant were added to the medium and cells were preincubated at 37°C / 5% CO₂ for 30 min, followed by adding 1 ml infection medium supplemented with polybrene (Sigma #107689) to a final concentration of 8µg/ml (Miyoshi et al., 1997; Davis et al., 2002). Then, plates were incubated for 72h at 37°C / 5% CO₂ before titer was determined via flow cytometry.

Infected HeLa cells were collected in 1.5 ml tubes 72 hours post infection (hpi) by aspirating the medium, washing the cells in PBS, adding 150 µl dissociation reagent containing trypsin and EDTA (GIBCO #25300-054), and 950µl growth medium after detachment to inactivate the trypsin. The cell suspension was centrifuged for 5 min at 800 x g, followed by washing with PBS and transfer to 5 ml flow cytometer tubes. Transduction efficiency was assessed by a BD FACSCalibur flow cytometer and analyzed using CellQuest software determining the percentage of fluorescent HeLa cells per well. The virus titer was determined using the formula calculating transduction units (TU) per ml according to White et al. (1999):

$$TU/ml = \frac{N * P}{V} * 1000 \quad (1)$$

N cell number at time of infection

P percentage of EGFP-positive cells [%]

V volume of concentrated viral supernatant [µl]

The percentage of fluorescent cells usually ranged between 1 and 20, therefore the probability of multiple infections of a single cell was considered negligible, which would otherwise lead to underestimation of the actual vector titer.

3.6 Titration of lentiviral vector RNA copy number via RT-qPCR

Viral RNA or total RNA was extracted from either concentrated or unconcentrated cell-free samples using the QIAGEN Viral RNA Mini kit or from HEK293 cell pellets using the QIAGEN RNeasy Mini Kit. The supplied protocols were conducted without modifications. All steps before lysis of vector particles or producer cells were carried out in a BSL2 laminar flow hood, the washing steps and elution in 50 µl nuclease-free water were performed under nuclease-free conditions at the bench according to the biosafety regulation that demands working with infectious material is allowed only in dedicated areas.

In order to remove residual DNA carried over from transfection, pHR-CMV-EGFP in particular, DNA was digested in the viral RNA extracts with DNase I by adding 1 µl of a 5 mg/ml DNase I stock together with 0.25 µl 1M CaCl₂, 0.25 µl recombinant RNase inhibitor (rRNasin; 20-40 U/µl;

Promega, #N2515) and incubation at 37°C for 30 min. DNase was inactivated by heating 15 min at 95°C.

RNA concentrations were determined using a PEQLAB NanoDrop UV/Vis spectrophotometer and ranged from roughly 100 ng/μl for extracts from cell-free samples to around 500 ng/μl for total RNA preparations.

Reverse transcription of viral RNA was done using Moloney Murine Leukemia Virus reverse transcriptase (Promega, #M1705). In each reaction, 2 μl RNA extract (200-800μg) were incubated with 2 μl of an appropriate reverse primer dilution (4μM) at 70°C for 5 min to resolve RNA secondary structures and facilitate annealing, followed by chilling on ice for 10 min. Then, 21 μl RT master mix consisting of 5 μl 5x M-MLV buffer, 1 μl 10mM dNTP mix, 0.375μl rRNAsin (20-40 U/μl), 13.125 μl Millipore water and 0.5μl M-MLV reverse transcriptase (200U/μl) were added. One cycle of 45°C for 1 h, 70°C for 15 min, 4°C hold was used for amplification on a thermocycler with heated lid. Reverse transcribed cDNA was used either directly for quantitative PCR (qPCR) or stored at -20°C.

Vector copy numbers were determined via quantitative PCR (qPCR) by comparing the threshold cycle values (Ct values) with a standard curve derived from a serial dilution of pHR-CMV-EGFP ranging from roughly 10⁷ copies/μl to 0.1 copies/μl. Each well of an Eppendorf Twintec 96-well plate included 1 μl reverse transcribed cDNA template or 1 μl of pHR-CMV-EGFP plasmid standards put into 9 μl qPCR master mix consisting of 5 μl KAPA SYBR® FAST qPCR mix (KAPABIOSYSTEMS, #KK4601), 1 μl of an appropriate reverse and forward primer dilution (4μM) each, and 2 μl Millipore water. Ct-values were recorded during 45 cycles of 95°C for 15 s, 55-57°C for 30 s (depending on the used primer pair) and 68°C for 20 s after 2 min denaturation at 95°C in the 520 nm channel of a Eppendorf Mastercycler® RealPlex².

3.7 Viral RNA fractionation from LDLR co-expressing cells

Virus was produced as described in HEK293 cells co-transfected with LDLR encoding plasmid and without as control in 10 cm² plates. Cell supernatant (10 ml) was transferred to 15 ml tubes (supernatant fraction, S), residual liquid was aspirated, followed by adding 10 ml PBS containing 10 mM EGTA to the cells. After incubation for 5 min, cells detached and were transferred to new 15 ml tubes for spinning cells down at 800 x g for 5 min. The cleared washing buffer was transferred to a third set of 15 ml tubes (wash fraction, W) and stored together with S at -80°C until viral RNA isolation. The cells were resuspend in DMEM / 2% FCS, counted in a Neubauer counting chamber and stored at -80°C until total RNA isolation (cell fraction, C). Avoid pipetting up and down the cells for resuspension at any step as this easily disrupts syncytia that form during virus production and releases intracellular viral RNA into W.

3.8 Cell lysis in buffer A (OGP lysis buffer)

HEK293 cells were collected in 1.5 ml tubes by scraping cells off the culture plates in 0.5-1 ml lysis buffer A (50mM Tris base, 50mM NaCl, 1% Octyl- β -D-glucopyranosid (OGP) (Carl Roth GmbH, #CN23.3), pH 7.4), followed by adding PMSF dissolved in isopropanol to a final concentration of 1 mM, incubation on ice for at least 30 minutes, brief vortexing, and another 30 minutes incubation on ice. PMSF crystals have to be redissolved by warming to room temperature and occasional vortexing. The lysate was cleared by centrifugation in a tabletop centrifuge at full speed ($\geq 14.000 \times g$) for 10 minutes. The protein concentration of the cleared lysate was measured using a NanoDrop UV-Vis spectrophotometer. Then, 400-800 μ l of cleared lysate were transferred to a new 1.5 ml tube, mixed with 100-200 μ l 5x reducing or non-reducing Laemmli sample buffer (50% glycerol, 10% SDS, 0.4M Tris pH 6.8, 0.5% bromophenol blue, with or without 4% β -mercaptoethanol) and boiled at 95°C for 10 minutes, followed by flash freezing in liquid nitrogen and storage on -20°C.

3.9 Cell lysis in buffer B (RIPA lysis buffer)

HEK293 cells were collected in 1.5 ml tubes either by scraping cells off the culture plates in 0.5 ml PBS or trypsinisation, followed by pelleting at $800 \times g$, inhibition of the trypsin with 1 ml growth medium and washing once in PBS to get rid of cell debris. Then, the pelleted cells were resuspended in 100 μ l pre-cooled RIPA lysis buffer (50mM Tris base, 150mM NaCl, 1% Triton X-100, 10mM EDTA, 0.5% Na-Deoxycholate, 0.1% SDS, 1mM PMSF, 5 μ M pepstatin A (Tocris, #1190), 1 tablet Roche Complete protease inhibitor cocktail per 10 ml) and the lysate was homogenised by pipetting up and down 20 times. The lysate was cleared by centrifugation in a tabletop centrifuge at full speed ($\geq 14.000 \times g$) for 10 minutes. The protein concentration of aliquots of the cleared lysate was measured via BCA assay (Pierce™ BCA Protein Assay Kit #23225). Then, the remaining volume of cleared lysate was split to two new 1.5 ml tubes and mixed with 5x reducing or non-reducing Laemmli sample buffer (50% glycerol, 10% SDS, 0.4M Tris pH 6.8, 0.5% bromophenol blue) and boiled at 95°C for 10 minutes, followed by flash freezing in liquid nitrogen and storage on -80°C. The procedure was completed as fast as possible to avoid loss of protein fragments due to residual lysosomal protease activity.

3.10 Western blot

A total of 10 μ g protein per lane was separated onto discontinuous Tris-glycine SDS-PAGE gels (8%) with 4.5% stacking gels. Samples were heated to 95°C for 5 min before loading to dissolve eventual SDS precipitates. The gels were run at 200V in Tris-glycine running buffer (25mM Tris, 250mM glycine, 3.5mM SDS, pH unadjusted). Afterwards, proteins were blotted onto PVDF

membranes with 0.45µm pore size (Millipore Immobilon-P, #IPVH00010) at 20V for 2h using transfer buffer (20mM Tris, 150mM glycine, 20% MeOH, pH unadjusted), followed by blocking in 2.5% skimmed milk powder in TBS + 0.1% Tween-20 (Sigma #P1379). The next day, the blocking buffer was saved and membranes were rinsed twice in PBS + 0.1% Tween-20 (PBST) before incubating in primary antibody dilutions for 1h at room temperature on a shaker. After washing the membranes three times in PBST for 10 min, the appropriate HRP-conjugated secondary antibody was diluted in saved blocking buffer and added to the membranes for 1h at room temperature on a shaker. Membranes were washed in PBST three times before detection via ECL (Thermoscientific SuperSignal West Pico, #34080).

3.11 Site-directed mutagenesis

A point mutation (W6STOP) or deletions (Δ SP, Δ LBD, Δ NPVY) were introduced into the LDLR coding sequence of RC200006 via a modified Quikchange or round-the-horn approach, respectively, using 5'-phosphorylated mutagenic primers. The reactions are shown schematically in figure 3.1.

The applied modified Quikchange approach is a one-step site-directed mutagenesis protocol with a pair of completely overlapping primers bearing the desired point mutation in each sequence of the primer pair (W6STOP_for, W6STOP_rev; Figure 3.1A). Linear amplification of the parent plasmid during thermal cycling (Table 3.2) on an Eppendorf Mastercycler yields a mutated plasmid with single-strand nicks that do not require *in vitro* ligation (Zheng et al., 2004; Liu and Naismith, 2008) next to the primer 5' ends. Afterwards, the parent plasmid was digested by adding 1 µl DpnI (20U/µl) and incubation at 37°C for 1h, followed by direct transformation of 2 µl PCR reaction via electroporation without prior purification of the PCR product. The deletion constructs *LDLR-Δ*SP, *LDLR-Δ*LBD and *LDLR-Δ*NPVY were generated by amplification (Table 3.2) from the same template (RC200006) using either the primer pair signal_for/signal_rev, LBD_for/LBD_rev or NPVY_for/NPVY_rev. Round-the-horn mutagenesis is an exponentially amplifying method and yields blunt-ended products (Moore, 2014), shown in figure 3.1B). After DpnI digesting, PCR mixes were loaded onto 1% preparative agarose gels and gel purified (PEQ Gold gel extraction kit). This step is essential as ligating the blunt-ended linear fragments from the PCR reaction directly is strongly inhibited by the crude PCR mix (personal communication from Sofiya Fedosyuk). Furthermore, cutting out bands excludes incompletely amplified DNA fragments. Around 50-100 ng of purified linear blunt-ended PCR products were ligated using 1 µl T4 ligase (3U/µl) on room temperature over night, supplemented with PEG8000 (2.5%) to support ligation via molecular crowding (Harrison and Zimmermann, 1984). Aliquots of 10X T4 ligase buffer (2µl each) were stored at -20°C for single use to avoid freeze-thaw cycles and degradation of ATP. Ligation products

were directly used for transformation by electroporation.

Subsequently, single colonies were picked with a sterile tooth pick and put into 3 ml LB medium supplemented with kanamycin (25µg/ml). Plasmid DNA was miniprep (OMEGA E.Z.N.A.® Plasmid DNA Mini Kit) after 16h and sent for sequencing either premixed with a sequencing primer (RC200006_for) or as pure DNA which was mixed with a standard primer (CMV-for) at the sequencing company. Aliquots of the miniprep cultures were mixed 1:1 with 70% sterile glycerol and stored at -80°C.

Appropriate thawing of the polymerase buffer proved essential for a successful PCR, because freezing the buffer eventually produced precipitates, most probably MgSO₄, which were redissolved by heating to 95°C for 5 min.

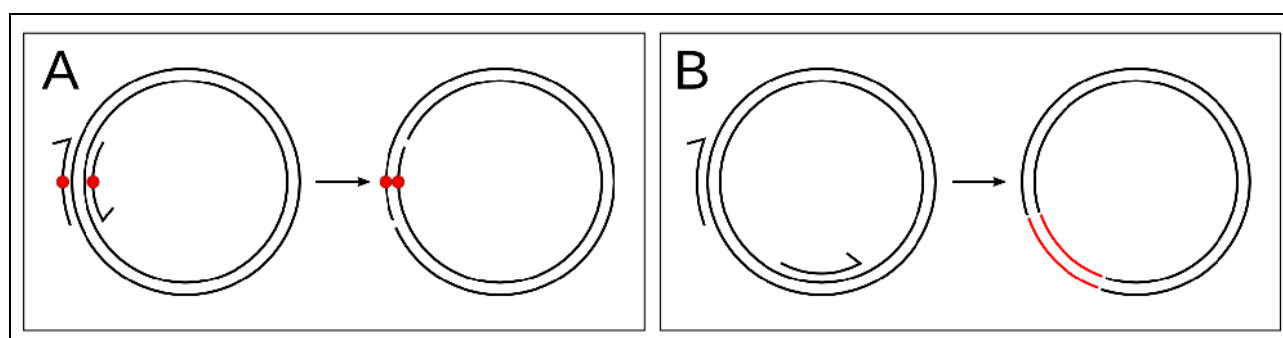


Figure 3.1. Graphical representation of the employed site-directed mutagenesis approaches. The 5'-3' direction of the primers is indicated by arrows. **A)** Modified Quikchange mutagenesis. Red dots denote the point mutation. The PCR product has single-strand nicks at the primer 5' ends. **B)** Round-the-horn mutagenesis. The deletion is indicated in red (not to scale). The PCR product is blunt-ended.

component	amount
Millipore water	ad 20 µl
Template plasmid	50-100 ng
Pfu buffer (10X)	2 µl
dNTP mix (10mM)	1 µl
Forward primer (10µM)	1 µl
Reverse primer (10µM)	1 µl
Pfu polymerase (2.5U/µl)	1 µl
total	20 µl

Table 3.2. Components of the PCR reactions.

step	temperature	time	
initial denaturation	95°C	5 min	
cycling	95°C	50 sec	18 repeats
	x°C	50 sec	
	72°C	15 min	
	72°C	15 min	
final extension	72°C	15 min	
stand-by	4°C	∞	

Table 3.3. PCR cycling conditions. The annealing temperature for the W6STOP reaction was 57°C, for *LDLR-ΔLBD* and *LDLR-ΔSP* 68°C, and *LDLR-ΔNPVY* 65°C.

3.12 Electroporation of XL1-Blue cells

An electroporation cuvette (2 mm electrode distance) was precooled at -20°C 15 min before transformation. After thawing an aliquot of XL1-Blue cells (50µl) on ice, 50-100 ng DNA was added and mixed with the cells by stirring gently with the pipettor tip. Incubation on ice was continued for 10 min, followed by transferring the suspension into a precooled electroporation cuvette and tapping the cuvette onto the bench until no air bubble spanned the electrodes. This step is vital as air bubbles lead to increased energy density around them which might kill the cells. The pulse program was 2500V, 335Ω and 15µF on a EQUIBIO EasyjecT Optima. After the pulse, 200 µl LB medium equilibrated to room temperature was added quickly to the suspension in the cuvette without pipetting up and down. Then, the suspension was transferred back to the tube, where incubation with DNA has taken place, and was incubated at 37°C for 1h shaking at 300rpm on a thermoblock. Aliquots of 100µl were plated onto selective LB agar plates containing the appropriate concentration of antibiotic, following incubation for 24h in a 37° incubator or at room temperature over a weekend. A control electroporation of XL1-Blue without added DNA and plating onto non-selective LB agar plates was carried out to assure cell viability after the transformation procedure. Cuvettes can be reused after rinsing them three times with distilled water and three times in 70% ethanol. The cuvettes placed in a beaker covered with aluminium foil can be autoclaved or put in a sterile incubator for drying. Afterwards, that container was stored on the bench until the next usage.

3.13 Indirect immunofluorescence microscopy

HEK293 cells seeded onto 18 mm glass coverslips (0.17 mm thickness) in 12-well plates, 1×10^5 cells per well. After transfection with respective virus production constructs and expression vectors as described and 48h incubation at 37°C / 5% CO₂, medium was aspirated and cells were washed once in PBS. Adding fluids to HEK293 cells easily blasts off cells from the coverslip, therefore tips have to be cut off to reduce hydrodynamic shearing forces. Afterwards, cells were fixed in 1 ml 2% PFA in PBS for 15 min, followed by adding 1 ml 25 mM NH₄Cl to quench reactive aldehyde for 30 min. Cells were rinsed once in PBS, before adding 1ml blocking buffer (BB) (1% BSA / 0.2% saponin in PBS) for at least 30 min. Blocking buffer was replaced with 20µl primary antibody dilutions in blocking buffer without an intermediate washing step. Primary antibody master mixes were prepared for dual stainings. After incubation at room temperature on a shaker (30 rpm) for at least 30 min in the 12-well plate covered with wet paper towel, cells were washed twice in PBS, before adding 20µl secondary antibody dilution for single stainings or dilution mastermix for double stainings for at least 30 min. Then, cells were washed twice in PBS and rinsed once with Hoechst33342 1:10000 in Millipore water, before mounting the cells in Mowiol (15µl per coverslip).

3.14 Quantification of Western Blots

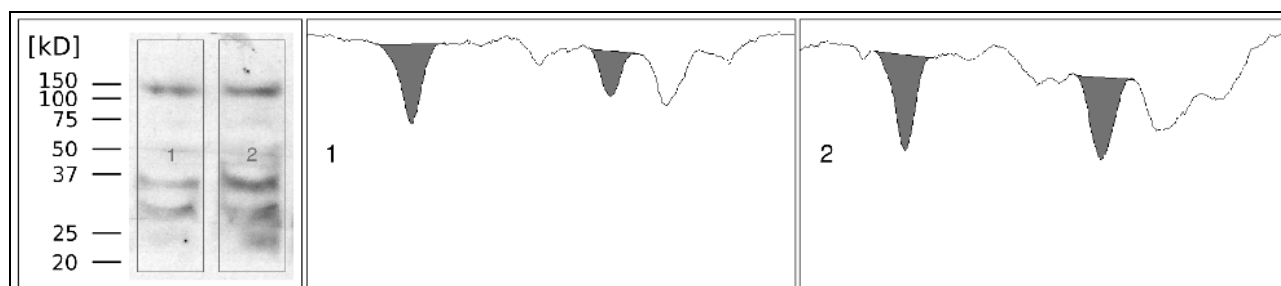


Figure 3.2. Densitometric analysis of Western blot signals via ImageJ. Evenly sized rectangles are drawn onto the scanned X-ray films (left panel). The corresponding optical density plots for the two lanes are shown in the middle (1) and right panel (2), which represent (from left to right) the average grey value of the pixel row in the respective rectangles on the blot from top to bottom. Peak areas of interest at around 150kD and 36kD are highlighted in dark grey. The analysis shown is a sample from figure 4.10.

X-ray films exposed to luminescent Western blot membranes were scanned to TIFF files with a standard office scanner (CanoScan 9950F) in transillumination mode and densitometrically analyzed using the GelAnalyzer plugin of ImageJ 1.47v software. The TIFF files were automatically white-corrected before analysis using GIMP software. The method is based on optical density plots representing the mean grey values from top to bottom, which are calculated from rectangular boxes drawn onto the lanes (Figure 3.2, *left*). Baselines for peaks of interest are inserted, which were selected and drawn determined by eye and hand, respectively. The peak integrals are then calculated from the enclosed peak areas (Miller, 2015), which is the recommended analysis parameter (Gassmann et al., 2009).

4 Results

4.1 Transfection efficiency of TurboFect and PEI

The transfection efficiency of polyethyleneimine (PEI) was assessed in comparison to TurboFect transfection reagent for transfecting HEK293 cells. Cells were harvested after virus production, during which EGFP expression occurs as a byproduct, and the percentage of fluorescent HEK293 cells per plate was determined with a BD FACSCalibur flow cytometer and CellQuest software (Table 4.1).

Reagent	NC	PC	LDLR 1:2	LDLR 1:8	ICAM1 1:2	ICAM1 1:8	TFRC 1:2	TFRC 1:8
TurboFect	0.00	47.35	19.28	47.36	42.53	32.26	37.45	43.08
PEI	0.00	87.30	52.04	55.45	93.70	94.90	91.89	94.20

Table 4.1. Transfection efficiencies of TurboFect compared to PEI. Data are percentage of EGFP-positive HEK293 cells from a single experiment.

The PEI-mediated transfection efficiency was on average twice as high as TurboFect mediated

transfection throughout the tested transfections. The transfection efficiency of the LDLR co-transfections is about 50%, whereas 90% of the cells were transfected in the positive control and the *ICAM1*- and *TFRC* controls. One might argue that this decrease in EGFP-positive cells is due to the presence of *LDLR* sequences, however, this is not replicated in the TurboFect batch. In conclusion, the usage of TurboFect was discontinued due to economical considerations.

4.2 Vector yield is independent of transmembrane protein presence

The construction of a lentiviral vector library from human ORFs under EF1 α promoter revealed an intrinsic bias among human genes affecting the resulting titer of produced vector (Škalamera et al., 2012). The strong promoter EF1 α facilitated over-expression of the respective ORF during vector production which were toxic to HEK293T cells in some cases as reported or putatively interfered with vector construction for various reasons. Therefore, the vector titer which was obtained by Al-Allaf (unpublished) might be simply due to the fact that highly abundant human CMV-driven low-density lipoprotein receptor (LDLR), blocks an event during vector production such as transcription or translation of vector components, vector assembly or budding.

LDLR as well as VSVG pass the ER and the Golgi during their biosynthesis in the cell, because both are transmembrane proteins. Al-Allaf (unpublished) did not observe a significant decrease in vector yield when the transgene was EGFP, a cytosolic protein, encoded in the viral transfer vector plasmid. Therefore, the expression of LDLR might overload the biosynthesis pathway of VSVG. As a result, lower amounts of VSVG would be available at the plasma membrane preventing budding of vector particles or leading to assembly of particles without surface protein that are non-infectious. The finding that HIV1 Gag alone is able to promote the formation of virus-like particles supports this hypothesis (Doan et al., 2004). If this overloading hypothesis is relevant, the expression of other transmembrane proteins such as intercellular adhesion molecule 1 (ICAM1) or transferrin receptor (TFRC) should also decrease the vector titer.

Vector was produced as described by transient transfection in 10 cm² plates. In addition to the vector, packaging and envelope constructs, expression plasmids encoding transmembrane receptor cDNA of LDLR, ICAM1 or TFRC were co-transfected at different weight ratios to pHR-CMV-EGFP. After concentrating the virus-containing cell supernatant by ultracentrifugation, HeLa cells were infected with aliquots of the virus preparations for titration. Before harvesting, the cells were imaged for EGFP expression on a ZEISS Axiovert 200M at 10X magnification. Then the number of transduced cells was determined via flow cytometry.

The microscopic analysis already revealed a striking pattern. The amount of EGFP-positive HeLa cells decreased dramatically the more *LDLR* was co-transfected during vector production (Figure 4.1A). In contrast, infection of HeLa cells with virus preparations from the positive control (PC)

and from the ICAM1 and TFRC controls of either ratio resulted in indistinguishable fluorescent cell densities.

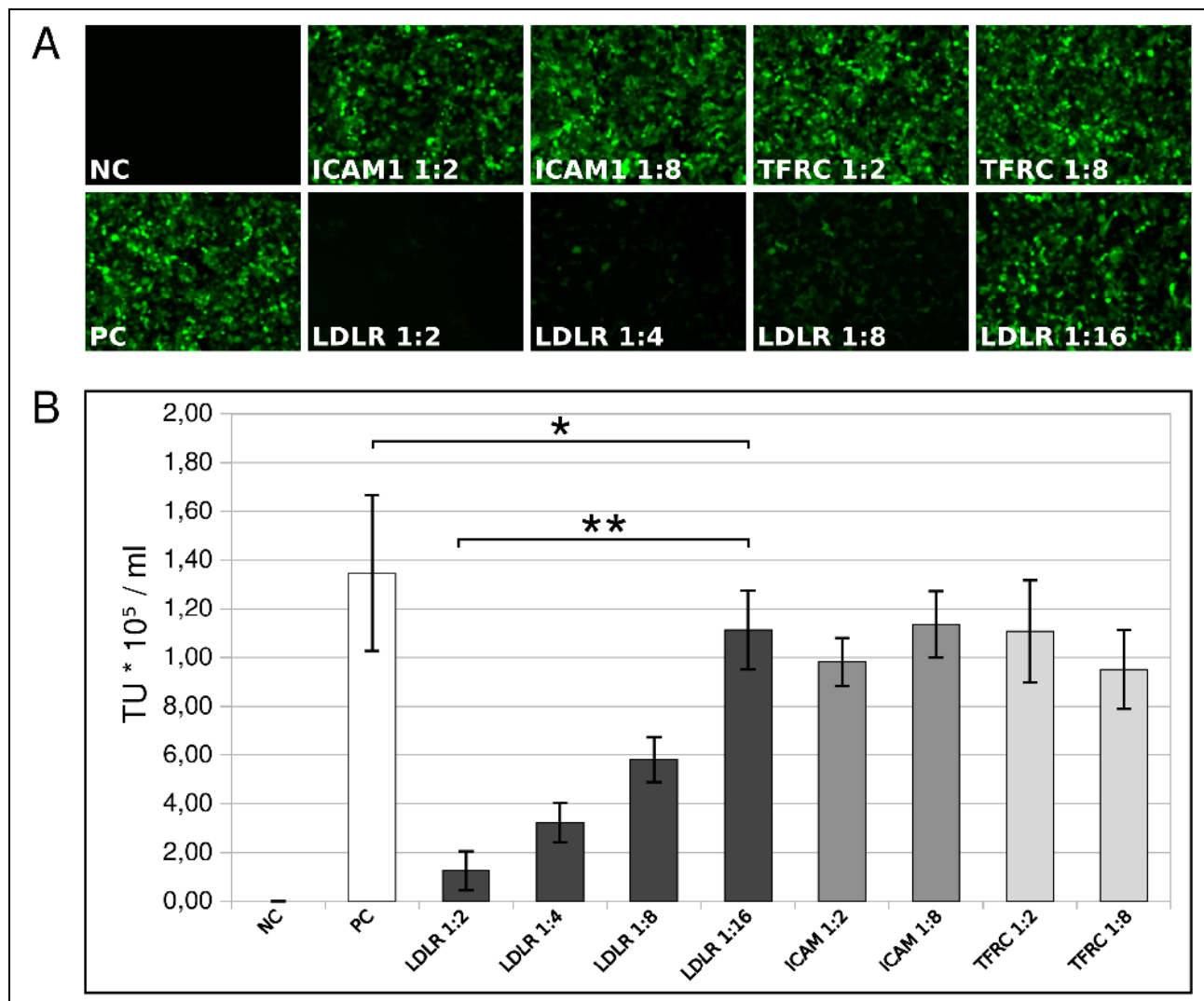


Figure 4.1. Determination of vector titer with respect to co-expression of transmembrane proteins. A) Fluorescence micrographs of HeLa cells transduced with EGFP. **B)** Transducing units (TU) in unconcentrated supernatant of the indicated virus preparations. Data are arithmetic mean \pm SEM for three biological replicates. * $p < 0.005$, ** $p < 0.0005$, one-way ANOVA.

The calculation of transducing units (TU) substantiate the microscopic observations and provide a quantitative estimation of the correlation of TU with the amount of LDLR plasmid transfected. The titer yield was around 1.5×10^5 TU/ml from the positive control (PC, Figure 4.1B), which matches the reported achievable titers for this type of production system (Naldini et al., 1996). The more LDLR plasmid was co-transfected during virus production, the less TU were produced (LDLR 1:2 to LDLR 1:16). One-way ANOVA revealed that the decrease in vector titer in response to LDLR cotransfection is highly significant ($p < 0.005$), whereas the concentration-dependent increase in vector titer inversely proportional to the LDLR amount bears even higher significance ($p < 0.0005$). Differences in vector titer between PC, LDLR 1:16 and ICAM1 as well as TFRC at either ratio are considered non-significant ($p > 0.03$) compared to the significance level of the LDLR

cotransfections. This reduction probably results from the expression of the respective transmembrane protein competing with the expression of viral components in the cell.

This result confirms that providing LDLR cDNA *in trans* induces a significant decrease in vector yield as found by Al-Allaf for LDLR present *in cis*. The presence of ICAM1 or TFRC cDNA does not result in significant changes in TU, but LDLR seems to interfere specifically with vector biosynthesis. Therefore, the argument that all three co-transfected cDNAs encoding membrane proteins would inhibit vector production for that reason does not hold water. This finding is also in accordance with the results from Skalamera and colleagues (Skalamera et al., 2012) who found transmembrane protein coding genes among low as well as high vector titer yielding ORFs.

4.3 LDLR-expression correlates with released vector copy number

Titerting a lentiviral vector via determining the transducing units per volume is limited to detecting infectious vector particles only. That assay does not allow for an assertion about the total vector particle count which might be present in the sample, albeit non-infectious. Although the co-transfection of LDLR apparently decreases the titer of the transducing vector as shown before, an equal number of vector particles might be released into the cell supernatant during vector production. The over-expression of LDLR could result in it's incorporation into the viral envelope during vector assembly and budding, which was reported for other host cell membrane proteins such as ICAM1 likewise in wildtype HIV1 (Paquette et al., 1998) or an HIV1-based packaging system (Bounou et al., 2004).

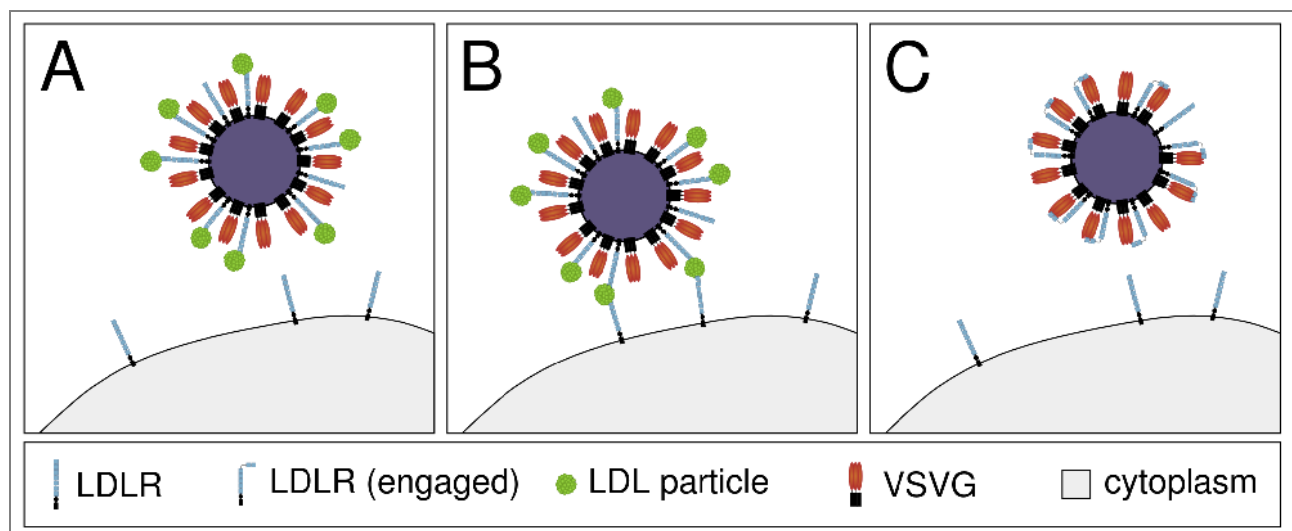


Figure 4.2. Schematic overview of possible events elicited by incorporation of LDLR packaged into the virion. **A)** LDL particles binding to vector-associated LDLR prevent binding to and infection of a recipient cell (HeLa). **B)** LDL-decorated vector particles bind to host-cell LDLR, preventing or making infection more efficient. **C)** Vector-associated LDLR binds to VSVG at the vector surface preventing binding to host-cell LDLR.

The presence of LDLR on the virus surface might not have any effect, however, it could also alter the vector's infection efficiency either positively or negatively. The cell supernatant contains LDL-

particles that could bind to virus-associated LDLR rendering the vector particle non-infectious by sterically hindering VSVG interacting with a recipient cell surface and/or its host cell receptor (Figure 4.2A). Taking the size difference of the lentiviral vector particle (~80-120 nm, Fleury et al., 2003, Sastry et al., 2005) and the average size of LDL particles (~22 nm, Kumar et al., 2011) into consideration, this model is only reasonable, if the stoichiometric ratio of LDLR to VSVG on the vector surface equals or is greater than one, otherwise the steric shielding might be incomplete. On the other hand, serum LDL particles could bridge virus-associated LDLR and cell-associated LDLR in a bivalent interaction. As a result, the vector could be prevented from infecting the cell by impairing endocytosis or infect the cell more effectively, because vector particles would enter the cell via ligand-mediated internalization of LDLR (Figure 4.2B), which is an essential step of the wildtype VSV infection route (Panda, 2011). Therefore, the latter case of LDL particles binding to surface-incorporated LDLR of a vector particle most probably fails to explain the apparent decrease of vector titer.

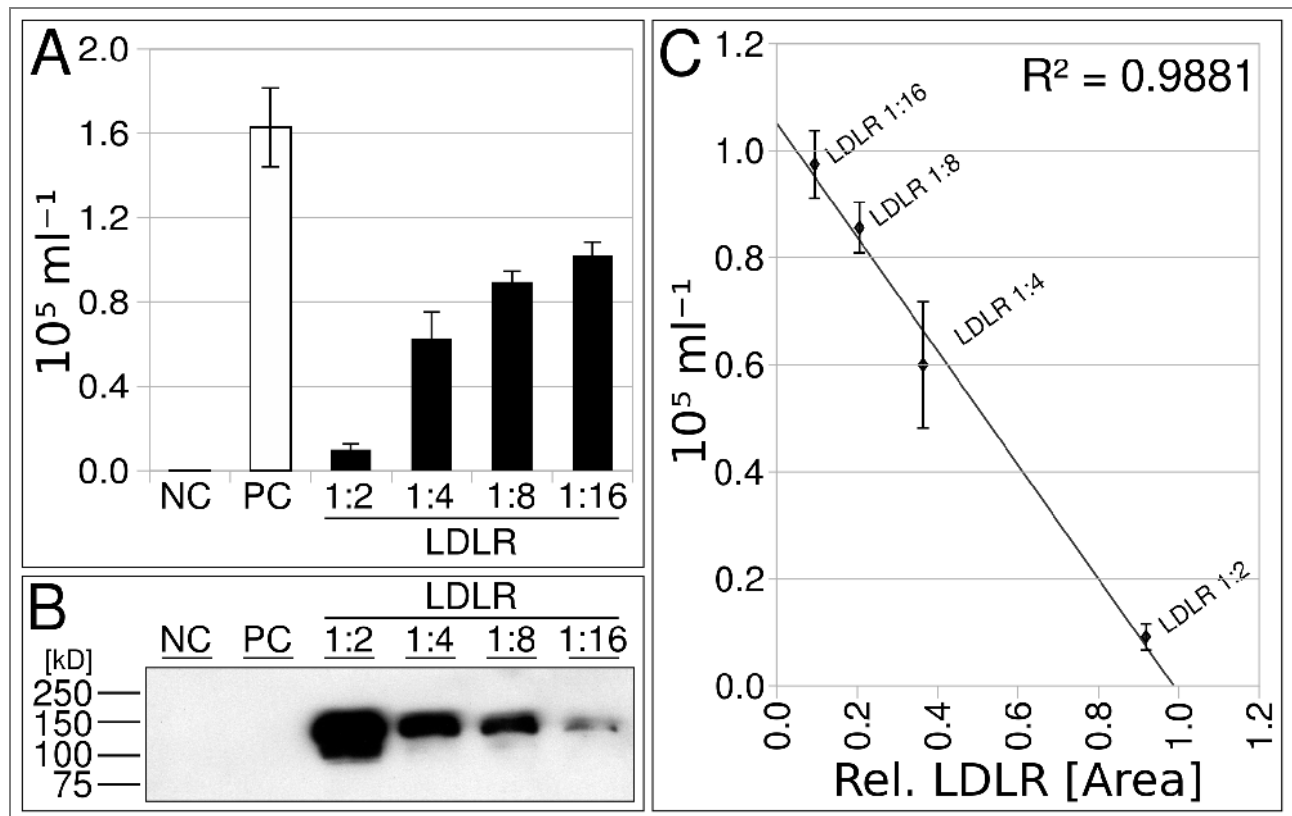


Figure 4.3. Determination of vector titer in correlation with the expression level of recombinant LDLR. **A)** Vector copy number in the supernatant of HEK293 producer cells. Data are arithmetic mean \pm 2SD of triplicate measurements. **B)** Western blot analysis of DDK-tagged LDLR expression levels. Scanned film image was automatically white corrected with GIMP. **C)** Linear correlation of the relative LDLR expression level quantified as described from panel B with vector copy number from panel A.

Recently, LDLR was identified as a host cell receptor for vesicular stomatitis virus (Finkelshtein et al., 2013). The authors showed that VSVG binds specifically to ligand-binding repeats present in LDLR and its family members. This interaction was required for the infection of a recipient cell,

however, virus-associated LDLR could putatively interact with adjacent VSVG molecules on the surface of released vector particles, which in turn makes interaction of VSVG with a recipient cell's LDLR and its infection impossible (Figure 4.2C).

In order to check whether the same particle count is produced irrespective of the extent of LDLR co-transfection that could only modulate a particle's specific infectivity, a reverse transcriptase quantitative PCR (RT-qPCR) assay was designed that does account for infectious as well as non-infectious particles. This method is commonly used to determine a virus titer as alternative to marker expression based assays (Sastry et al., 2002; Greenberg et al., 2006).

Vector copy number was determined via measuring the amount of EGFP coding sequences in viral RNA extracts from concentrated cell supernatant. The probes (primer pair EGFP) annealed to nucleotides 362 to 381 and 432 to 455 of the EGFP coding sequence on reverse transcribed cDNA as well as on serial dilutions of pHR-CMV-EGFP, which was used as standard. In parallel, HEK293 cells were lysed after virus harvest in lysis buffer A containing Octyl- β -D-glucopyranosid (OGP), analyzed for DDK-tagged LDLR on Western Blot and quantified as described.

Again, a significant decrease of vector titer with increasing amount of co-transfected LDLR was observed. Figure 4.3A shows the vector copy numbers obtained via RT-qPCR back-calculated to the unconcentrated supernatant.

This result proves the hypothesis wrong that specific vector infectivity is modulated by virus-associated LDLR. The actual released vector copy number rather than the specific infectivity of the particles is declining. In addition, the decrease in vector copy number highly correlates with LDLR expression level (figure 4.3C) suggesting an interference of the LDLR protein with vector production. The question whether the receptor protein or its mRNA is responsible for the observed effect is addressed in subsequent experiments.

As observed by another group (Sanburn and Cornetta, 1999), the vector titers determined via RT-qPCR reflect the biological titer obtained from transducing unit determination via flow cytometry. This means that each released vector particle can be considered infectious under the experimental conditions in this work, regardless of LDLR expression.

4.4 Partitioning of vector RNA in supernatant, cell surface and interior

The actual decrease in released vector copy number raises the question of what happens to the other vector copies as long as they are not found in the supernatant and RNA transcription proceeds unaffected in presence of LDLR. There are several possibilities ranging from 1) a putative negative transcriptional feedback that LDLR over-expression exerts on the formation of viral RNA molecules, which is highly speculative and has never been described up to the author's knowledge (Figure 4.4A), to 2) equal transcription of viral RNA that is differently distributed between the

intracellular space, the cell surface and the supernatant due to interference of LDLR over-expression with one or more steps in the viral assembly sequence. As there is obviously no or a negligible extent of virus-associated LDLR interacting with virus-associated VSVG at the vector particle surface, this particular interaction could take place at another location such as between nascent vector particles and the plasma membrane (Figure 4.4B). Under the assumption that the vector is properly assembling and budding in presence of LDLR, cell-surface localized LDLR might interact with virus-associated VSVG and/or vice versa. As a result, vector particles would accumulate at the cell surface rather than being released into the medium as a function of LDLR expression. In addition, the possibility of multivalent interactions might inhibit internalization. Alternatively, viral RNA could accumulate in the cytoplasm in case the assembly of virions fails in presence of LDLR. The intracellular copy numbers would show an inverse trend compared to the released vector RNA in that the more LDLR is expressed the more viral RNA would be found in the cytoplasm (Figure 4.4C).

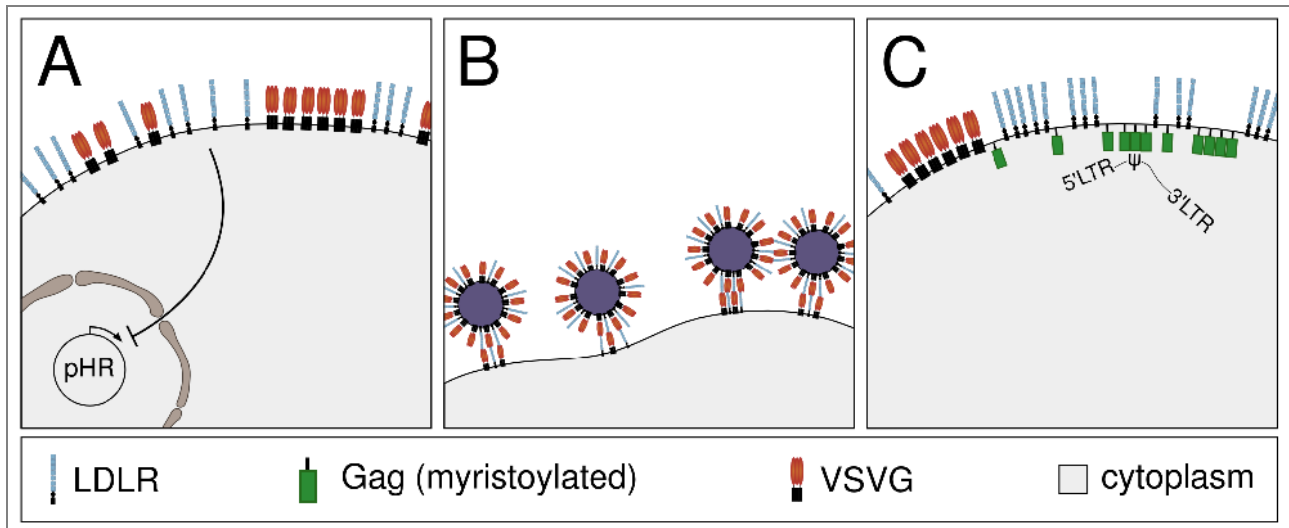


Figure 4.4. Hypothetical molecular events leading to different spatial distribution of viral RNA (5'LTR- ψ -3'LTR). **A)** LDLR expression at the cell surface represses transcription of viral RNA from pHR-CMV-EGFP by an unknown mechanism. **B)** Accumulation of nascent vector particles at the cell surface by multivalent LDLR-VSVG interactions between cell and virus, but also virus and virus. **C)** Failure of productive vector assembly and/or budding leading to accumulation of unpackaged viral RNA in the cell.

Therefore, the partitioning of viral RNA between supernatant (*S fraction*), the cell surface (*W fraction*) and from inside the cell (*C fraction*) in HEK293 cells was analyzed by RT-qPCR measuring the amount of HIV-1 packaging sequences (ψ) via ψ -specific primers. A different primer pair was used for this experiment as two different transcripts are present in the cell, each of them carrying EGFP coding sequences (viral RNA transcribed from 5'LTR and EGFP mRNA transcribed from CMV promoter of pHR-CMV-EGFP). Adhering to the usage of the primer pair EGFP_for/EGFP_rev would measure both RNA species and wrong conclusions might be drawn from the results. After harvesting *S*, cells were washed once under Ca^{2+} -depleting conditions with

10 ml PBS / 10mM EGTA which destroys the structural integrity of LDLR (Zhao and Michaely, 2009) by withdrawal of receptor-integrated Ca^{2+} ions and eventually releases cell-surface bound VSVG-decorated vector particles. Afterwards, the cells were collected in DMEM / 2% FCS and counted before total RNA isolation allowing a determination of copy number per cell rather than volume. The determination of vector RNA copy number inside the cell, at the cell-surface and the supernatant revealed a striking decrease in total vector RNA summed up from the three fractions (Figure 4.5A). This is totally unexpected, because the sum of vector RNA was anticipated equal among all LDLR co-transfections and the positive control. Therefore, vector RNA which was missing in the supernatant in the previous as well as in this experiment should have shown up in either the wash or the cell fraction. However, the results indicate that vector RNA neither accumulates at the cell surface nor in the cytoplasm in presence of LDLR over-expression.

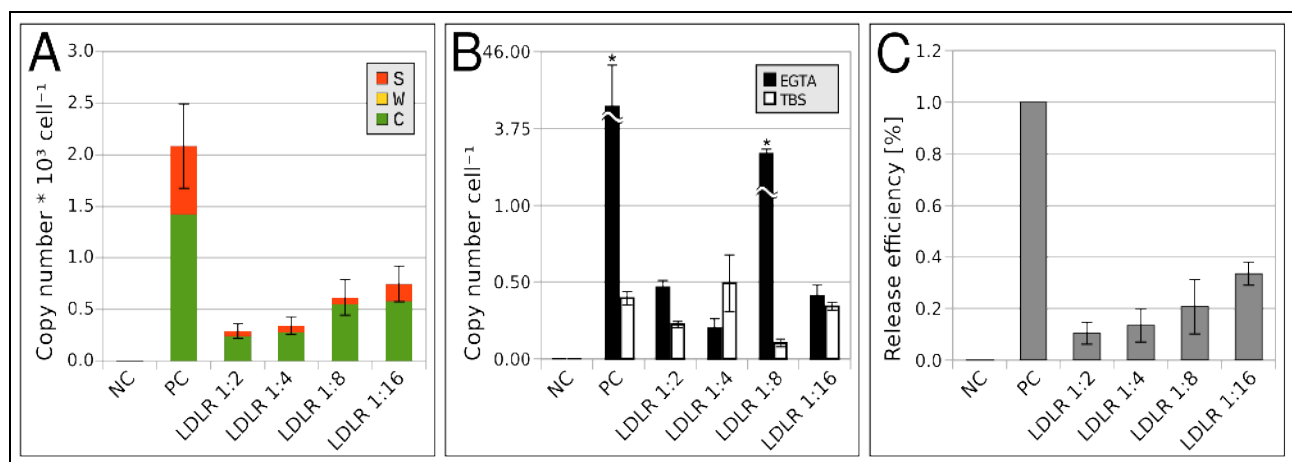


Figure 4.5. Distribution of viral RNA copy numbers in transfected HEK293 cells co-transfected with LDLR. **A)** Sum of vector RNA found inside the cell (green), the wash fraction (yellow) and the supernatant (orange). Data are arithmetic mean \pm SEM of three biological replicates. **B)** Vector RNA copy numbers per cell found in the wash fractions of cells washed in EGTA buffer (solid bars) or TBS (open bars). Data are arithmetic mean \pm 2SD from duplicate measurements. Asterisks denote outliers. **C)** Release efficiency of vector RNA represented by the ratio of released (S) to unreleased (C) ψ -containing RNA copy numbers normalised to the positive control. Data are from A..

The second striking finding is that the wash fraction is nearly devoid of vector particles. On average 0.81 ± 0.28 particles per cell for the LDLR co-transfections compared to 6.8 ± 4.1 particles per cell for the positive control were found in the wash fraction. The difference seems substantial, however, these numbers are vanishingly low compared to the copy numbers determined in the other fractions. This observation raises the justified question of whether the Ca^{2+} -depleting conditions were actually sufficient to detach vector particles from the cell surface.

Therefore, the feasibility of surface removal of vector particles was independently assayed by comparing the employed Ca^{2+} -depleting conditions with washing the cells in TBS, which is considered to behave inert to a putative LDLR-VSVG interaction or LDLR alone. Two additional batches of virus were produced under identical conditions. Cells of the first batch were gently

washed in PBS / 10mM EGTA, the cells of the second batch were washed in TBS. Following viral RNA extraction and RT-qPCR as before, the average copy numbers of 0.36 ± 0.14 particles per EGTA-washed cell and 0.31 ± 0.15 particles per TBS-washed cell were obtained (Figure 4.5B). The EGTA-washing is obviously harsher than washing with TBS, as PC and LDLR 1:8 were considered to contain ψ -containing RNA leaked out from inside the cells due to rupture of syncytia and were excluded from statistical calculations for this reason. The insignificant difference ($p > 0.7$, one-way ANOVA) of the average detachable vector particles in presence or absence of LDLR could either indicate that 1) the conformation of LDLR is insensitive to EGTA, which would contradict previous findings of Zhao and Michaely (2009), 2) there is no binding of VSVG-decorated particles to LDLR at the cell surface, or 3) there actually is hardly any vector particle adsorbed at all at the cell surface specifically or unspecifically.

Coincidentally, the release efficiency of vector RNA was found to decrease significantly with increasing LDLR expression by calculating a ratio of released (S) to unreleased RNA (C), that is viral RNA packaged into released virions or viral RNA retained in the cytoplasm, respectively (Figure 4.5C). Although the sum of vector RNA decreases, also the proportion of released vector particles with respect to the total amount of vector RNA found is declining. This suggests that two superimposing effects, an overall reduced level of viral RNA production and/or stability and a putative budding/release defect in particular, underlie the observed decrease in released vector particles.

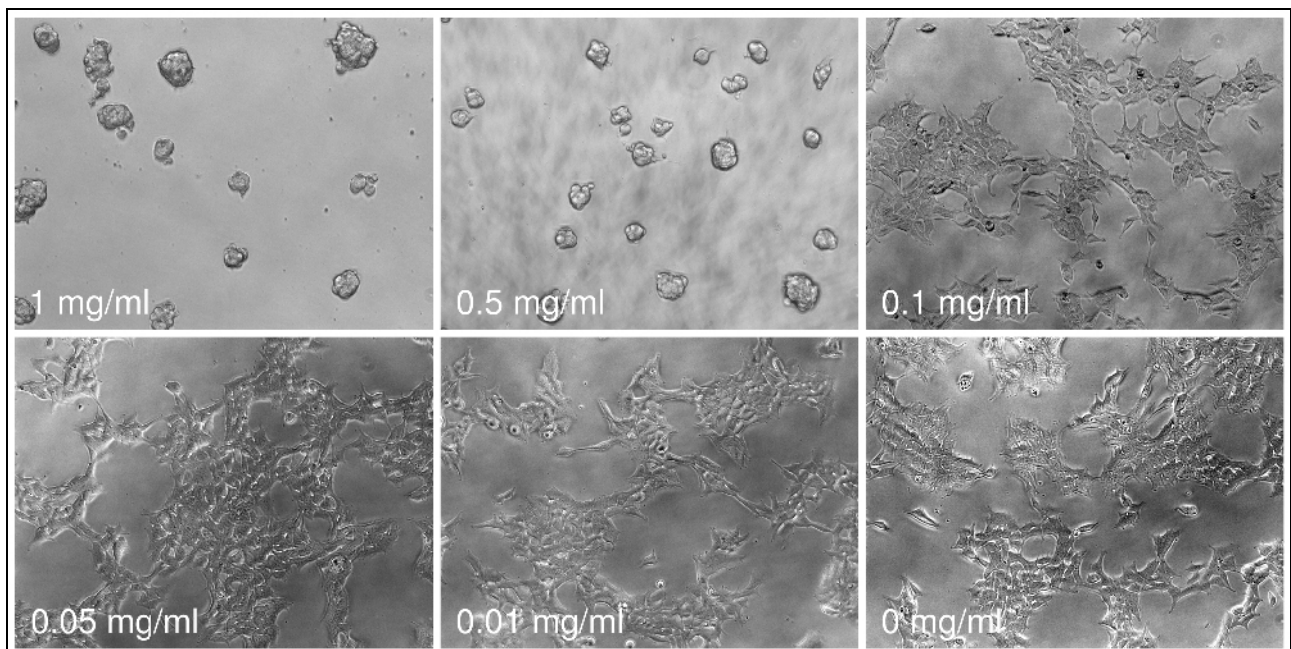


Figure 4.6. Suramin cytotoxicity assay. HEK293 cells were incubated in growth medium containing the indicated concentrations of suramin.

In parallel, the efficacy of suramin (a kind gift from Marcela Hermann), an inhibitor of the LDLR-LDL interaction *in vitro* (Schneider et al., 1982) and *in vivo* (Martins et al., 2000), was tested for

washing off vector particles from the cell surface. This was unsuccessful, because washing the cells in PBS supplemented with 1 mg/ml suramin induced a cytopathic effect within seconds. Therefore, the maximum tolerable concentration was determined in a cytotoxicity assay. HEK293 cells were incubated in growth medium containing suramin at concentrations between 0 mg/ml and 1 mg/ml (Figure 4.6). Cell morphology remained normal up to a concentration of 0.1 mg/ml, but showed a strong cytopathic effect at 0.5 mg/ml and higher. Obviously, HEK293 cells do not tolerate suramin doses, which were used in live-cell assays elsewhere (Martins et al., 2000). For example, Martins and colleagues (2000) used a minimum suramin concentration of 0.5 mg/ml to abolish interaction of LDL and chylomicron remnants with LDLR on mouse skin fibroblasts. These findings led the author to the conclusion that suramin is not compatible with washing off vector particles from HEK293 cells, because it could not be assured that the cells stayed intact during the experimental procedure and that leaked out intracellular viral RNA was measured in the wash fraction, due to the cytopathic effect.

4.5 Vector particles are not subject to degradation

The reduced release efficiency of vector particles as well as the absence of particles accumulating at the cell surface led to the hypothesis that nascent viral particles are rapidly internalized facilitated by ligand-mediated internalisation of LDLR and targeted for lysosomal degradation instead of being released into the supernatant. Under the assumption that viral RNA transcription is not influenced by LDLR, the apparent reduction in viral RNA production might be caused by nucleolytic decay of viral RNA from internalized vector particles in the lysosome (Figure 4.7, 1a). Alternatively, an internalized vector particle might fuse with the membrane of an endosomal compartment and release its capsid and ribonucleoprotein particle (RNP) into the cytoplasm (Figure 4.7, 1b). This would mimic the infection route of wildtype VSV (Panda, 2011). The release of the HIV-RNP (Figure 4.7, 2) would explain the reduction in vector RNA as shown above (Figure 4.5), because after shedding the virion's contents into the cytosol, the HIV-RNP contained in the produced vector particles would start reverse transcription, which destroys the RNA template (Sarafianos et al., 2009). As a result, this could create the gradual decrease in total vector RNA copy number as a function of LDLR expression.

A spectrum of differently sized fragments of VSVG as a result of degradation was expected to result in smears on Western Blot of whole cell lysates from LDLR co-expressing cells, but neither in the positive nor negative control. Fragments of Gag would most probably not appear in pathway 1b of figure 4.7, because the contents of the vector particle would be shed into the cytosol upon fusion with the endosomal membrane. Therefore, VSVG was chosen as analytical target.

The isolation of viral RNA fragments was considered to fail due to an expected very short half life

of the respective RNA molecules in the cell lysates. The activity of lysosomal nucleases might diminish at neutral pH of the lysis buffer, however, residual activity during the sample preparations could not be excluded. For this reason, detecting RNA fragments was dismissed in favour of searching for VSVG protein fragments. Their C-terminal epitope is considered to have a sufficiently long half-life allowing the successful isolation and detection of the fragments.

The employed lysis buffer B contained inhibitors for all classes of proteases including lysosomal cathepsins such as the cysteine proteases cathepsin B, H and L (Barrett and Kirschke, 1981) as well as the aspartate protease cathepsin D (Dean, 1979) which have various mechanisms of action (Koga et al., 1991, Bohley and Seglen, 1992), to efficiently stop any enzymatic activity at the moment of breaking up the cells. Complete inhibition of proteases and quick sample handling was pursued, since the half-life of proteins processed by lysosomal proteolysis is 8 minutes (Bohley and Seglen, 1992). Therefore, each lysate preparation took less than 10 minutes from breaking up the cells to freezing the cleared lysates at -80°C ready-to-use for analysis.

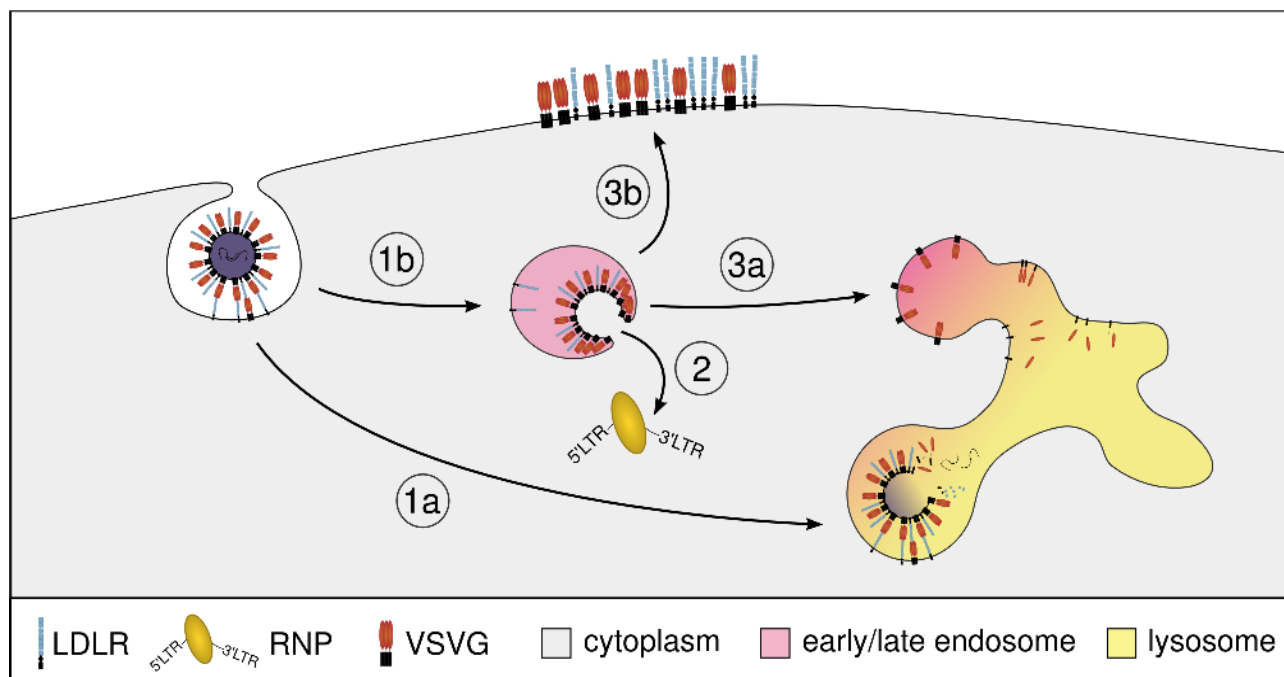


Figure 4.7. Schematic representation of the hypothesis of vector particle internalisation and lysosomal degradation in presence of overexpressed LDLR. 1a) Following internalisation, a vector particle is directly targeted for degradation in the lysosome. 1b) Alternatively, an internalised vector particle might fuse with the endosomal membrane after acidification, 2) release its ribonucleoprotein particle (RNP) and 3a) its remaining components might become subjected to degradation in the lysosome. Contrary, endosome-associated VSVG might 3b) recycled to the plasme membrane alongside LDLR.

The viral protein VSVG was successfully detected at the expected height via enhanced chemiluminescence (ECL) on Western Blot (58kD, Figure 4.8). However, no smears were found which would be indicative of proteolytic degradation of VSVG. The presence of a more than three-fold excess (Barrett and Dingle, 1972) of pepstatin as well as the proprietary cysteine protease

inhibitors is considered to have reliably inhibited proteolysis during sample preparation, so loss of epitopes on the protein fragments, and therefore a failure in detecting them, can be excluded. For this reason, the absence of VSVG degradation is considered assured disproving the hypothesis of vector particle internalization and subsequent lysosomal degradation.

The result agrees with the absence of LDLR degradation in figure 4.3B. However, one could argue that endosome-associated VSVG is actively recycled alongside LDLR to the plasma membrane preventing lysosomal degradation (Figure 4.7, 3b). That could be an alternative explanation for the absence of VSVG and LDLR degradation fragments. Differences in lysate preparation were controlled by detecting γ -Tubulin as loading control in a replicate gel run in parallel (Figure 4.8, lower panel).

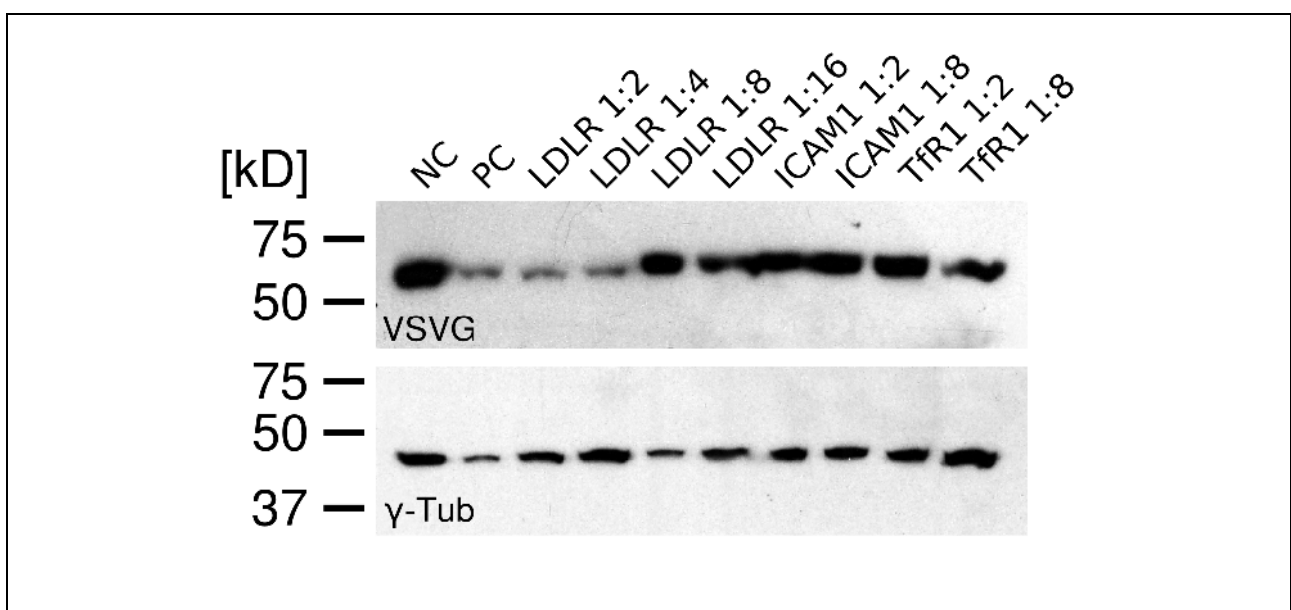


Figure 4.8. Western Blot analysis of VSVG degradation and expression in HEK293 whole cell lysates. A total of 10 μ g protein was loaded per lane of an 8% SDS-Tris/Glycine polyacrylamide gel. The upper panel shows VSVG detected with (rabbit) ThermoScientific #PA1-30128 (1:5000 in 1% BSA in PBST) and (goat) Jackson #111-035-003 α -rabbit::HRP (1:10000). The lower panel shows γ -tubulin detected with (mouse) Sigma #T5326 (1:5000 in 1% BSA in PBST) and (goat) Jackson #115-035-062 α -mouse::HRP (1:10000) as loading control.

4.6 Up- and downregulation of endogenous LDLR in HEK293 cells

In order to evaluate whether up- or downregulating endogenous LDLR can be used to replace the over-expression of recombinant LDLR or serve as control, respectively, cells were grown under sterol-depleting conditions such as replacement of FCS in the growth medium by fatty acid free BSA or delipidated FCS to upregulate endogenous LDLR (eLDLR). Addition of pitavastatin (10 μ M corresponding to 4 μ g/ml) to the growth medium in addition to the sterol-reduced culture conditions was chosen to maximally increase eLDLR expression. Pitavastatin was found to be most effective at upregulating eLDLR in HepG2 cells (Morikawa et al., 2000). Supplementing the growth medium with 12 μ g/ml cholesterol and 2 μ g/ml 25-OH-cholesterol was expected to downregulate eLDLR as

done earlier (Hofer et al., 1994).

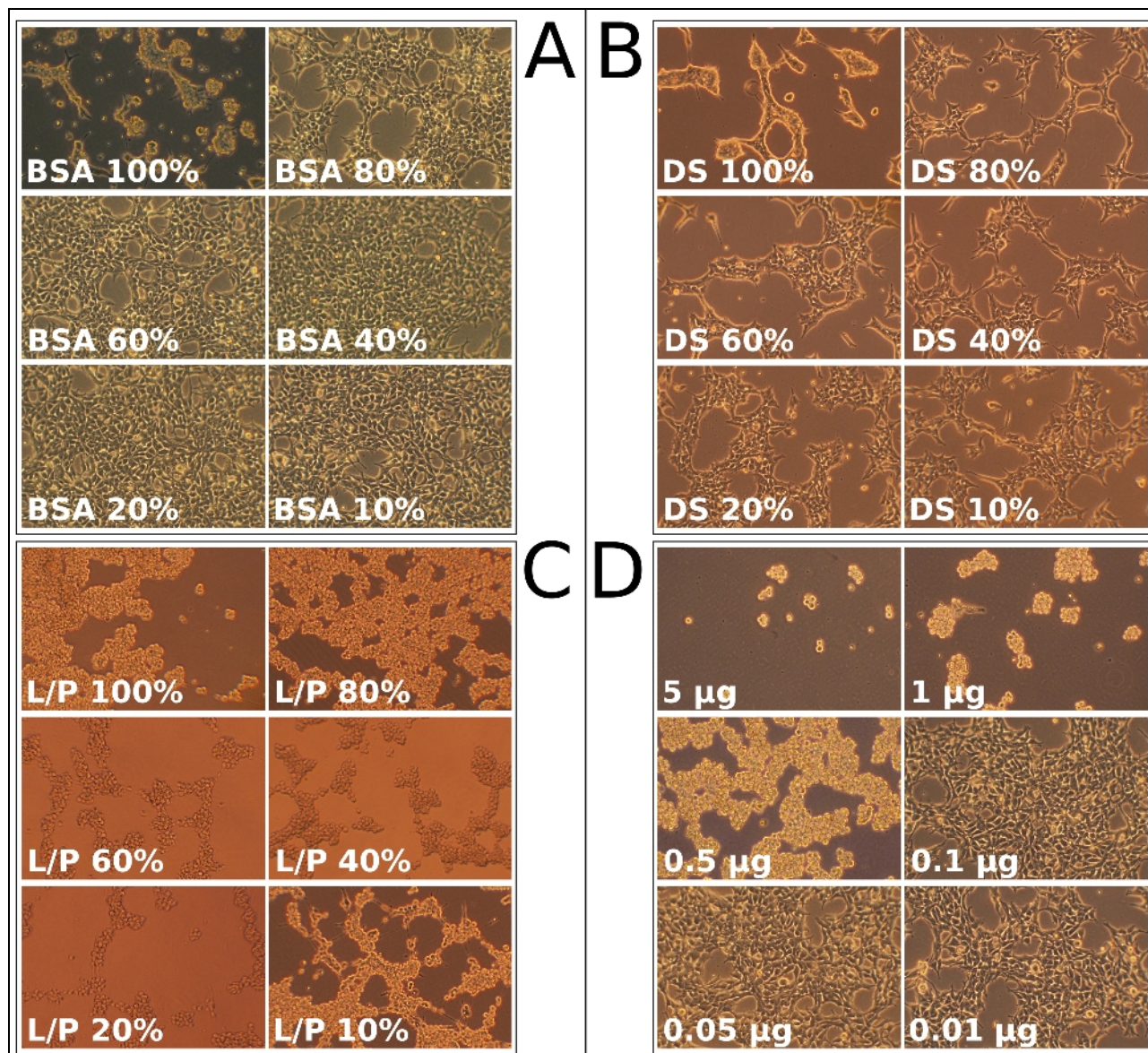


Figure 4.9. Differential interference contrast micrographs of HEK293 cultured in different media. **A)** DMEM / 1% (w/v) fatty acid free BSA. **B)** Delipidated serum (DS). **C)** Delipidated serum supplemented with 4 µg/ml endconcentration pitavastatin (L/P). **D)** FCS supplemented with the indicated amounts of pitavastatin. Indicated percentages inform about the proportion of normal growth medium content of the medium, eg. 'BSA 80%' refers to 80% DMEM / 1% (w/v) fatty acid free BSA plus 20% normal growth medium and so forth. All micrographs were taken at 10x magnification.

Unexpectedly, all of three attempts of up-regulating eLDLR induced cytopathic effects in HEK293 cells already after 24 h. Therefore, several media compositions were tested in terms of DMEM with fatty acid free BSA (1%) or delipidated FCS (10%) mixed with normal growth medium at different proportions to check, which level of sterol/lipid depletion is tolerated by HEK293 cells. Accordingly, different concentrations of pitavastatin in normal growth medium were tested ranging from 0.01 µg/ml (0.025 µM) to 5 µg/ml (12.5 µM).

Culturing HEK293 cells in DMEM / 1% (w/v) fatty acid free BSA leads to detachment from the culture dish and clumping after 24 h (Figure 4.9A). Mixing the BSA medium with 20% (v/v)

normal growth medium or higher rescues the cells' adherence to the dish (BSA 80% to BSA 10%). Delipidated serum (LPDS) has a similar effect, cells detach from the dish and associate with each other to form cell rolls (Figure 4.9B). The phenotype is again rescued by 20% (v/v) or more normal growth medium contained in the culture medium. Nevertheless, confluency of the monolayer was not achieved after 24 h indicating a growth retardation effect elicited by LPDS. Similarly, cell detachment occurs in delipidated serum supplemented with 4 µg/ml pitavastatin (L/P) after 24 h (Figure 4.9C). Mixing L/P medium with 20%, 40%, 60%, 80% or even 90% normal growth

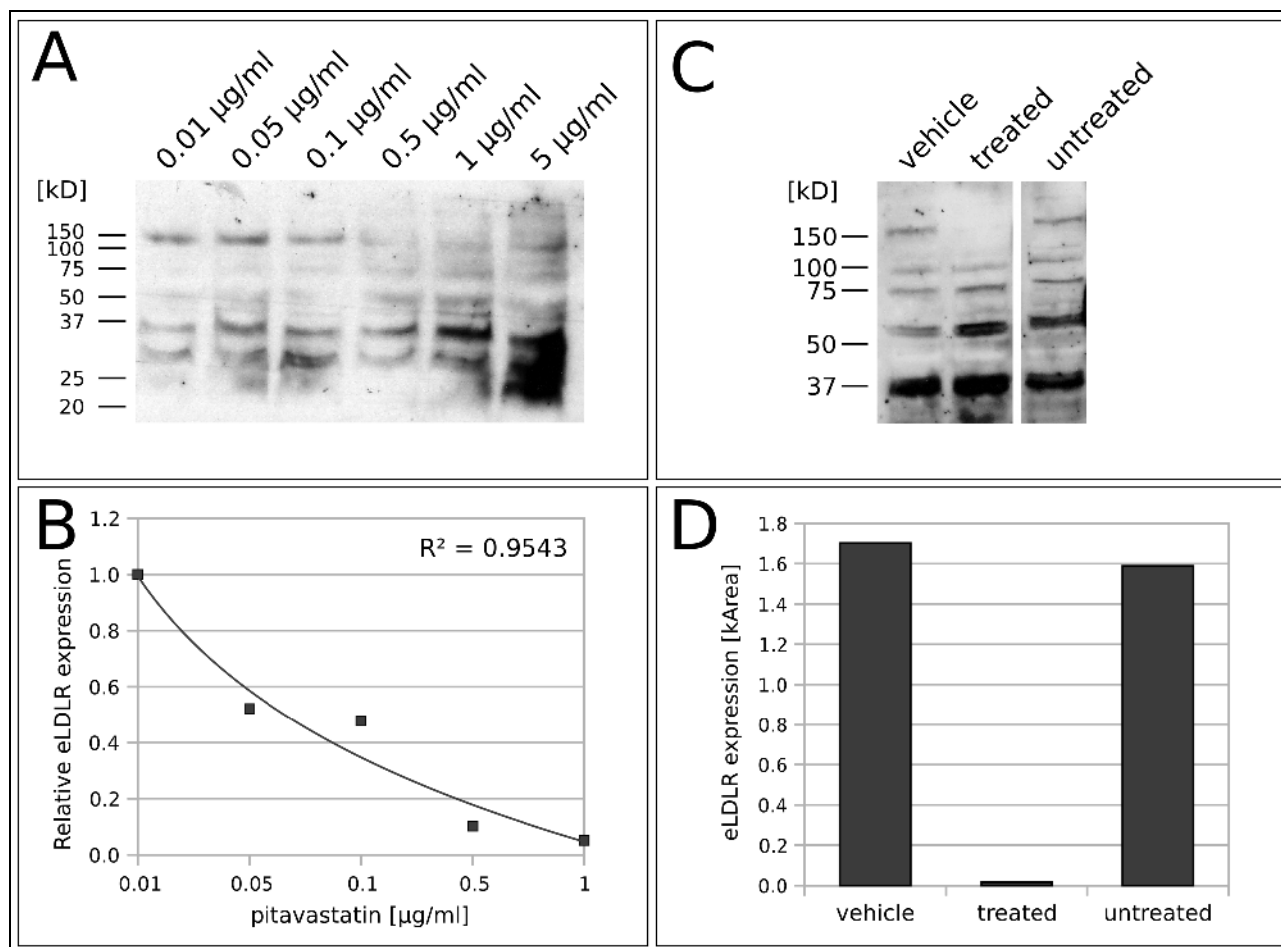


Figure 4.10. Regulation of eLDLR via pitavastatin and cholesterol/25-OH-cholesterol. **A)** Western blot analysis of untransfected HEK293 whole cell lysates prepared from pitavastatin treated cells shown in figure 4.9 via OGP lysis. LDLR was detected via chicken α -292 antiserum (1:250 in PBST) and goat α -chicken::HRP (1:10000). Note the decreasing density of the band at 150kD. **B)** Dose-response curve showing an inverse logarithmic correlation of eLDLR expression level and pitavastatin concentration. Data is derived from A), normalized to the band at 37kD. **C)** Western blot analysis of untransfected HEK293 whole cell lysates prepared from ethanol-treated control (vehicle), cholesterol (12µg/ml) / 25-OH-cholesterol (2µg/ml) treated or untreated cells. LDLR was detected via chicken α -292 antiserum (1:250 in PBST) and goat α -chicken::HRP (1:10000). Note the absence of the band at 150kD in the treated cells. **D)** Quantification of the eLDLR expression level in vehicle control, treated and untreated control lanes from C. eLDLR levels in vehicle and untreated controls are indistinguishable in comparison to the expression level of the treated cells.

medium is not able to rescue the phenotype. However, the cell rolls forming in presence of LPDS alone were not observed, all cells kept an individual spherical morphology, although they

aggregated in floating clumps. The IC₅₀ of pitavastatin in wildtype HEK293 was reported to be 4µg/ml, corresponding to about 10µM (Zhang et al., 2013). However, this concentration effectively killed the cells after 24 h (Figure 4.9D). Concentrations starting from 0.1µg/ml and below did not lead to cytopathic effects. Nevertheless, cells cultured in DMEM/FCS (10%) and different pitavastatin concentrations shown in figure 4.9D were harvested and analyzed for eLDLR expression regardless of cell viability to check whether any pitavastatin-mediated upregulation yields an expression level comparable to the ectopically expressed LDLR. Cells were lysed in OGP-lysis buffer as described and eLDLR was detected via a chicken polyclonal antiserum (α-292, lot #6) raised against the aminoterminal 292 residues of human LDLR in-house.

Surprisingly, pitavastatin reduces the expression of eLDLR in a negative non-linear dose-response in HEK293. The higher the pitavastatin concentration, the less eLDLR was detected (Figure 4.10A), which is considered to be the band at around 150kD that was normalized to the unspecific band at 37kD. The eLDLR expression level is highly correlated with the introduced amounts of pitavastatin (Figure 4.10B). Statins mediate upregulation of SREBP-responsive genes such as eLDLR and PCSK9 in liver cells (Horton et al., 2003; Maxwell et al., 2003) and other cell types (Pocathikorn et al., 2010). The protease PCSK9 is degrading LDLR (Maxwell and Breslow, 2004). The results are difficult to interpret due to the observed cytotoxicity, however, pitavastatin might increase PCSK9 expression more efficiently than that of eLDLR in HEK293. As a result, the eLDLR level decreases in response to higher pitavastatin concentrations due to degradation via PCSK9.

Endogenous LDLR was successfully downregulated by adding 12µg/ml cholesterol and 2µg/ml 25-OH-cholesterol. Western Blot analysis of whole cell lysates revealed that the eLDLR expression level dropped nearly below the detection limit (Figure 4.10C, *treated*). Although again a lot of background signals show up, the missing band at around 150kD is obvious. Lane 1 (ethanol control) shows that ethanol, the solvent for cholesterol and 25-OH-cholesterol, does not influence eLDLR expression compared to the untreated control.

4.7 Comparison of endogenous and ectopically expressed LDLR

To check whether the expression levels of the DDK tagged LDLR construct provided *in trans* during virus production in HEK293 cells and eLDLR differ and how much, OGP whole cell lysates of HEK293 cells transfected with 1.6 µg RC200006 or untransfected were produced. Western blot analysis using the same chicken α-292 antiserum as above revealed a striking difference of LDLR and eLDLR in transfected and untransfected cells, respectively (Figure 4.11). The dense dark spot spanning 100kD to 150kD on the left lane (transfected) demonstrates that the difference between ectopically expressed LDLR construct and eLDLR expression level (right lane, narrow band at 150kD) is tremendous. The fold-change LDLR expression level from untransfected to

transfected is estimated to be about 100 or more as the blot could not reliably be quantified. Therefore, one can deduce that the endogenous receptor does not or very little interfere with vector production, because vector production in cells triple-transfected with pHR-CMV-EGFP, psPAX2 and pMD2.G yields expected titers. Moreover, the observed titer lowering effects arise by the non-physiologic over-expression of LDLR.

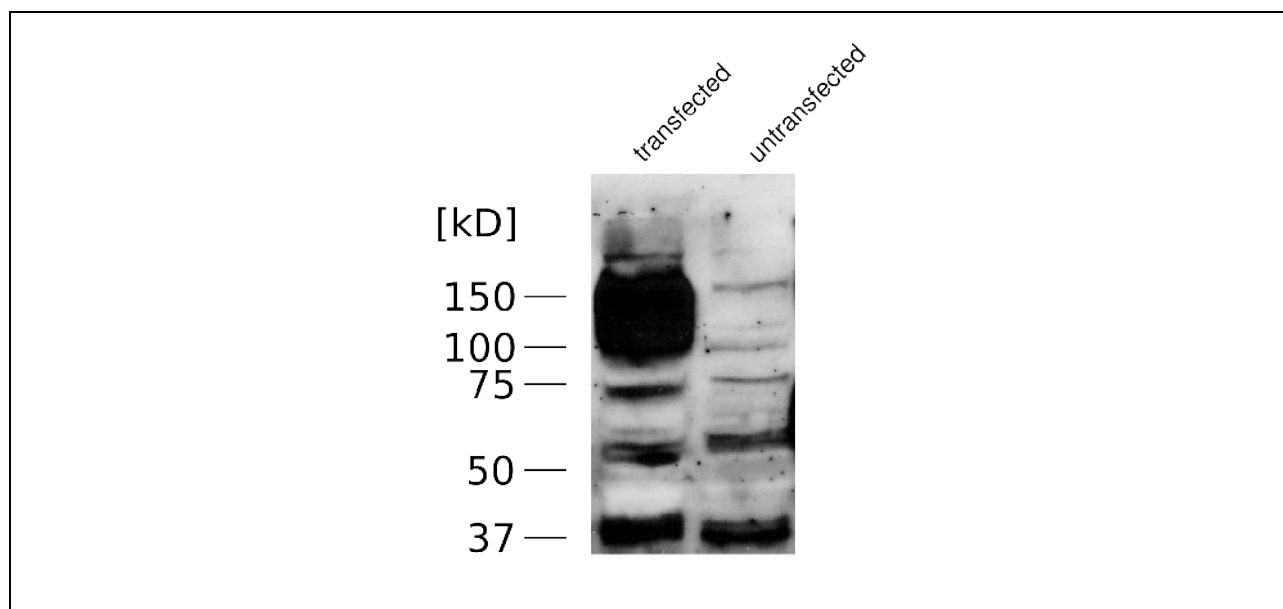


Figure 4.11. Western blot analysis of transfected (left lane) or untransfected (right lane) HEK293 whole cell lysates. LDLR (ectopically expressed from transfected RC200006 as well as eLDLR) was detected via chicken α -292 antiserum (1:250 in PBST) and goat α -chicken::HRP (1:10000).

4.8 LDLR deletion constructs

The generation of an LDLR nonsense mutant carrying a premature stop codon instead of the sixth codon (W6STOP) was performed to show that the observed reduction in released vector particles can actually be attributed to functional LDLR protein rather than its mRNA or DNA sequences. In addition, deletion of functional domains from the LDLR expression vector RC200006 were prepared to gain a more detailed insight into which protein domain interferes with vector production. The constructs either lacked the signal peptide (Δ SP), the ligand binding domain (Δ LBD) or the internalization signal (Δ NPVY) to interfere with subcellular localization, binding to VSVG, or internalisation of LDLR, respectively.

The sixth codon (TGG) coding for tryptophan (W) in the W6STOP mutant was successfully changed to a stop codon (TGA). As a result translation will prematurely stop prior to synthesis of any functional domain of LDLR. The Δ SP mutant lacks 69 nucleotides from nucleotide 4 to 72 of the *LDLR* coding sequence. The Δ LBD mutant lacks 867 nucleotides from nucleotide 73 to 939 of the *LDLR* coding sequence. One codon of the EGF-like precursor domain had to be included in the deleted stretch to match annealing temperatures of the primers. Finally, 12 nucleotides from

nucleotide 2473 to 2484 of the *LDLR* coding sequence were excised in the Δ NPVY mutant.

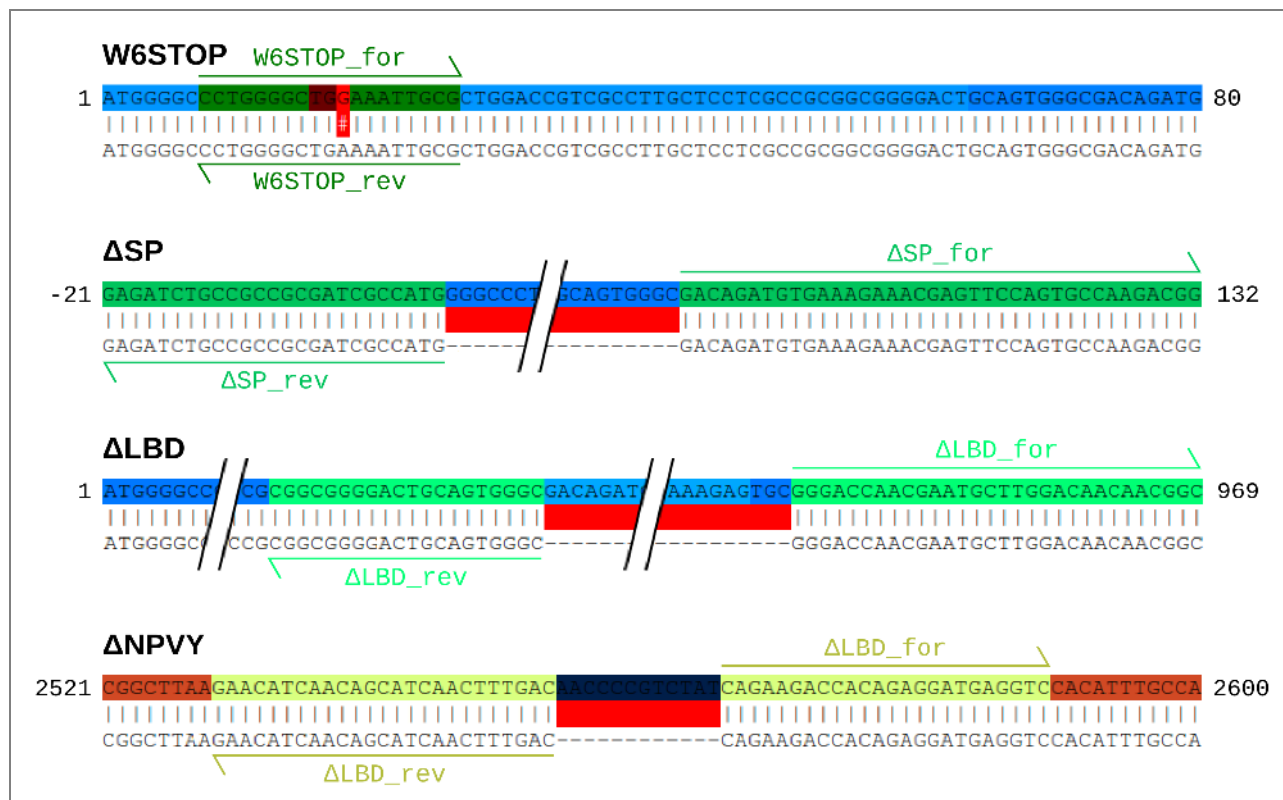


Figure 4.12. Alignments of the sequencing results for selected clones (lower strands) to the template sequence (upper strands). The point mutation or deleted sequences are highlighted in red. Sequence interruptions by double bars denote blanked out sequence ranges. For each clone, the positions and 5'-3' directions of the mutagenic primers are indicated by arrows.

After the verification of clones via sequencing (Figure 4.12), the expression and the molecular weights of the mutant proteins were analyzed by transfecting HEK293 cells and Western Blot analysis of whole cell lysates to show that the mutated LDLR-derived proteins are still expressed after deleting the corresponding coding sequences.

The run distance of *LDLR*- Δ SP, *LDLR*- Δ LBD and *LDLR*- Δ NPVY proteins was compared to the apparent molecular weight of the DDK-tagged wildtype LDLR as positive control. The wildtype LDLR control lane shows a triple band at 100-150kD most probably representing different stages of glycosylation (Cummings et al., 1983).

The *LDLR*- Δ SP protein lacks 23 aminoacids (~2.5kD) and runs faster due to the reduced molecular weight (Figure 4.13), however, the size difference of around 50kD can not be due to the few missing aminoacids alone. The protein is engineered to stay cytosolic caused by the mutation, therefore, the deletion together with absence of glycosylation reduces the molecular weight to around 90kD, compared to 95kD molecular weight of the lowest band in the wildtype control, which represents presumably the unglycosylated form. Moreover, the single band instead the three-band pattern supports the expectation of absent glycosylation.

The *LDLR*- Δ LBD mutant lacking 289 aminoacids (~30kD) runs below 100kD and matches well

with the expectation. The three-band pattern is found again, although stretched. The three bands are again indicative for different (non-)glycosylated forms of LDLR, which are all shifted down by around 30kD.

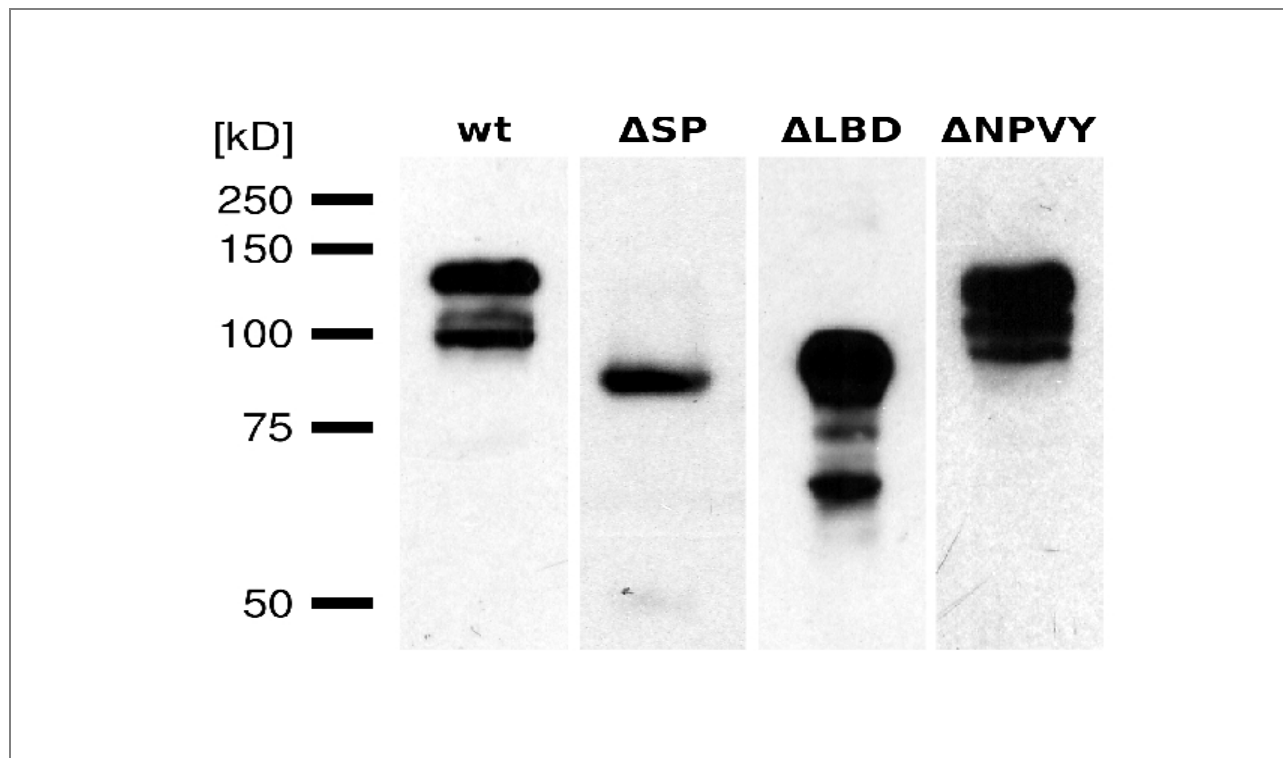


Figure 4.13. Western blot analysis of mutant recombinant LDLR proteins. The three-band pattern of wildtype (wt), *LDLR*- Δ LBD (Δ LBD) and *LDLR*- Δ NPVY (Δ NPVY) is considered to represent differently glycosylated forms. Note the absence of this pattern in *LDLR*- Δ SP (Δ SP), which stays cytosolic. DDK-tag was detected with (mouse) α -DDK (Origene #TA50011) 1:1000 in 1%BSA/PBST and (goat) α -mouse (Jackson #115-035-062) 1:10000. All bands are from the same blot, but have different exposure times. Scanned films were automatically white-corrected using GIMP software.

There is no difference in run distance of the *LDLR*- Δ NPVY protein compared to the wildtype, because the deletion spans only 4 aminoacids. Nevertheless, the three-band pattern indicates successful processing in the Golgi. The W6STOP mutant cannot be detected on Western Blot, because the C-terminal DDK-tag is missing from the resulting nonsense fragment.

4.9 Syncytia formation correlates with released vector yield

Finkelshtein and colleagues (2013) reported that the ligand binding domain of LDLR is at least part of the binding interface with VSVG, so the proteins expressed from the generated deletion constructs change this interaction in different ways. Consequently, their influence on released vector yield might vanish indicating the functional domain of wildtype LDLR that is responsible for a decrease in vector yield.

A deleted the signal peptide (Δ SP) prevents any incidence that an LDLR molecule comes into spatial contact with a VSVG molecule at all, because the translation of *LDLR*- Δ SP no longer happens at the rough endoplasmatic reticulum (ER) compared to VSVG and other integral

membrane proteins. As a result, translated *LDLR-ΔSP* stays cytosolic and vector production should occur unaffected.

Secondly, a missing ligand binding domain from LDLR (*LDLR-ΔLBD*) makes a specific interaction of *LDLR-ΔLBD* with VSVG impossible (Finkelshtein et al., 2013), although both proteins take the same route during synthesis and intracellular transport. The resulting vector titer is expected to be similar to the positive control, however, a slight decrease might occur, because the coexpression of LDLR could decrease the efficiency of VSVG expression by crowding the secretory pathway before reaching the plasma membrane.

Finally, the excised internalisation signal (*LDLR-ΔNPVY*) prevents recycling of LDLR from the plasma membrane (Chen et al., 1990). As a consequence, the receptor would accumulate at the cell surface where multivalent VSVG-LDLR interactions might sequester VSVG preventing productive progression of viral assembly or budding by changing the physical membrane properties such as increasing rigidity. As a result, partially or fully assembled viral capsids are retained cytoplasmatically, because budding becomes energetically unfavourable. In this case, the question remains of what reduces the total ψ -containing RNA copy number, as observed in the fractionation experiments. In any case, the non-internalizable LDLR mutant will show unequivocally whether LDLR internalisation is decisive for the decrease in released vector copy number.

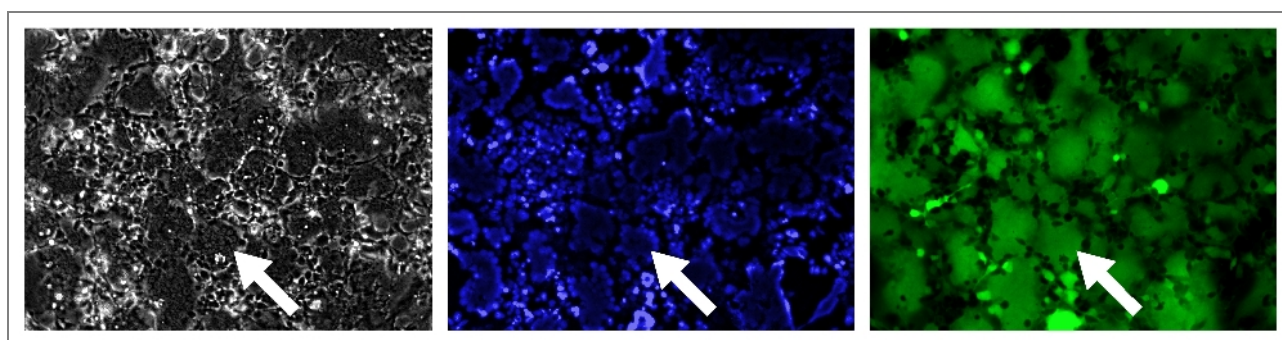


Figure 4.14. Live-cell fluorescence microscopy of syncytia in virus-producing HEK293 cells 24 hpt. The same field of view was imaged in differential interference contrast (DIC) channel (left), in DAPI channel (middle) and GFP channel (right). The arrows point to the same exemplary syncytium in the different imaging channels. Syncytic foci (arrow) appear darker as unfused cells in DIC and contain herded nuclei which have a shared cytoplasm.

Live-cell imaging of virus-producing HEK293 cells revealed differences in syncytia formation in response to co-expression of the mutant receptor proteins. Syncytia are multinucleated cell-like structures resulting from cell-cell fusion during expression of viral fusion proteins in virus packaging cells or virus-infected cells *in vivo*. This has been observed for viral glycoproteins such as Jaagsiekte sheep retrovirus (JSRV) envelope (Env) or influenza A hemagglutinin (HA) (Kun et al., 2013), also cell surface expression of VSVG in particular has been reported to readily fuse cells (Sun et al., 2008). Syncytia formation is characterized by appearance of foci in the cell monolayer consisting of ganged up nuclei surrounded by a shared cytoplasm and plasma membrane (Figure

4.14) already 24 hpt. Eventually, the foci extend into the third dimension. A syncytium is defined here as five or more nuclei sharing one cytoplasm, because two-, three- or four-nucleated syncytia could originate from a single cell that has undergone one or two cell divisions.

Vector production yields EGFP expression from pHR-CMV-EGFP as a byproduct in the packaging cells. Therefore, cytoplasmic EGFP can diffuse in the cytoplasm shared by the horde of nuclei upon cell-cell fusion, also if only one of the fusion partners was EGFP-positive. However, EGFP stays confined to single cells, if cells do not fuse as a result of absence of cell-surface localized VSVG (Sun et al., 2008).

Syncytia formation was observed to be indiscernible in the positive control (PC) from the ICAM1 and TFRC co-transfection controls and spans nearly the whole culture dish (Figure 4.15). The negative control (NC) does not express EGFP, but syncytia were observed in the DIC channel as well identical to the left image in figure 4.14. This shows that syncytia formation is independent from virus production or release.

The co-transfection of wildtype *LDLR* completely prevents syncytia formation at high *LDLR* ratios (*LDLR* 1:2, *LDLR* 1:4), but syncytia occur again with decreasing the *LDLR* ratio (*LDLR* 1:8, *LDLR* 1:16). However, syncytia formation is normal upon co-transfecting *LDLR*-ΔSP at any ratio (ΔSP 1:2 – ΔSP 1:16). Obviously, cytosolic LDLR protein does not interfere with VSVG surface expression, because the extracellular parts of LDLR and VSVG never get a chance to interact. Syncytia formation of HEK293 cells co-transfected with mutant *LDLR* devoid of its ligand-binding domain (*LDLR*-ΔLBD) is similar at all ratios, although lower as compared to *LDLR*-ΔSP or the control cells. This indicates that the expression of the mutant protein might occupy the maturation pathway for integral membrane proteins up to a certain degree and therefore impair the surface localization of VSVG unspecifically (ΔLBD 1:2 – ΔLBD 1:16), which is also reflected by a reduction of released transducing units (Figure 4.16).

Unexpectedly, the presence of *LDLR* lacking the internalisation signal (*LDLR*-ΔNPVY) yields an identical syncytia pattern as the wildtype control, meaning absence syncytia at high ratios (ΔNPVY 1:2, ΔNPVY 1:4), but syncytia at lower ratios (ΔNPVY 1:8, ΔNPVY 1:16). Concomitantly, the resulting vector titer increases with decreasing *LDLR*-ΔNPVY ratio (Figure 4.16). This proves that internalisation of LDLR does not play a role in decreasing the titer.

As expected, co-transfection of the *LDLR*-W6STOP mutant does not change the extent of syncytia formation. The translation of the receptor coding sequence is engineered to stop prematurely preventing the expression of a functional protein. This shows clearly that the LDLR protein is interfering with vector production. In addition, the results show that the protein exerts the effect via its ligand binding domain, which correlates with the findings from Finkelshtein and colleagues (2013). Moreover, cytosolic LDLR (*LDLR*-ΔSP) obviously does not interfere with vector

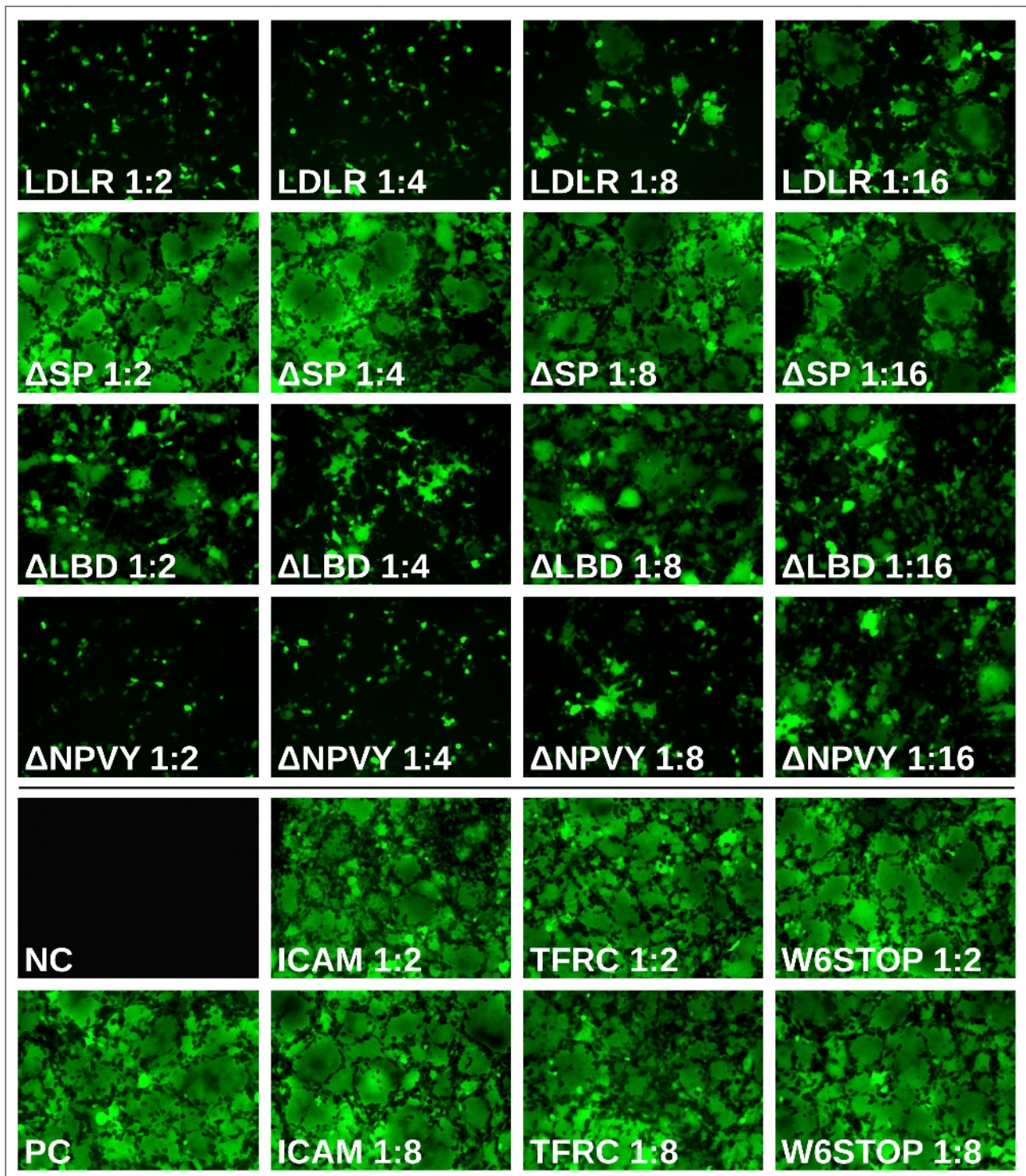


Figure 4.15. Live-cell fluorescence micrographs of HEK293 syncytia during virus production. As expected, fluorescence is absent in negative control (NC). Syncytia formation is identical in the positive control (PC), the ICAM1- and TFRC controls and cells co-transfected with *LDLR-W6STOP*. Syncytia are absent in presence of full-length LDLR at high ratios (LDLR 1:2, LDLR 1:4) and markedly reduced at lower ratios (LDLR 1:8, LDLR 1:16). The co-transfection ratio has no influence on the syncytia pattern in case of LDLR- Δ SP and LDLR- Δ LBD. In presence of LDLR- Δ NPVY, syncytia are again absent at high ratios (Δ NPVY 1:2, Δ NPVY1:4), and appear when reducing the amount of LDLR- Δ NPVY, similar to full-length LDLR.

production or release, although it contains a functional LBD, which suggests that LDLR is

interacting with VSVG at or on the way to the plasma membrane.

In parallel, transducing units (TU) were determined in the conditioned cell culture supernatants via flow cytometry (Figure 4.16). Again, positive control (PC) as well as the ICAM1- and TFRC controls yield titers in the range of 10⁵ TU/ml. As expected, co-transfection of W6STOP, LDLR- Δ SP or LDLR- Δ LBD does not influence vector production, because the titers match the positive control. Interestingly, there is a strong decrease of TU as a function of co-transfecting LDLR- Δ NPVY resulting in a titer decrease of up to 100-fold. This clearly shows that vector production is not influenced by NPxY-mediated internalization of LDLR, however, alternative mechanisms might facilitate internalization of LDLR.

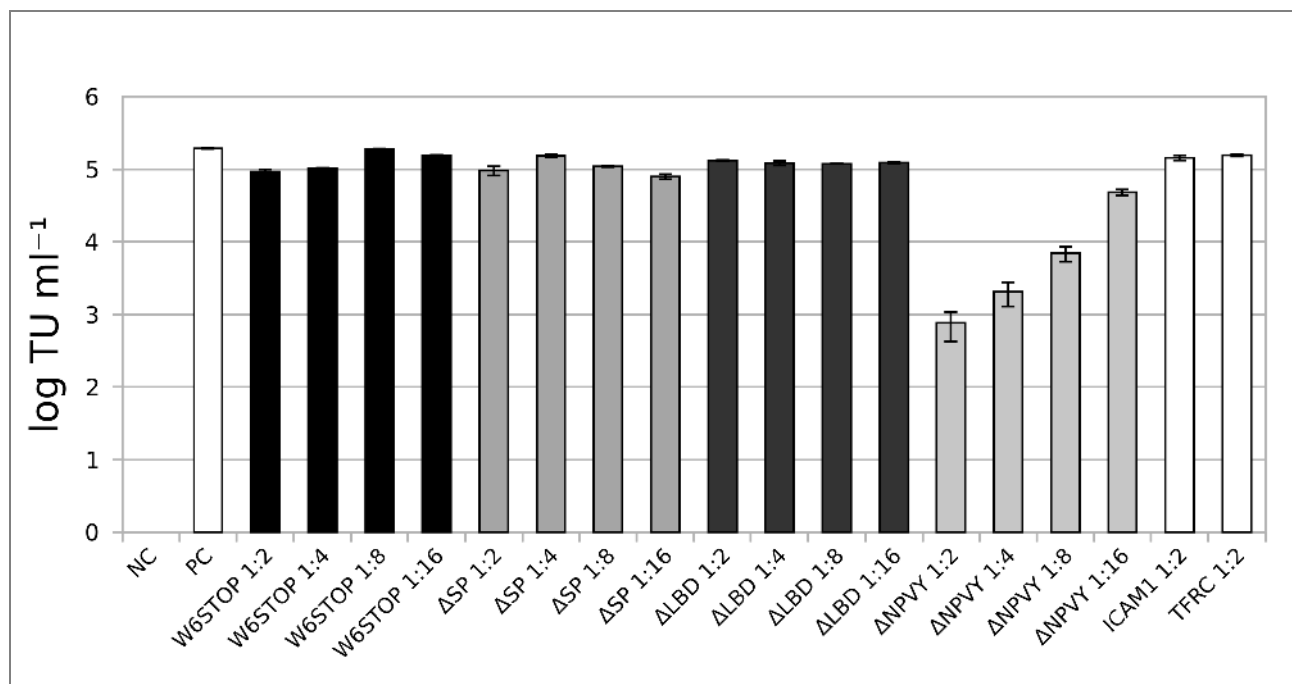


Figure 4.16. Transducing units (TU/ml) of released vector determined via flow cytometry from the supernatants of the corresponding cells imaged for syncytia. Note the strong decrease in vector titer in Δ NPVY as a function of co-transfected LDLR- Δ NPVY, which is not reflected by LDLR- Δ SP, LDLR- Δ LBD or W6STOP that have titers in the range of the positive control and the ICAM1 and TFRC controls. Data are arithmetic mean \pm 2SD from triplicate measurements.

4.10 VSVG mRNA levels are not a function of LDLR expression

Reduced syncytia formation is a result of reduced cell surface expression of VSVG (Sun et al., 2008). LDLR expression could interfere with VSVG expression on different levels including transcription of VSVG mRNA or translation of the protein. The VSVG protein expression level is independent from LDLR expression as shown above. To check whether LDLR expression is impacting VSVG mRNA transcription, an RT-qPCR assay was developed employing the VSVG_for/ VSVG_rev primer pair to measure VSVG mRNA levels in total RNA using a serial dilution of pMD2.G as standard.

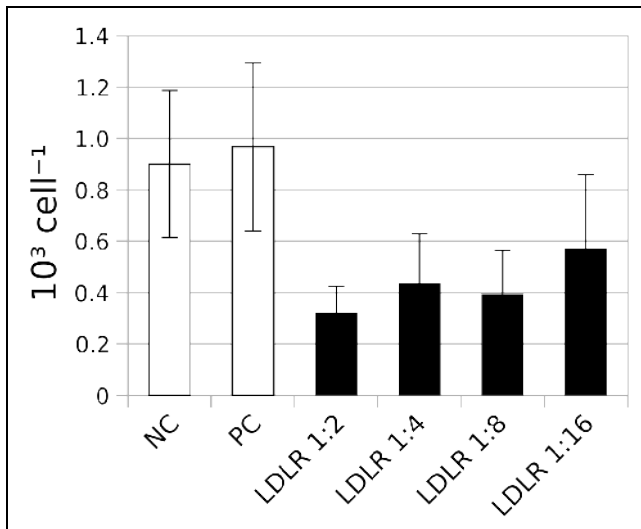


Figure 4.17. VSVG mRNA levels in total RNA isolated from transfected HEK293 after virus production. Data are arithmetic mean \pm SEM of 3 independent experiments.

As expected, the copy number of VSVG mRNA in the negative control (NC) and the positive control (PC) are similar (Figure 4.17), because pMD2.G is the only expression plasmid which is CMV-driven in both experiments. The VSVG mRNA levels in presence of LDLR decreases to around 50% compared to the positive control, because the *LDLR* expression plasmid is also CMV-driven, so the reduction is considered to be caused by a transcription factor sequestration effect. The reduction is not a function of LDLR expression ($p > 0.1$, one-way ANOVA). This

result shows that VSVG expression is unaffected at transcriptional level in addition to the translational dimension, and that the reduced surface expression is likely to be caused by altered intracellular transport of VSVG induced by LDLR expression.

4.11 VSVG and LDLR localize to a perinuclear compartment

The non-internalizable LDLR mutant (*LDLR-ΔNPVY*) revealed that released vector titer decrease occurs independently of LDLR-mediated internalization of nascent vector particles. However, internalisation of nascent vector particles might still occur via one or more alternative pathways (Martins et al., 2000; Sorrentino et al., 2013). To definitely exclude that internalization of nascent vector particles is taking place in full-length *LDLR* co-transfected cells, colocalization of VSVG and early endosome antigen (EEA1) was analyzed via indirect immunofluorescence. In parallel, the distribution of VSVG inside the cell might provide clues about altered localization of VSVG.

The immunofluorescence analysis required the omission of the vector construct pHR-CMV-EGFP from the transfection mixes, otherwise the EGFP expression would have created a fluorescence background that devours the EEA1 signals. It has been shown that HIV1 Gag expression alone leads to assembly of viral cores even in the absence of packaging signal (ψ) containing RNA (Doan et al., 2004). Therefore, the presence of viral RNA is not considered essential for drawing valid conclusions from the results, because the observed effects will be independent from RNA packaging.

The micrographs show HEK293 cells immunofluorescently labelled 48 hpt (Figure 4.19). The cell membranes of syncytic bodies in the control (cells transfected with envelope and packaging construct) as well as the *ICAM1* and *TFRC* co-transfection experiments contain small red speckles,

which corresponds to VSVG microdomains at the cell surface that form autonomously (Brown and Lyles, 2003). The extensive syncytia formation distributes VSVG protein and mRNA to almost every cell, so that only very few cells stay devoid of VSVG. The distribution of early endosomes marked via EEA1 is centralized in syncytia, for example in *TFRC*, but does never correlate with the localization of VSVG. In contrast, the disperse VSVG staining is absent in cells co-transfected with full-length *LDLR*, and shows dense perinuclear signals instead. Again, EEA1 signals do not correlate with the VSVG pattern, therefore internalisation of nascent vector particles is definitely excluded. The absence of colocalization of EEA1 and VSVG together with the dense intracellular VSVG signals indicates that VSVG accumulates in a perinuclear compartment rather than quantitatively reaching the plasma membrane. Some VSVG molecules reach it anyway, but their number is obviously too small to elicit cell-cell fusion, which is the reason why the VSVG staining is confined to few cells only.

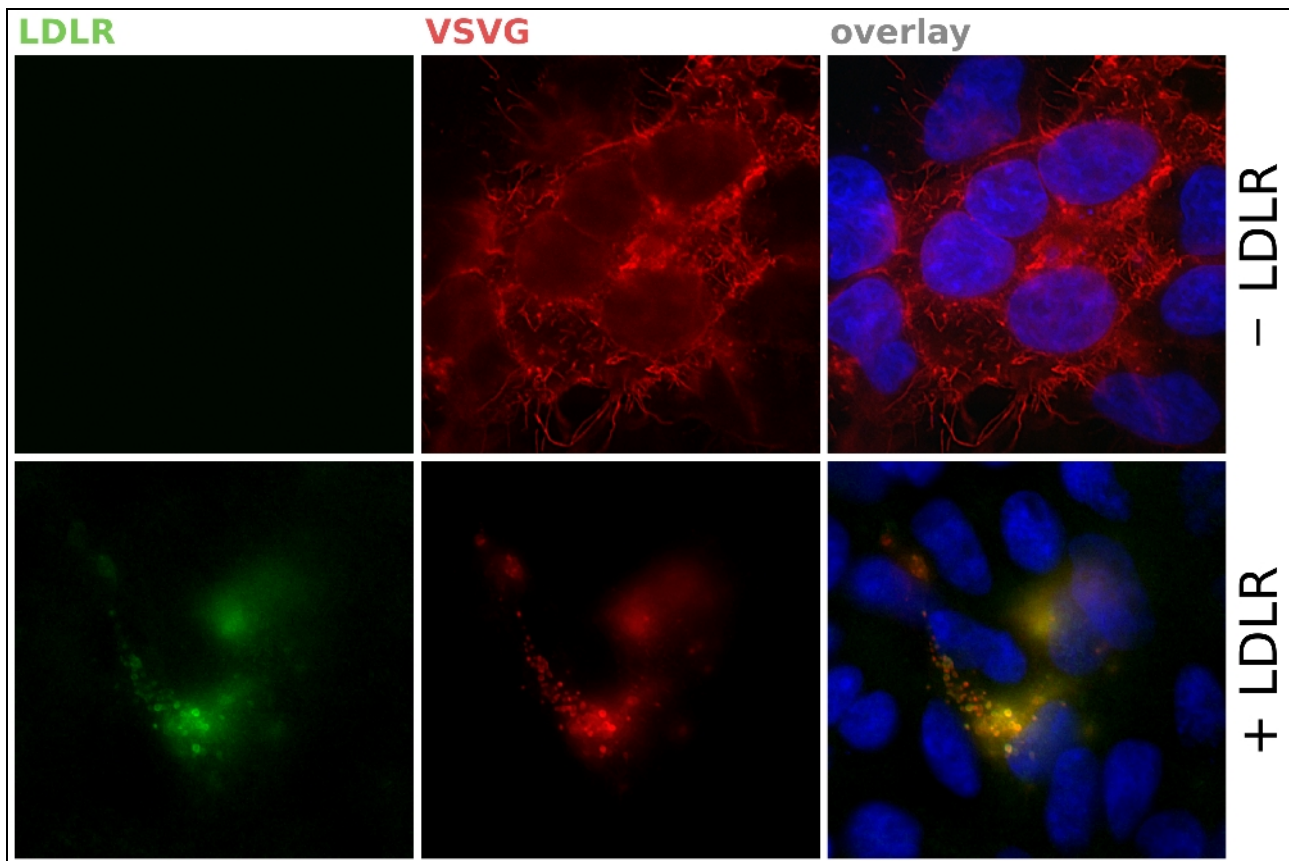


Figure 4.18. Indirect immunofluorescence of VSVG and LDLR in transfected HEK293 cells. Cells were transfected with envelope and packaging constructs only (–LDLR), or additionally co-transfected with LDLR expression plasmid (+LDLR). VSVG is shown in red, LDLR in green and nuclei are blue. Images were taken using a Zeiss 100x Plan-Apo 1.40 DIC oil objective on a Zeiss Axioplan 2 epifluorescence microscope. Images were deconvolved using the deconvolution filter of the G'MIC GIMP plugin package (version 1.5.4).

In parallel, colocalization of VSVG and LDLR was assayed via indirect immunofluorescence double-staining for VSVG and ectopically expressed LDLR via its DDK-tag (Figure 4.18). The absence of LDLR enables syncytia formation as before (–LDLR), because VSVG can reach the

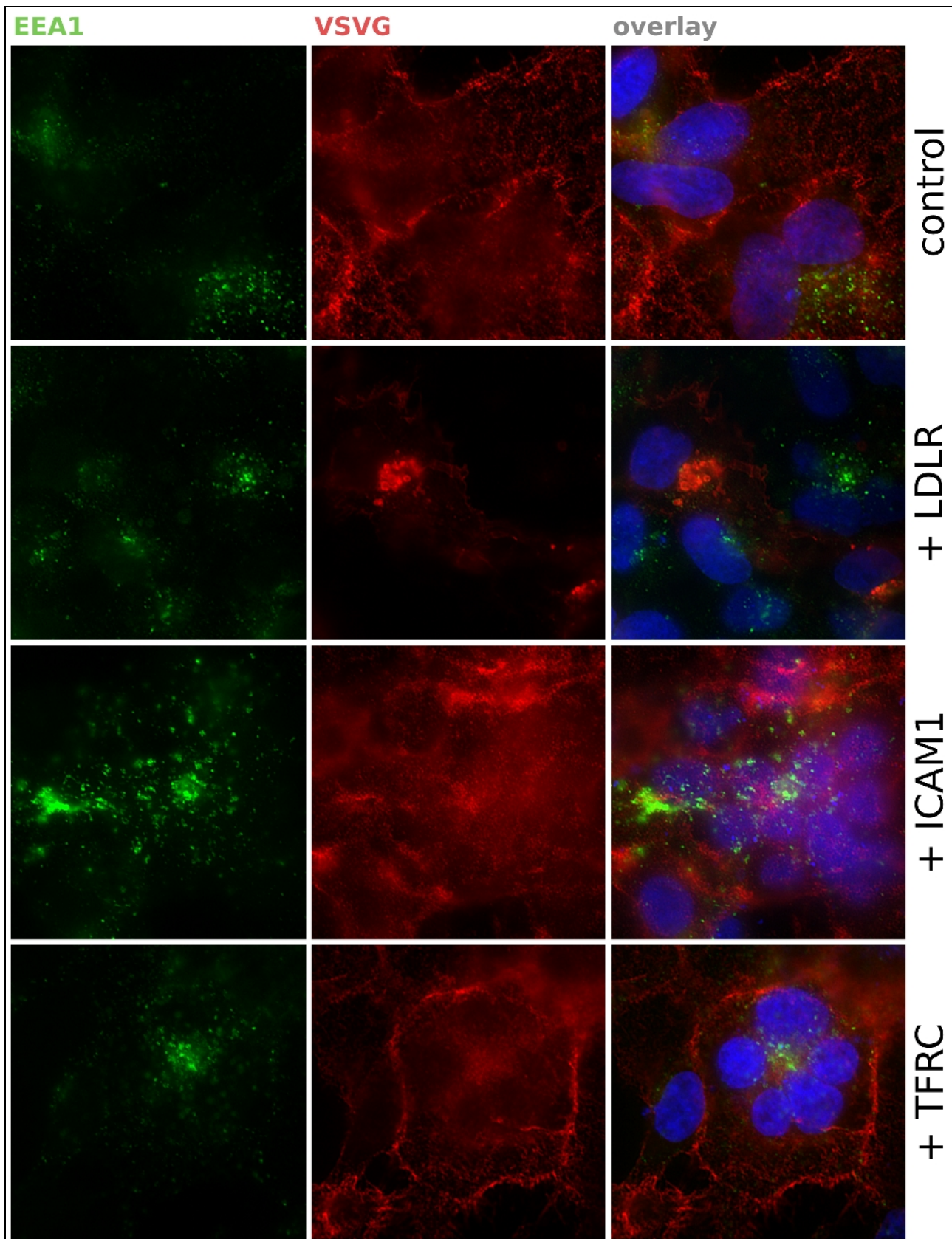


Figure 4.19. Indirect immunofluorescence of VSVG and EEA1 in transfected HEK293 cells. Cells were transfected with envelope and packaging constructs only (control), or additionally co-transfected with the indicated expression plasmid. VSVG is shown in red, EEA1 in green and nuclei are blue. Images were taken using a Zeiss 100x Plan-Apo 1.40 DIC oil objective on a Zeiss Axioplan 2 epifluorescence microscope. Images were deconvolved using the deconvolution filter of the G'MIC GIMP plugin package (version 1.5.4).

plasma membrane. The thread-like structures result from filopodia that lost contact to the coverslip during sample preparation. The co-expression of LDLR (+LDLR) prevents syncytia formation and leads to the formation of spherical compartments where VSVG and LDLR are present and colocalize which is a strong indication of their interaction.

As a consequence, the question arises of what are these perinuclear compartments? During and following translation at the rough ER and trimerization in the ER (Doms et al., 1988), VSVG might form complexes or aggregates with LDLR that accumulate in the ER lumen forming Russell bodies (Kopito and Sitia, 2000). Similar results were obtained by simultaneously expressing HIV1 Env and its host-cell receptor CD4 fused with an ER retention signal, which led to complex formation of Env and mutant CD4 in the ER as well as reduced surface expression of Env (Raja et al., 1993). In contrast, an interaction between LDLR and VSVG could also take place in the Golgi, where both are glycosylated which could be a prerequisite for interaction (Yoshimura et al., 1987).

4.12 LDLR prevents VSVG progression to the Golgi

The absence of internalisation of nascent vector particles provides no explanation for the decrease in vector RNA yield transcribed from pHR-CMV-EGFP as determined by RT-qPCR. A reduced surface expression of VSVG would explain a decrease in TU released into the supernatant, because the available amount of VSVG could be not enough for enveloping infectious vector particles. However, the intracellular copy number of vector RNA also decreases substantially, so a negative transcriptional feedback or direct inhibition of vector RNA transcription conferred by LDLR is assumed to act at some point during vector production.

A mechanism which could be triggered by LDLR-VSVG complexes in the secretory pathway is the ER-based unfolded protein response (UPR) which tries to balance ER homeostasis via different strategies including transcriptional feedback regulation, rerouting of misfolded proteins to degradation or enhancing chaperone activity in dilated ER cisternae (reviewed in Chakrabarti et al., 2011). Expression of viral proteins issues a challenge to the ER, because of the high amounts of protein synthesized (Zhang and Wang, 2012). ER stress induced by VSVG in particular was reported (Machamer et al., 1990). However, under the assumption that a putative LDLR-VSVG interaction depends on proper glycosylation, a similar mechanism could be elicited in the Golgi. The dilation of Golgi cisternae by LDLR-VSVG aggregates could be a signal to stop or pause transcriptional processes, which would explain the decrease in viral RNA yield measured above.

To test this hypothesis, cells were double stained for VSVG and the *cis*-Golgi marker GM130 (Figure 4.20). VSVG colocalizes with GM130 in absence of LDLR, which means that VSVG can progress through the secretory pathway to the cell surface without problems. However, in presence of LDLR the surface expression of VSVG is absent and VSVG localizes to spherical structures

instead that are spatially unrelated with GM130. Taken together, the spherical structures are not Golgi intracisternal accumulations of VSVG, and the expression of LDLR prevents VSVG from reaching the Golgi beforehand.

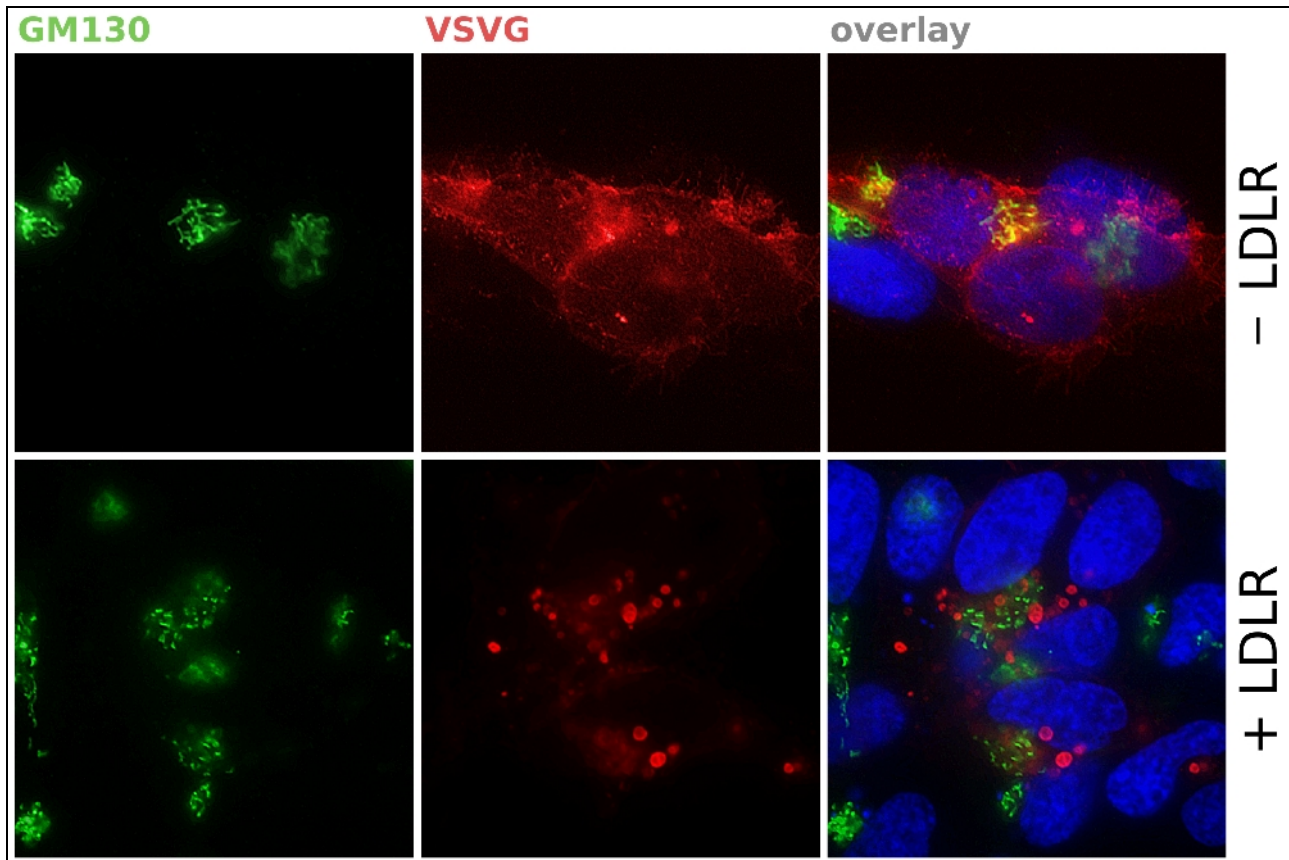


Figure 4.20. Indirect immunofluorescence of VSVG and GM130 in transfected HEK293 cells. Cells were transfected with envelope and packaging constructs only (–LDLR), or additionally co-transfected with LDLR expression plasmid (+LDLR). VSVG is shown in red, GM130 in green and nuclei are blue. Images were taken using a Zeiss 100x Plan-Apo 1.40 DIC oil objective on a Zeiss Axioplan 2 epifluorescence microscope. Images were deconvolved using the deconvolution filter of the G'MIC GIMP plugin package (version 1.5.4).

4.13 VSVG colocalizes with the ERGIC and lysosomal compartments

Following translation at the rough ER, newly synthesized proteins are transported along the secretory pathway. The ER-Golgi intermediate compartment (ERGIC) is the immediate organelle that secretory proteins encounter after the ER. The ERGIC is a sorting platform between the ER and the Golgi where on the anterograde transport of a given protein to the Golgi is decided. Low quality proteins such as misfolded or aggregated polypeptides are redirected back to the ER, subjected to chaperone-mediated refolding or disposal in the lysosome (reviewed in Appenzeller-Herzog and Hauri, 2006). As a result, the quality control mechanisms can lead to the formation of intraluminal land fill structures in the ER called Russel bodies or cytoplasmic accumulations termed aggresomes. Russell bodies colocalize with calnexin, but not with protein disulfide isomerase (PDI), whereas aggresomes localize to microtubule organisation centers (MTOC) and are surrounded by vimentin

cages (Kopito and Sitia, 2000). To identify the perinuclear VSVG-positive compartments, indirect immunofluorescence co-stainings were performed on HEK293 cells transfected with packaging and envelope constructs with or without LDLR expression plasmid. The vector construct was again omitted from the transfection mixes to avoid cytoplasmic EGFP background. Colocalisation was assayed by dual staining of VSVG together with either the ER markers calnexin and PDI (Kopito and Sitia, 2000), the ERGIC marker ERGIC53 (Appenzeller-Herzog and Hauri, 2006), the lysosome marker lysosome associated membrane protein 2 (LAMP2) (Carlsson and Fukuda, 1989).

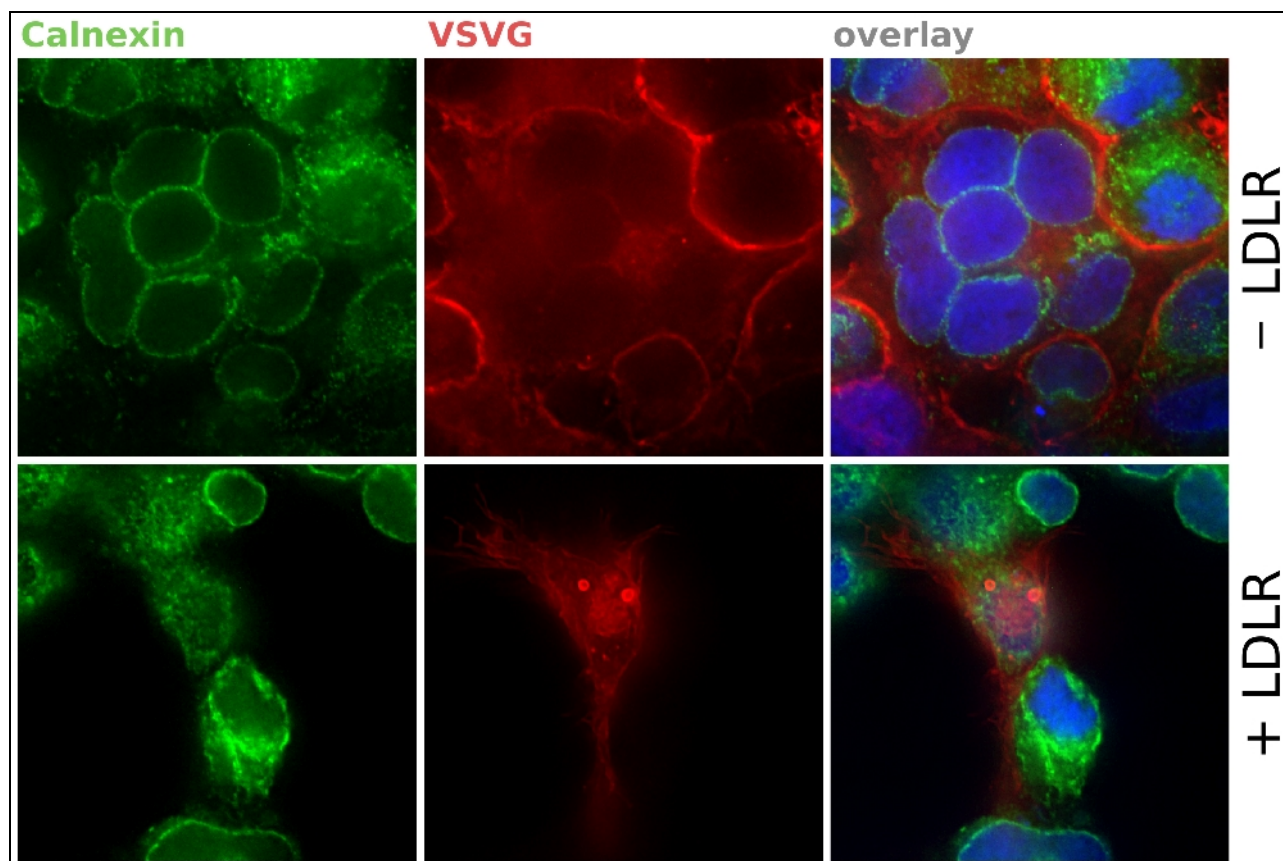


Figure 4.21. Indirect immunofluorescence of VSVG and calnexin in transfected HEK293 cells. Cells were transfected with envelope and packaging constructs only (–LDLR), or additionally co-transfected with LDLR expression plasmid (+LDLR). VSVG is shown in red, calnexin in green and nuclei are blue. Images were taken using a Zeiss 100x Plan-Apo 1.40 DIC oil objective on a Zeiss Axioplan 2 epifluorescence microscope. Images were deconvolved using the deconvolution filter of G'MIC GIMP plugin package (version 1.5.4).

VSVG was not found to colocalize with calnexin, so the spherical VSVG-positive structures forming in presence of LDLR are not Russell bodies (Figure 4.21). However, strong colocalisation of VSVG with ERGIC53 was detected in presence, but not in absence, of LDLR (Figure 4.22). That implies that the ERGIC is the location where VSVG and LDLR recognize each other and where the interference effect of LDLR onto vector production originates. The distribution of VSVG in presence of LDLR looks different than in figure 4.20, which is considered to represent an earlier stage of protein sorting where the VSVG-LDLR complexes start being transported away from the ERGIC.

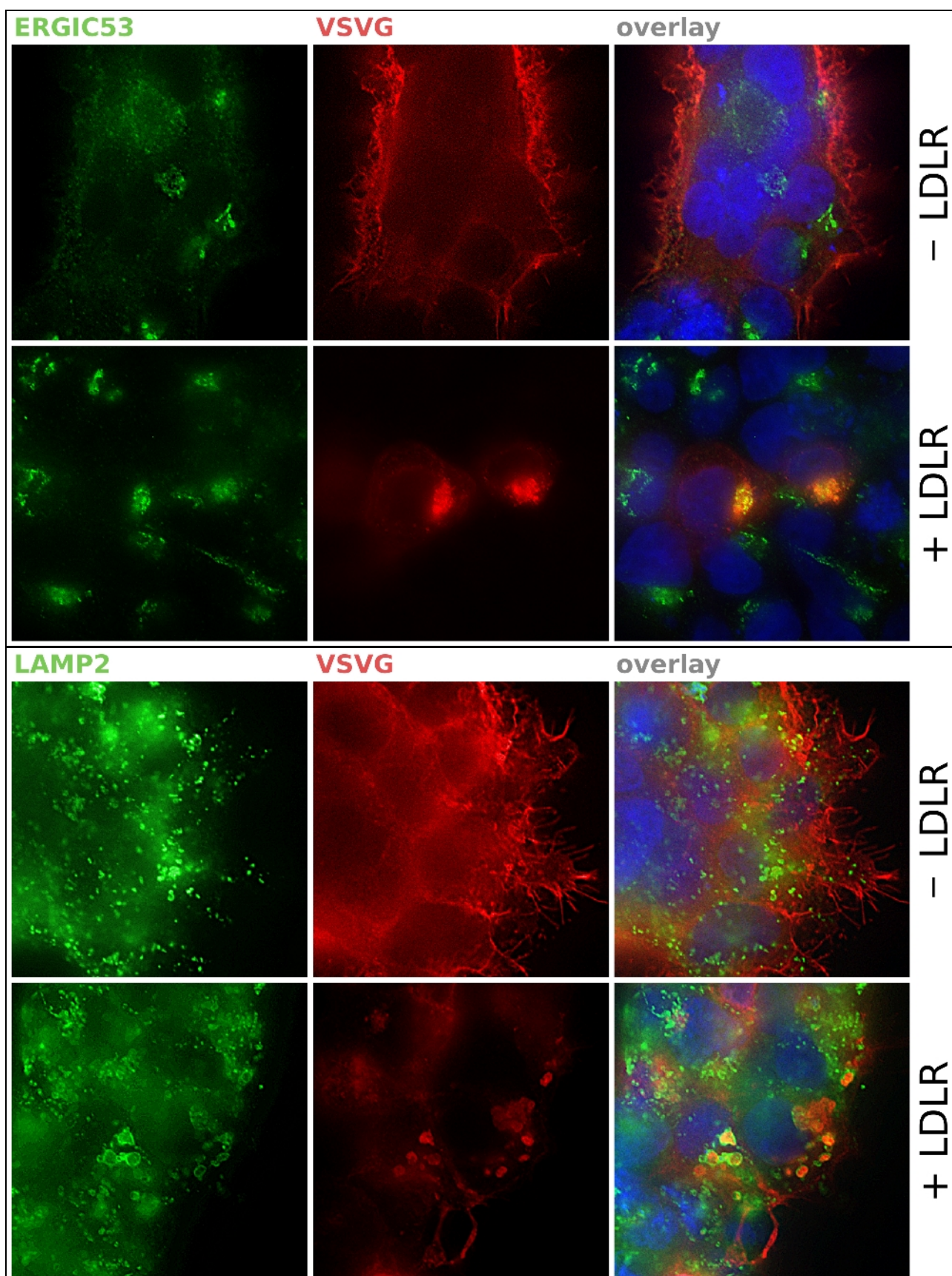


Figure 4.22. Indirect immunofluorescence of VSVG and ERGIC53 or LAMP2 in transfected HEK293 cells. Cells were transfected with envelope and packaging constructs only (-LDLR), or additionally co-transfected with LDLR expression plasmid (+LDLR). VSVG is shown in red, ERGIC53 or LAMP2 in green and nuclei are blue. Images were taken using a Zeiss 100x Plan-Apo 1.40 DIC oil objective on a Zeiss Axioplan 2 epifluorescence microscope. Images were deconvolved using the deconvolution filter of the G'MIC GIMP plugin package (version 1.5.4).

In parallel, VSVG was found enclosed by LAMP2-positive structures (Fehler: Referenz nicht gefunden) in presence of LDLR. After the quality checkpoint in the ERGIC, VSVG-LDLR complexes obviously fail to refold or dissociate, so the rerouting to lysosomal compartments is initiated. The events happening in that compartments remain to be characterized.

5 Discussion

The treatment of FH with gene therapeutic viral vectors holds alluring advantages in comparison to conventional therapies. The LDL-C lowering effect of the administration of functional LDLR alleles to hetero- or homozygotic FH patients in particular is permanent, requires only minimal invasive measures and avoids cutbacks in the quality of life of patients originating from regular appearance at health care centers.

The application of a lentiviral vector in pre-clinical trials in Watanabe heritable hyperlipidaemic (WHHL) rabbits having defective LDLR (Kankkonen et al., 2004) demonstrated the importance of proper vector design in terms of appropriate choices of the surface glycoprotein as well as the promoter for transduced genes in terms of cell targeting and transgene expression. The application of VSVG-pseudotyped vectors led to a low transduction rate of liver cells, because the VSVG pseudotype confers low serum resistance (DePolo et al., 2000). In addition, WHHL rabbits bear a deletion in the ligand-binding domain of LDLR, which is a host cell receptor for VSV (Finkelshtein et al., 2013), but the deletion could be distinct from the LDLR-VSVG binding interface. In spite of a low transduction rate the serum LDL-C was reduced by roughly 40%. However, only hepatocytes were tested for LDLR expression from a liver-specific (LSP) and CMV promoter. The latter is only active in non-hepatic cells which has to be considered in vector designs.

The production a VSVG-pseudotyped EIAV-based lentiviral vector encoding human LDLR under control of CMV promoter resulted in very low titer yield (Al-Allaf, unpublshed). In this work, genome mixing experiments showed a concentration-dependent effect of providing a *LDLR* expression construct *in trans* during packaging of a VSVG-pseudotyped HIV1-based lentiviral vector. Again, dramatic decreases in vector yield were observed which were specific to LDLR expression.

Mutational analysis revealed that the complete exclusion of LDLR from the secretory pathway or secreted LDLR missing the ligand-binding domain rescued vector production. Together with reduced surface expression of VSVG, an intracellular receptor-ligand interaction of LDLR and VSVG is likely, extending the findings of Finkelshtein and colleagues (2013). However, a direct proof for an intracellular LDLR-VSVG interaction in addition to colocalization is still pending. This could be done via fluorescence resonance energy transfer (FRET) experiments involving fusion constructs of VSVG and cyan fluorescent protein (CFP) as well as LDLR and yellow fluorescent protein (YFP), for example.

The ectopic expression of full-length LDLR led to the appearance of intracellular accumulations of VSVG, which do not result from internalisation of nascent vector particles as shown by colocalization with the early endosome marker EEA1. This observation together with the reduced

syncytia formation in presence of *LDLR-ΔNPVY* indicates that VSVG accumulates intracellularly at some stage before reaching the plasma membrane and that alternative internalization routes of LDLR are not used.

Similarly, VSVG is not found in the Golgi upon LDLR expression revealing that altered protein sorting is triggered even before that stage of the secretory pathway. In the following, colocalisation assays with ERGIC53 clearly demonstrated that VSVG is transported to the ERGIC posttranslationally, but is then redirected into the lumen of a compartment bearing the lysosomal marker LAMP. However, what happens there remains to be characterized, because degradation of VSVG was not detected on Western Blot. The VSVG accumulations could represent aggresomes, which were enclosed by lysosomal membrane, but were indegradable or simply not degraded yet. Another point, which has to be considered, is that the C-terminal epitope for the primary VSVG antibody could become quickly degraded, therefore preventing the detection of VSVG fragments on Western Blot. Nevertheless, the luminal staining would also be absent, if the C-terminus was lost quickly due to lysosomal hydrolases. In conclusion, the observed granules could represent accumulations of VSVG-LDLR complexes that are not digested, because they do not exhibit properties of misfolded proteins.

The exact nature of an intracellular VSVG-LDLR interaction remains to be elucidated, however, a proof-of-concept that intracellular ligand binding by LDLR is a relevant process was reported for the receptor's designated ligand apoB (Gillian-Daniel et al., 2002). Besides a physiologic receptor-ligand interaction starting in the ER as shown for other surface glycoprotein and host cell receptor pairs such as HIV1 Env and a mutant CD4 fused to an ER-retention signal (Raja et al., 1993), an interaction of LDLR-VSVG receptor-ligand complexation could occur not until reaching the ERGIC or could result from co-translational intermolecular disulfide formation in the ER, because both molecules contain a variety of cysteine residues. Under normal circumstances, LDLR family members are complexed with receptor-associated protein (RAP) preventing premature ligand interactions (Fisher et al., 2006), which was shown to dissociate from LDLR related protein (LRP) in the ERGIC due to acidic pH (Bu et al., 1995), thereby LDLR could be rendered binding competent for VSVG. As a result, the receptor-ligand complex is redirected for disposal or intracellular dumping. The model (Figure 5.1) describes the restriction for VSVG-pseudotyped vector production that is generated by the co-expression of the pseudotype's host cell receptor. This scheme could also hold true for other host cell receptor and surface glycoprotein pairs, which is worthwhile to be considered when designing future gene therapy vectors.

Concomitant with VSVG accumulation, highly significant reductions of vector RNA transcription was observed. The mechanism underlying this effect provides space for speculations. It is well established that ER-mediated quality control pathways include transcriptional feedback in terms of

transcriptional activation of chaperones (reviewed in Arvan et al., 2002). Similarly, negative transcriptional feedback could be elicited restricting vector RNA yield via signals emerging from the ERGIC in presence of LDLR-VSVG complexes. In contrast, VSVG mRNA transcribed from a CMV-promoter is only insignificantly reduced suggesting a mechanism that acts on LTR-driven transcription specifically.

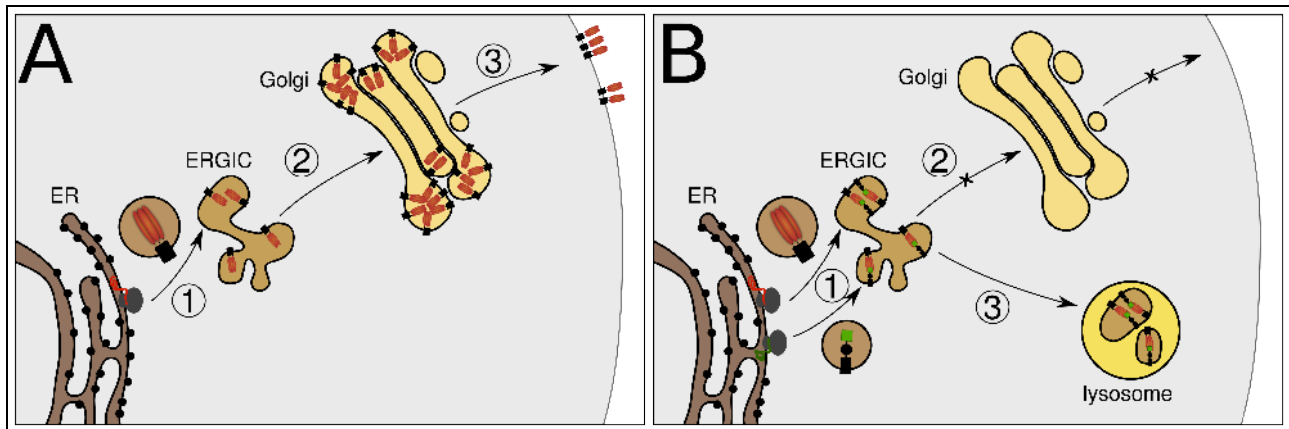


Figure 5.1. Model of VSVG-LDLR ligand-receptor complexation induced redirection. **A)** Normally, following synthesis at the rough ER (1), VSVG is transported through the ERGIC (2) and the Golgi to the plasma membrane (3). **B)** In presence of LDLR, VSVG engages in complex formation in the ERGIC (1), which triggers quality control mechanisms preventing progress to the Golgi (2) and leading to redirection to lysosomal compartments (3).

This work has shown that the vector production process would benefit from a modification to generate a gene therapy vector for FH encoding LDLR under control of a constitutive promoter at high titers. A possible way to achieve high vector yield in this case is preventing the expression of the transgene during vector production, for example via replacing the CMV-promoter of vector-encoded LDLR with either (1) a repressor element similar to Tet-off systems, (2) a target cell- or tissue-specific promoter such as LSP, or (3) one or more sterol-response elements (SRE) similar to the genomic LDLR locus (Wang et al., 1993). Option (1) allows switching off the expression of the vector's payload during vector production via supplementing the medium with a repressive drug that is absent in the patient. Next, approach (2) requires the selection of a proper promoter to allow transgene expression in target cells, but not in packaging cells. Finally, using optimization (3) would promote the incorporation of the administered LDLR coding sequence into physiologic regulation networks in patient cells, where endogenous LDLR expression is mediated by SRE-driven transcription activated by SRE binding proteins (Horton et al., 2003). Administering a functional physiologically regulatable LDLR coding sequence to FH patients would perfectly restore their LDL-C metabolism. Imitating the physiologic regulation and integrating introduced coding sequences into their native regulatory environment are demands that one can impose on a highly developed gene therapy vector suitable for therapeutic application.

A clinician's responsibility is to protect patients from iatrogenic effects elicited by a treatment itself.

Treating FH via a gene therapy vector that transmits only a non-physiologically regulated LDLR coding sequence could negatively affect a patient's sterol homeostasis leading to extremely low LDL-C levels. Although this has shown to be associated with decreased risk of CAD (Cohen et al., 2006), a diagnose of haematological and lymphoid malignancies would be impeded, because these diseases are also associated with or indicated by low serum LDL-C levels (Marenah et al., 1983; Pugliese et al., 2010), so false-positive diagnoses could occur or true malignancies might be overlooked. In conclusion, improperly designed vectors require additional risk analyses, which can be economized to speed up the development of a therapy for FH.

To date, gene therapy vectors contain multiple attenuating features that reduce or make the appearance of RCLs virtually impossible, however, the broad application still suffers from the fact that the insertion of proviral DNA into the genome occurs at random. This is a serious biosafety concern, because insertional mutagenesis mediated by retroviral vectors led to lymphoproliferative syndromes in two patients with X chromosome-linked severe combined immune deficiency (X-SCID) (Hacein-Bey-Abina et al., 2003). Due to the nature of retroviruses, transformation of cells into malignant or pre-malignant stages does not primarily depend on the gene being transduced. As long as this issue is not sorted out, the ethical justification of the therapeutic application of retroviral vectors remains questionable, however, it lays the foundation for important research in the field of gene therapy.

6 Acknowledgements

The plasmid pHR-CMV-EGFP was a gift from Inder Verma (Addgene plasmid # 14858), pMD2.G and psPAX2 were gifts from Didier Trono (Addgene plasmid # 12259; Addgene plasmid # 12260). Renate Fuchs provided a full range of primary antibodies used in the colocalization assays. Work was funded by the Saudi Arabian government via a collaboration with Faisal Al-Allaf. Sandra Kleinberger devoted herself to teaching the author working with virus cell culture.

The author thanks all members of Dieter Blaas and Heinrich Kowalski groups for their continuous commitment to inspiring talks, constructive suggestions and supportive efforts. In particular, Dieter deserves every praise for providing a challenging and productive research environment that allows focussing on doing science.

7 Abbreviations

CAD – Coronary artery disease
DMEM – Dulbecco's modified eagle medium
EGFP – Enhanced green fluorescent protein
EIAV – Equine infectious anaemia virus
ER – Endoplasmatic reticulum
ERGIC – ER-Golgi intermediate compartment
FCS – Fetal calf serum
FH – Familial hypercholesterolaemia
HIV1 – Human immunodeficiency virus type 1
ICAM1 – Intercellular adhesion molecule 1
LAMP2 – Lysosome associated membrane protein 2
LDLR – Low-density lipoprotein receptor
LSP – Liver-specific promoter
MTOC – Microtubule organising center
PDI – Protein disulfide isomerase
PEI – Polyethyleneimine
RCL – Replication-competent lentivirus
SIN – Self-inactivation
SRE – Sterol response element
SREBP – SRE binding protein
TfR1 – Transferrin receptor 1
TFRC – TfR1 coding sequence
VSV – Vesicular stomatitis virus
VSVG – Vesicular stomatitis virus glycoprotein

References

- Al Shamsi I.R., Al Dhaheri N.S., Phillip P.S., Mustafa F., Rizvi T.A. (2011) Reciprocal cross-packaging of primate lentiviral (HIV-1 and SIV) RNAs by heterologous non-lentiviral MPMV proteins. *Virus Research*, 155(1), 352-357
- Al-Allaf F. A., Coutelle C., Waddington S.N., David A.L., Harbottle R., Themis M. (2010) LDLR-Gene therapy for familial hypercholesterolaemia: problems, progress, and perspectives. *International Archives of Medicine*, 3(36)
- Appenzeller-Herzog C., Hauri H-P. (2006) The ER-Golgi intermediate compartment (ERGIC): in search of its identity and function. *Journal of Cell Science*, 119(Pt 11), 2173-2183
- Arias-Moreno X., Velazquez-Campoy A., Rodríguez J.C., Pocoví M., Sancho J. (2008) Mechanism of Low Density Lipoprotein (LDL) Release in the Endosome. *The Journal of Biological Chemistry*, 283(33), 22670-22679
- Arvan P., Zhao X., Ramos-Castaneda J., Chang A. (2002) Secretory pathway quality control operating in Golgi, plasmalemmal, and endosomal systems. *Traffic*, 3(11), 771-780
- Barrett A.J., Dingle J.T. (1972) The Inhibition of Tissue Acid Proteinases by Pepstatin. *Biochemical Journal*, 127(2), 439-441
- Barrett A.J., Kirschke H. (1981) Cathepsin B, Cathepsin H, and cathepsin L. *Methods in Enzymology*, 80(Pt.C), 535-561
- Blacklow S.C., Kim P.S. (1996) Protein folding and calcium binding defects arising from familial hypercholesterolemia mutations of the LDL receptor. *Nature Structural Biology*, 3(9), 758-762
- Bohley P., Seglen P.O. (1992) Proteases and proteolysis in the lysosome. *Experientia*, 48(2), 151-157
- Bounou S., Giguère J-F., Cantin R., Gilbert C., Imbeault M., Martin G., Tremblay M.J. (2004) The importance of virus-associated host ICAM-1 in human immunodeficiency virus type 1 dissemination depends on the cellular context. *The FASEB Journal*, 18(11), 1294-1296
- Brown E.L., Lyles D.S. (2003) Organization of the Vesicular Stomatitis Virus Glycoprotein into Membrane Microdomains Occurs Independently of Intracellular Viral Components. *Journal of Virology*, 77(7), 3985-3992
- Brown M.S., Goldstein J.L. (1983) Lipoprotein receptors in the liver. Control signals for plasma cholesterol traffic.. *The Journal of Clinical Investigation*, 72(3), 743-747
- Brown M.S., Goldstein, J.S. (1986) A receptor-mediated pathway for cholesterol homeostasis. *Science*, 232(4746), 34-47
- Bu G., Geuze H.J., Strous G.J., Schwartz A.L. (1995) 39 kDa receptor-associated protein is an ER resident protein and molecular chaperone for LDL receptor-related protein. *The EMBO Journal*, 14(10), 2269-2280
- Burnett J.R., Hooper A.J. (2008) Common and Rare Gene Variants Affecting Plasma LDL Cholesterol. *The Clinical Biochemist Reviews*, 29(1), 11-26
- Burns J.C., Friedmann T., Driever W., Burrascano M., Yee J.K. (1993) Vesicular stomatitis virus G glycoprotein pseudotyped retroviral vectors: concentration to very high titer and efficient gene transfer into mammalian and nonmammalian cells. *PNAS*, 90(17), 8033-8037
- Carlsson S.R., Fukuda M. (1989) Structure of Human Lysosomal Membrane Glycoprotein 1. *The Journal of Biological chemistry*, 264(34), 20526-20531
- Cavazza A., Cocchiarella F., Bartholomae C., Schmidt M., Pincelli C., Larcher F., Mavilio F. (2013) Self-inactivating MLV vectors have a reduced genotoxic profile in human epidermal keratinocytes. *Gene therapy*, 20(9), 949-957
- Chakrabarti A., Chen A.W., Varner J.D. (2011) A review of the mammalian unfolded protein response. *Biotechnology and Bioengineering*, 108(12), 2777-2793
- Chen W.J., Goldstein J.L., Brown M.S (1990) NPXY, a sequence often found in cytoplasmic tails, is required for coated pit-mediated internalization of the low density lipoprotein receptor. *The Journal of Biological Chemistry*, 265(6), 3116-3123
- Choi K.H., Basma H., Singh J., Cheng P-W. (2005) Activation of CMV promoter-controlled glycosyltransferase and beta-galactosidase glycogenes by butyrate, trichostatin A, and 5-Aza-2'-deoxycytidine. *Glycoconjugate Journal*, 22(1-2), 63-69
- Cohen J.C., Boerwinkle E., Mosley T.H. Jr., Hobbs H.H. (2006) Sequence variations in PCSK9, low LDL, and protection against coronary heart disease. *New England Journal of Medicine*, 354(12), 1264-1272
- Cornetta K., Yao J., Jasti A., Koop S., Douglas M., Hsu D., Couture L.A., Hawkins T., Duffy L. (2011) Replication-competent Lentivirus Analysis of Clinical Grade Vector Products. *Molecular Therapy*, 19(3), 557-566
- Cronin J., Zhang X.Y., Reiser J. (2005) Altering the Tropism of Lentiviral Vectors through Pseudotyping.

- Cuchel M., Bruckert E., Ginsberg H.N., Raal F.J., Santos R.D., Hegele R.A., Kuivenhoven J.A., Nordestgaard B.G., Descamps O.S., Steinhagen-Thiessen E., Tybjaerg-Hansen A., Watts G.F., Aversa M., Boileau C., Borén J., Catapano A.L., Defesche J.C., Hovingh G.K., Humphries S.E., Kovanen P.T., Masana L., Pajukanta P., Parhofer K.G., Ray K.K., Stalenhoef A.F., Stroes E., Taskinen M.R., Wiegman A., Wiklund O., Chapman M.J. (2014) Homozygous familial hypercholesterolaemia: new insights and guidance for clinicians to improve detection and clinical management. A position paper from the Consensus Panel on Familial Hypercholesterolaemia of the European Atherosclerosis Society. *European Heart Journal*, 35(32), 2145-2157
- Cummings R.D., Kornfeld S., Schneider W.J., Hobgood K.K., Tolleshaug H., Brown M.S., Goldstein J.L. (1983) Biosynthesis of N- and O-linked oligosaccharides of the low density lipoprotein receptor. *The Journal of Biological Chemistry*, 258(24), 15261-15273
- Damgaard D., Jensen J.M., Larsen M.L., Soerensen V.R., Jensen H.K., Gregersen N., Jensen L.G., Faergeman O. (2004) No genetic linkage or molecular evidence for involvement of the PCSK9, ARH or CYP7A1 genes in the Familial Hypercholesterolemia phenotype in a sample of Danish families without pathogenic mutations in the LDL receptor and apoB genes. *Atherosclerosis*, 177(2), 415-422
- Davis C.G., Elhammer A., Russell D.W., Schneider W.J., Kornfeld S., Brown M.S., Goldstein J.L. (1986) Deletion of clustered O-linked carbohydrates does not impair function of low density lipoprotein receptor in transfected fibroblasts. *The Journal of Biological Chemistry*, 261(6), 2828-2838
- Davis C.G., Goldstein J.L., Südhof T.C., Anderson R.G.W., Russell D.W., Brown M.S. (1987) Acid-dependent ligand dissociation and recycling of LDL receptor mediated by growth factor homology region. *Nature*, 326(6115), 760-765
- Davis H. E., Morgana J. R., Yarmush M. L. (2002) Polybrene increases retrovirus gene transfer efficiency by enhancing receptor-independent virus adsorption on target cell membranes. *Biophysical Chemistry*, 97(2-3), 159-172
- De Rijck J., Vandekerckhove L., Christ F., Debyser Z. (2007) Lentiviral nuclear import: a complex interplay between virus and host. *Bioessays*, 29(5), 441-451
- Dean R.T. (1979) Macrophage Protein Turnover - Evidence for lysosomal participation in basal proteolysis. *The Journal of Biochemistry*, 180(2), 339-345
- DePolo N.J., Reed J.D., Sheridan P.L., Townsend K., Sauter S.L., Jolly D.J., Dubensky T.W. Jr. (2000) VSV-G pseudotyped lentiviral vector particles produced in human cells are inactivated by human serum. *Molecular Therapy*, 2(3), 218-222
- Doan L.X., Li M., Chen C., Yao Q. (2004) Virus-like particles as HIV-1 vaccines. *Reviews in Medical Virology*, 15(2), 75-88
- Doms R.W., Ruusala A., Machamer C., Helenius J., Helenius A., Rose J.K. (1988) Differential effects of mutations in three domains on folding, quaternary structure, and intracellular transport of vesicular stomatitis virus G protein. *Journal of Cell Biology*, 107(1), 89-99
- Dull T., Zufferey R., Kelly M., Mandel R.J., Nguyen M., Trono D., Naldini L. (1998) A Third-Generation Lentivirus Vector with a Conditional Packaging System. *Journal of Virology*, 72(11), 8463-8471
- Durand S., Cimorelli A. (2011) The Inside Out of Lentiviral Vectors. *Viruses*, 3(2), 132-159
- Esser V., Russell D.W. (1988) Transport-deficient Mutations in the Low Density Lipoprotein Receptor. *The Journal of Biological Chemistry*, 263(26), 13276-13281
- Fass D., Blacklow S., Kim P.S., Berger J.M. (1997) Molecular basis of familial hypercholesterolaemia from structure of LDL receptor module. *Nature*, 388(6643), 691-693
- Finkelshtein D., Werman A., Novick D., Barak S., Rubinstein M. (2013) LDL receptor and its family members serve as the cellular receptors for vesicular stomatitis virus. *PNAS*, 110(18), 7306-7311
- Fisher C., Beglova N., Blacklow S.C. (2006) Structure of an LDLR-RAP complex reveals a general mode for ligand recognition by lipoprotein receptors. *Molecular Cell*, 22(2), 277-283
- Fleury S., Simeoni E., Zuppinger C., Déglon N., von Segesser L.K., Kappenberger L., Vassalli G. (2003) Multiply Attenuated, Self-Inactivating Lentiviral Vectors Efficiently Deliver and Express Genes for Extended Periods of Time in Adult Rat Cardiomyocytes In Vivo. *Circulation*, 107(18), 2375-2382
- Fries E., Rothman J.E. (1980) Transport of vesicular stomatitis virus glycoprotein in a cell-free extract. *PNAS*, 77(7), 3870-3874
- Gassmann M., Grenacher B., Rohde B., Johannes Vogel J. (2009) Quantifying Western blots: Pitfalls of densitometry. *Electrophoresis*, 30(11), 1845-1855
- Ghani K., Wang X., de Campos-Lima P.O., Olszewska M., Kamen A., Rivière I., Caruso M. (2009) Efficient Human Hematopoietic Cell Transduction Using RD114- and GALV-Pseudotyped Retroviral Vectors Produced in Suspension and Serum-Free Media. *Human Gene Therapy*, 20(9), 966-974
- Gheysen D., Jacobs E., de Foresta F., Thiriart C., Francotte M., Thines D., De Wilde M. (1989) Assembly and release of HIV-1 precursor Pr55gag virus-like particles from recombinant baculovirus-infected insect

cells. *Cell*, 59(1), 103-112

- Gillian-Daniel D.L., Bates P.W., Tebon A., Attie A.D.** (2002) Endoplasmic reticulum localization of the low density lipoprotein receptor mediates presecretory degradation of apolipoprotein B. *PNAS*, 99(7), 4337-4342
- Goldstein J.L., Brown M.S.** (1974) Binding and Degradation of Low Density Lipoproteins by Cultured Human Fibroblasts. *The Journal of Biological Chemistry*, 249(16), 5133-5162
- Goldstein J.L., Brown M.S., Anderson R.G., Russell D.W., Schneider W.J.** (1985) Receptor-Mediated Endocytosis: Concepts Emerging from the LDL Receptor System. *Annual review of cell biology*, 1(1), 1-39
- Greenberg K.P., Lee E.S., Schaffer D.V., Flannery J.G.** (2006) Gene delivery o the retina using lentiviral vectors. *Advances in Experimental Medicine and Biology*, 572(IV), 255-266
- Gruh I., Wunderlich S., Winkler M., Schwanke K., Heinke J., Blömer U., Ruhparwar A., Rohde B., Li R.K., Haverich A., Martin U.** (2008) Human CMV immediate-early enhancer: a useful tool to enhance cell-type-specific expression from lentiviral vectors. *The Journal of Gene Medicine*, 10(1), 21-32
- Hacein-Bey-Abina S., von Kalle C., Schmidt M., Le Deist F., Wulffraat N., McIntyre E., Radford I., Valle J.L., Fraser C.C., Cavazzana-Calvo M., Fischer A.** (2003) A Serious Adverse Event after Successful Gene Therapy for X-Linked Severe Combined Immunodeficiency. *New England Journal of Medicine*, 348(3), 255-256
- Harrison B., Zimmermann S.B.** (1984) Polymer-stimulated ligation - enhanced ligation of oligo- and polynucleotides by T4 RNA ligase in polymer solutions. *Nucleic Acids Research*, 12(21), 8235-8251
- Hastie E., Cataldi M., Marriott I., Grdzeliashvili V.Z.** (2013) Understanding and altering cell tropism of vesicular stomatitis virus. *Virus research*, 176(1-2), 16-32
- Hofer F., M Gruenberger, Kowalski H., Machat H., Huettinger M., Kuechler E., Blaas D.** (1994) Members of the low lipoprotein receptor family mediate cell entry of a minor-group common cold virus. *PNAS*, 91(5), 1839-1842
- Höfig I., Barth S., Salomon M., Jagusch V., Atkinson M.J., Anastasov N., Thirion C.** (2014) Systematic improvement of lentivirus transduction protocols by antibody fragments fused to VSV-G as envelope glycoprotein. *Biomaterials*, 35(13), 4204-4212
- Horton J.D., Shah N.A., Warrington J.A., Anderson N.N., Park S.W., Brown M.S., Goldstein J.L.** (2003) Combined analysis of oligonucleotide microarray data from transgenic and knockout mice identifies direct SREBP target genes. *PNAS*, 100(21), 12027-12032
- Ikeda Y., Collins M. K.L., Radcliffe P. A., Mitrophanous K. A., Takeuchi Y** (2002) Gene transduction efficiency in cells of different species by HIV and EIAV vectors. *Gene Therapy*, 9(14), 932-938
- Innerarity T.L., Weisgraber K.H., Arnold K.S., Mahley R.W., Krauss R.M., Vega G.L., Grundy S.M.** (1987) Familial defective apolipoprotein B-100: low density lipoproteins with abnormal receptor binding. *PNAS*, 84(19), 6919-6923
- Ishibashi S., Brown M.S., Goldstein J.L., Gerard R.D., Hammer R.E., Herz J.** (1993) Hypercholesterolemia in Low Density Lipoprotein Receptor Knockout Mice and its Reversal by Adenovirus-mediated Gene Delivery. *The Journal of Clinical Investigation*, 92(2), 883-893
- Ivanchenko S., Godinez W.J., Lampe M., Kräusslich H-G., Eils R., Rohr K., Bräuchle C., Müller B., Lamb D.C.** (2009) Dynamics of HIV-1 Assembly and Release. *PLoS Pathogens*, 5(11), e1000652
- Kafri T., van Praag H., Ouyang L., Gage F.H., Verma I.M.** (1999) A Packaging Cell Line for Lentivirus Vectors. *Journal of Virology*, 73(1), 576-584
- Kankkonen H. M., Vahakangas E., Marr R. A., Pakkanen T., Laurema A., Leppanen P., Jalkanen J., Verma I. M., Yla-Herttuala S.** (2004) Long-Term Lowering of Plasma Cholesterol Levels in LDL-Receptor-Deficient WHHL Rabbits by Gene Therapy. *Molecular therapy*, 9(4), 548-556
- Kingsley D.M., Krieger M.** (1984) Receptor-mediated endocytosis of low density lipoprotein - Somatic cell mutants define multiple genes required for expression of surface-receptor activity. *PNAS*, 81(17), 5454-5458
- Koga H., Yamada H., Nishimura Y., Kato K., Imoto T.** (1991) Multiple proteolytic action of rat liver cathepsin B: specificities and pH-dependences of the endo- and exopeptidase activities. *The Journal of Biochemistry*, 110(2), 179-188
- Kopito R.R., Sitia R.** (2000) Aggresomes and Russell bodies. Symptoms of cellular indigestion?. *EMBO Reports*, 1(3), 225-231
- Koul P.A., Jan R.A., Wahid A.B., Bhat T.A., Mudassir S.M.** (2007) Familial Hypercholesterolaemia. *Saudi Med J*, 28(4), 628-630
- Kumar V., Butcher S.J., Öörni K., Engelhardt P., Heikkinen J., Kaski K., Alakorpela M., Kovanen P.T.** (2011) Three-Dimensional cryoEM Reconstruction of Native LDL Particles to 16Å Resolution at Physiological Body Temperature. *PLoS*, 6(6), e18841
- Landau, N.R.; Page, K.A.; Littman, D.R.** (1991) Pseudotyping with human T-cell leukemia virus type I broadens the human immunodeficiency virus host range. *Journal of Virology*, 65(1), 162-169

- Leigh S.E., Foster A.H., Whittall R.A., Hubbart C.S., Humphries S.E.** (2008) Update and analysis of the University College London low density lipoprotein receptor familial hypercholesterolemia database. *Annals of Human Genetics*, 72(pt 4), 485-498
- Leren T.P.** (2014) Sorting an LDL receptor with bound PCSK9 to intracellular degradation. *Atherosclerosis*, 237(1), 76-81
- Li K., Markosyan R.M., Zheng Y-M., Golfetto O., Bungart B., Li M., Ding S., He Y., Liang C., Lee J.C., Gratton E., Cohen F.S., Liu S-L.** (2013) IFITM Proteins Restrict Viral Membrane Hemifusion. *PLOS Pathogens*, 9(1), e1003124
- Liu H., Naismith J.H.** (2008) An efficient one-step site-directed deletion, insertion, single and multiple-site plasmid mutagenesis protocol. *BMC Biotechnology*, 8(91), 1472-6750
- Lu J.K., Chen T.T., Allen S.K., Matsubara T., Burns J.C.** (1996) Production of transgenic dwarf surfclams, *Mulinia lateralis*, with pantropic retroviral vectors. *PNAS*, 93(8), 3482-3486
- Lucas T.M., Lyddon T.D., Cannon P.M., Johnson M.C.** (2010) Pseudotyping Incompatibility between HIV-1 and Gibbon ApeLeukemia Virus Env Is Modulated by Vpu. *Journal of Virology*, 84(6), 2666-2674
- Machamer C.E., Doms R.W., Bole D.G., Helenius A., Rose J.K.** (1990) Heavy chain binding protein recognizes incompletely disulfide-bonded forms of vesicular stomatitis virus G protein. *The Journal of Biological Chemistry*, 265(12), 6879-6883
- Marais A.D.** (2004) Familial Hypercholesterolaemia. *The Clinical Biochemist Reviews*, 25(1), 49-68
- Marenah C.B., Lewis B., Hassall D., La Ville A., Cortese C., Mitchell W.D., Bruckdorfer K.R., Slavin B., Miller N.E., Turner P.R., Heduan E.** (1983) Hypocholesterolaemia and non-cardiovascular disease: metabolic studies on subjects with low plasma cholesterol concentrations. *British Medical Journal (Clinical research Etd.)*, 286(6378), 1603-1606
- Martins I.J., Hone E., Chi C., Seydel U., Martins R.N., Redgrave T.G.** (2000) Relative roles of LDLr and LRP in the metabolism of chylomicron remnants in genetically manipulated mice. *Journal of Lipid Research*, 41(2), 205-213
- Maxwell K.N., Breslow J.L.** (2004) Adenoviral-mediated expression of Pcsk9 in mice results in a low-density lipoprotein receptor knockout phenotype. *PNAS*, 101(18), 7100-7105
- Maxwell K.N., Soccio R.E., Duncan E.M., Sehayek E., Breslow J.L.** (2003) Novel putative SREBP and LXR target genes identified by microarray analysis in liver of cholesterol-fed mice. *Journal of Lipid Research*, 44(11), 2109-2119
- Milionis H., Liamis G., Elisaf M.** (2015) Proprotein convertase subtilisin kexin 9 inhibitors: next generation in lipid-lowering therapy. *Expert Opinion on Biological Therapy*, 15(2), 287-298
- Miller L.** (2015), Analyzing gels and western blots with ImageJ [WWW document]. <http://lukemiller.org/index.php/2010/11/analyzing-gels-and-western-blots-with-image-j/> (Accessed 2015-01-02)
- Miyoshi H., Blömer U., Takahashi M., Gage F.H., Verma I.M.** (1998) Development of a Self-Inactivating Lentiviral Vector. *Journal of Virology*, 72(10), 8150-8157
- Miyoshi H., Takahashi M., Gage F.H., Verma I.M.** (1997) Stable and efficient gene transfer into the retina using an HIV-based lentiviral vector. *PNAS*, 94(19), 10319-10323
- Moore S.** (2014), Round-the-horn site-directed mutagenesis [WWW document]. http://openwetware.org/wiki/%27Round-the-horn_site-directed_mutagenesis (Accessed 2014-10-10)
- Morikawa S., Umetani M., Nakagawa S., Yamazaki H., Suganami H., Inoue K., Kitahara M., Hamakubo T., Kodama T., Saito Y.** (2000) The relative induction of mRNA for HMGCoA and LDL receptor by five different HMGCoA reductase inhibitors in cultured human cells. *Journal of atherosclerosis and thrombosis*, 7(3), 138-144
- Mozas P., Galetto R., Albajar M., Ros E., Pocoví M., Rodríguez-Rey J.C.** (2002) A mutation (-49C>T) in the promoter of the low density lipoprotein receptor gene associated with familial hypercholesterolemia. *Journal of Lipid Research*, 43(1), 13-18
- Naldini L.** (1998) Lentiviruses as gene transfer agents for delivery to non-dividing cells. *Current opinion in biotechnology*, 9(5), 457-463
- Naldini L., Blömer U., Gallay P., Ory D., Mulligan R., Gage F.H., Verma I.M., Trono D.** (1996) In vivo gene delivery and stable transduction of nondividing cells by a lentiviral vector. *Science*, 272(5259), 263-267
- Naoumova R.P., Tosi I., Patel D., Neuwirth C., Horswell S.D., Marais A.D., van Heyningen C., Soutar A.K.** (2005) Severe Hypercholesterolemia in Four British Families With the D374Y Mutation in the PCSK9 Gene. *Atherosclerosis, thrombosis, and vascular biology*, 25(12), 2654-2660
- Naviaux R.K., E Costanzi, Haas M., Verma I.M.** (1996) The pCL vector system: rapid production of helper-free, high-titer, recombinant retroviruses. *Journal of Virology*, 70(8), 5701-5705
- O'Rourke J.P., Newbound G.C., Kohn D.B., Olsen J.C., Bunnell B.A.** (2002) Comparison of Gene Transfer Efficiencies and Gene Expression Levels Achieved with Equine Infectious Anemia Virus- and Human Immunodeficiency Virus Type 1-Derived Lentivirus Vectors. *Journal of Virology*, 76(3), 1510-1515

- Page K.A., Landau N.R., Littman D.R.** (1990) Construction and use of a human immunodeficiency virus vector for analysis of virus infectivity. *Journal of Virology*, 64(11), 5270-5276
- Page M.M., Ekinici E.I., Jones R.M., Angus P.W., Gow P.J., O'Brien R.C.** (2014) Liver transplantation for the treatment of homozygous familial hypercholesterolaemia in an era of emerging lipid-lowering therapies. *Internal Medicine Journal*, 44(6), 601-604
- Panda, D.** (2011) Identification Of Host Proteins Required For Vesicular Stomatitis Virus Infection. *Dissertations and Theses in Veterinary and Biomedical Science, University of Nebraska - Lincoln*
- Paquette J-M., Fortin J-F., Blanchard L., Tremblay M.J** (1998) Level of ICAM-1 Surface Expression on Virus Producer Cells Influences both the Amount of Virion-Bound Host ICAM-1 and Human Immunodeficiency Virus Type 1 Infectivity. *Journal of Virology*, 72(11), 9329-9336
- Parveen Z., Mukhtar M., Goodrich A., Acheampong E., Dornburg R., Pomerantz R.J.** () Cross-Packaging of Human Immunodeficiency Virus Type 1 Vector RNA by Spleen Necrosis Virus Proteins: Construction of a New Generation of Spleen Necrosis Virus-Derived Retroviral Vectors. *Journal of Virology*, 78(12), 6480-6488
- Parveen Z., Mukhtara M., Rafic M., Wenger D.A., Siddiqui K.M., Siler C.A., Dietzschold B., Pomerantz R.J., Schnell M.J., Dornburg R.** (2003) Cell-type-specific gene delivery into neuronal cells in vitro and in vivo. *Virology*, 314(1), 74-83
- Pocathikorn A., Taylor R.R., Mamotte C.D.** (2010) Atorvastatin increases expression of low-density lipoprotein receptor mRNA in human circulating mononuclear cells. *Clinical and Experimental Pharmacology and Physiology*, 37(4), 471-476
- Pugliese L., Bernardini I., Pacifico N., Peverini M., Damaskopoulou E., Cataldi S., Albi E.** (2010) Severe hypocholesterolaemia is often neglected in haematological malignancies. *European Journal of Cancer*, 46(9), 1735-1743
- Raja N.U., Vincent M.J., Jabbar M.A.** (1993) Analysis of endoproteolytic cleavage and intracellular transport of human immunodeficiency virus type 1 envelope glycoproteins using mutant CD4 molecules bearing the transmembrane endoplasmic reticulum retention signal. *Journal of General Virology*, 74(Pt 10), 2085-2097
- Rudenko G., Henry L., Henderson K., Ichtchenko K., Brown M.S., Goldstein J.L., Deisenhofer J.** (2002) Structure of the LDL receptor extracellular domain at endosomal pH. *Science*, 298(5602), 2353-2358
- Russell D.W., Schneider W.J., Yamamoto T., Luskey K.L., Brown M.S., Goldstein J.L.** (1984) Domain map of the LDL receptor: Sequence homology with the epidermal growth factor precursor. *Cell*, 37(2), 577-585
- Russell D.W., Yamamoto T., Schneider W.J., Slaughter C.J., Brown M.S., Goldstein J.L.** (1983) cDNA cloning of the bovine low density lipoprotein receptor: feedback regulation of a receptor mRNA. *PNAS*, 80(24), 7501-7505
- Sanburn N., Cornetta K.** (1999) Rapid titer determination using quantitative real-time PCR. *Gene Therapy*, 7(6), 1340-1345
- Sandrin V., Boson B., Salmon P., Gay W., Nègre D., Le Grand R., Trono D., Cosset F.L.** (2002) Lentiviral vectors pseudotyped with a modified RD114 envelope glycoprotein show increased stability in sera and augmented transduction of primary lymphocytes and CD34+ cells derived from human and nonhuman primates. *Blood*, 100(3), 823-832
- Sarafianos S.G., Marchand B., Das K., Himmel D., Parniak M. A., Hughes S.H., Arnold E.** (2009) Structure and function of HIV-1 reverse transcriptase: molecular mechanisms of polymerization and inhibition. *Structure*, 17(5), 693-713
- Sastry L., Johnson T., Hobson M.J., Smucker B., Cornetta K.** (2002) Titering lentiviral vectors: Comparison of DNA, RNA and marker expression methods. *Gene Therapy*, 9(17), 1155-1162
- Sastry L., Miller C., Johnson T., Jasti A., Gattone V., Cornetta K.** (2005) Assessing Lentiviral Vector Quality Using Transmission Electron Microscopy. *Molecular Therapy*, 11(Suppl. 1), S191
- Scandinavian Simvastatin Survival Study Group** (1994) Randomised trial of cholesterol lowering in 4444 patients with coronary heart disease: the Scandinavian Simvastatin Survival Study (4S). *The Lancet*, 344(8934), 1383-1389
- Schneede A., Schmidt C.K., Hölttä-Vuori M., Heeren J., Willenborg M., Blanz J., Domanskyy M., Breiden B., Brodesser S., Landgrebe J., Sandhoff K., Ikonen E., Saftig P., Eskelinen E.L.** (2011) Role for LAMP-2 in endosomal cholesterol transport. *Journal of cellular and molecular medicine*, 15(2), 280-295
- Schneider W.J., Beisiegel U., Goldstein J.L., Brown M.S.** (1982) Purification of the low density lipoprotein receptor, an acidic glycoprotein of 164,000 molecular weight. *The Journal of Biological Chemistry*, 257(5), 2664-2673
- Shepherd J.** (1998) Preventing coronary artery disease in the West of Scotland: implications for primary prevention. *American Journal of Cardiology*, 82(10B), 57T-59T
- Skalamera D., Dahmer M., Purdon A.S., Wilson B.M., Ranall M.V., Blumenthal A., Gabrielli B., Gonda**

- T.J.** (2012) Generation of a Genome Scale Lentiviral Vector Library for EF1 α Promoter-Driven Expression of Human ORFs and Identification of Human Genes Affecting Viral Titer. *PLoS*, 7(12), e51733
- Soria L.F., Ludwig E.H., Clarke H.R., Vega G.L., Grundy S.M., McCarthy B.J.** (1989) Association between a specific apolipoprotein B mutation and familial defective apolipoprotein B-100. *PNAS*, 86(2), 587-591
- Sorrentino V., Nelson J.K., Maspero E., Marques A.R., Scheer L., Polo S., Zelcer N.** (2013) The LXR-IDOL axis defines a clathrin-, caveolae-, and dynamin-independent endocytic route for LDLR internalization and lysosomal degradation. *Journal of Lipid Research*, 54(8), 2174-2184
- Soutar A.K., Naoumova R.P.** (2007) Mechanisms of Disease: genetic causes of familial hypercholesterolemia. *Nature Clinical Practice Cardiovascular Medicine*, 4(4), 214-225
- Spector D.H., Wade E., Wright D.A., Koval V., Clark C., Jaquish D., Spector S.A.** (1990) Human immunodeficiency virus pseudotypes with expanded cellular and species tropism. *Journal of Virology*, 64(5), 2298-2308
- Stefanutti C., Thompson G.R.** (2015) Lipoprotein apheresis in the management of familial hypercholesterolaemia: historical perspective and recent advances. *Current atherosclerosis reports*, 17(1), 465
- Südhof T.C., Goldstein J.L., Brown M.S., Russell D.W.** (1985) The LDL receptor gene: a mosaic of exons shared with different proteins. *Science*, 228(4701), 815-822
- Sun X., Belouzard S., Whittaker G. R.** (2008) Molecular Architecture of the Bipartite Fusion Loops of Vesicular Stomatitis Virus Glycoprotein G, a Class III Viral Fusion Protein. *Journal of Biological Chemistry*, 263(10), 6418-6427
- Sundquist W.I., Kräusslich H-G.** (2012) HIV-1 Assembly, Budding, and Maturation. *Cold Spring Harb Perspectives in Medicine*, 2(7), a006924
- Tolleshaug H., Goldstein J.L., Schneider W.J., Brown M.S.** (1982) Posttranslational processing of the LDL receptor and its genetic disruption in familial hypercholesterolemia. *Cell*, 30(3), 715-724
- Turner B.M.** (1991) Histone acetylation and control of gene expression. *Journal of Cell Science*, 99(Pt 1), 13-20
- Uchida Y., Maezawa Y., Uchida Y., Hiruta N., Shimoyama E., Kawai S.** (2013) Localization of oxidized low-density lipoprotein and its relation to plaque morphology in human coronary artery. *PLoS One*, 8(2), e55188
- van den Bosch H.C., Vos L.D.** (1998) Images in clinical medicine. Achilles'-tendon xanthoma in familial hypercholesterolemia.. *The New England Journal of Medicine*, 338(22), 1591
- Wade P.A., Pruss D., Wolffe A.P.** (1997) Histone acetylation: chromatin in action. *Trends in Biochemical Sciences*, 22(4), 128-132
- Wang X., Briggs M.R., Hua X., Yokoyama C., Goldstein J.L., Brown M.S.** (1993) Nuclear Protein That Binds Sterol Regulatory Element of Low Density Lipoprotein Receptor Promoter. II. Purification and characterization.. *The Journal of Biological Chemistry*, 268(19), 14497-14504
- White S.M., Renda M., Nam N-Y., Klimatcheva E., Zhu Y., Fisk J., Halterman M., Rimel B.J., Federoff H., Pandya S., Rosenblatt J.D., Planelles V.** (1999) Lentivirus Vectors Using Human and Simian Immunodeficiency Virus Elements. *Journal of Virology*, 73(4), 2832-2840
- Wiegman A., de Groot E., Hutten B.A., Rodenburg J., Gort J., Bakker H.D., Sijbrands E.J., Kastelein J.J.** (2004) Arterial intima-media thickness in children heterozygous for familial hypercholesterolemia. *The Lancet*, 363(9406), 369-370
- Wu X., Wakefield J.K., Liu H., Xiao H., Kralovics R., Prchal J.T., Kappes J.C.** (2000) Development of a Novel Trans-Lentiviral Vector That Affords Predictable Safety. *Molecular therapy*, 2(1), 47-55
- Yoshimura A., Yoshida T., Seguchi T., Waki M., Ono M., Kuwano M.** (1987) Low binding capacity and altered O-linked glycosylation of low density lipoprotein receptor in a monensin-resistant mutant of Chinese hamster ovary cells. *The Journal of Biological Chemistry*, 262(27), 13299-13308
- Zhang L., Wang A.** (2012) Virus-induced ER stress and the unfolded protein response. *Frontiers in Plant Science*, 293(3), eCollection 2012
- Zhang X., Scialis R.J., Feng B., Leach K.** (2013) Detection of Statin Cytotoxicity Is Increased in Cells Expressing the OATP1B1 Transporter. *Toxicological Sciences*, 134(1), 73-82
- Zhao Z., Michaely P.** (2009) The Role of Calcium in Lipoprotein Release by the LDL Receptor. *Biochemistry*, 48(30), 7313-7324
- Zheng L., Baumann U., Reymond J-L.** (2004) An efficient one-step site-directed and site-saturation mutagenesis protocol. *Nucleic Acids Research*, 32(14), e115
- Zhu Z.H., Chen S.S., Huang A.S.** (1990) Phenotypic mixing between human immunodeficiency virus and vesicular stomatitis virus or herpes simplex virus. *Journal of Acquired Immune Deficiency Syndromes*, 3(3), 215-219
- Škalamera D., Dahmer M., Purdon A.S., Wilson B.M., Ranall M.V., Blumenthal A., Gabrielli B., Gonda T.J.** (2012) Generation of a Genome Scale Lentiviral Vector Library for EF1 α Promoter-Driven Expression of Human ORFs and Identification of Human Genes Affecting Viral Titer. *PLoS*, 7(12), e51733

Abstract

The titer of a HIV1-based VSVG-pseudotyped lentiviral vector produced in HEK293 cells decreases as a function of LDLR over-expression. In contrast, co-expression of either ICAM-1 or TfR1 does not reduce vector production. Reverse transcription quantitative PCR (RT-qPCR) revealed a decrease in vector RNA yield rather than a reduction of the specific infectivity of vector particles. Live-cell fluorescence microscopy showed decreased syncytia formation of HEK293 cells during vector production suggesting reduced surface expression of VSVG. Co-expression of LDLR deletion constructs instead full length LDLR lacking either the signal peptide (*LDLR-ΔSP*), the ligand-binding domain (*LDLR-ΔLBD*) or the internalisation signal (*LDLR-ΔNPVY*) demonstrated that the ligand-binding domain of LDLR is responsible for decreased VSVG surface expression which corresponded with decreased vector titer. VSVG protein expression levels were unaffected, as shown by Western Blot analysis. Similarly, the copy number of VSVG mRNA showed only insignificant differences in presence and absence of LDLR according to RT-qPCR, therefore transcriptional feedback onto VSVG expression was excluded. Colocalisation of VSVG with markers of intracellular compartments (ERGIC53, GM130, LAMP2) and LDLR, respectively, was assayed via indirect immunofluorescence to uncover intracellular rerouting processes. Dense VSVG-positive spherical structures were found colocalizing with ERGIC53, LAMP2 and LDLR, but not with GM130. Previously, Finkelshtein and colleagues (2013) identified LDLR as a host-cell receptor for VSVG. Thus, the over-expression of both, LDLR and VSVG, during vector production could lead to their intracellular interaction, which could trigger a type of unfolded protein response redirecting the transport of VSVG-LDLR complexes or aggregates to lysosomes instead the Golgi.

Zusammenfassung

Der Titer eines HIV1-basierten VSVG-pseudotypisierten lentiviralen Vektors produziert in HEK293 Zellen wird abhängig von der Expression humanen LDL-Rezeptors (LDLR) vermindert. Im Gegensatz dazu, Ko-Expression von ICAM-1 oder TfR1 reduziert die Vektorproduktion nicht. Reverse Transkription und quantitative PCR (RT-qPCR) enthüllte eine Verminderung der Ausbeute an Vektor RNA statt einer Reduktion der spezifischen Infektivität der Vektorpartikel. Fluoreszenzmikroskopie lebender Zellen zeigte verminderte Syncytium-Bildung von HEK293 Zellen während der Vektorproduktion, was auf reduzierte Zelloberflächenexpression von VSVG schließen lässt. Ko-Expression von LDLR Deletionskonstrukten statt Wildtyp-LDLR, denen entweder das Signalpeptid (*LDLR-ΔSP*), die Ligandenbindungsdomäne (*LDLR-ΔLBD*) oder das Internalisierungssignal (*LDLR-ΔNPVY*) fehlt, veranschaulicht, dass die Ligandenbindungsdomäne von LDLR verantwortlich für die reduzierte VSVG Zelloberflächenexpression ist, was mit vermindertem Vektortiter korrespondiert. Das Expressionsniveau von VSVG bleibt unverändert, wie eine Western Blot Analyse ergab. Ebenso zeigte die Kopiezahl an VSVG mRNA nur insignifikante Unterschiede in An- und Abwesenheit von LDLR laut RT-qPCR. Daher wird auch transkriptionelles Feedback auf die VSVG-Expression ausgeschlossen. Kolo-kalisierung von VSVG mit Markern verschiedener intrazellulärer Kompartimente (ERGIC53, GM130, LAMP2) sowie LDLR selbst mittels indirekter Immunofluoreszenz deckte intrazelluläre Umleitungsprozesse auf. VSVG-positive vesikuläre Strukturen kolo-kalisiert mit ERGIC53 und LAMP2 sowie LDLR, aber nicht mit GM130. Finkelshtein und Kollegen (2013) konnten kürzlich zeigen, dass LDLR ein Wirtszellrezeptor für VSVG ist. Daher könnte die Überexpression von LDLR und VSVG während der Vektorproduktion zu deren intrazellulären Interaktion führen, was Protein-Qualitätskontrollmechanismen auslösen könnte, die VSVG-LDLR Komplexe oder Aggregate zu Lysosomen umleiten anstatt das Fortschreiten auf dem Sekretionsweg durch den Golgi zu erlauben.

Curriculum vitae

EDUCATION

03/2012-04/2015: Master studies in Molecular Cell Biology, MFPL, University of Vienna

10/2008-12/2011: Bachelor studies in Molecular Biology, MFPL, University of Vienna

09/2000-06/2008: Graduation from high school, K. M. Hofbauer Gymnasium, Katzelsdorf

RESEARCH EXPERIENCE

01/2014-02/2015: Master thesis in Blaas Lab, Max F. Perutz Laboratories (MFPL) Vienna. Subject of studies: „Impacts of human LDLR overexpression on the production of a VSVG-pseudotyped lentiviral vector“. Methods applied: Virus cell culture, transfection, transduction, live-cell microscopy, RT-qPCR, PCR, cloning, bacterial transformation, Western Blot, immunofluorescence microscopy.

07/2013: Research internship in Weitzer Lab, Max F. Perutz Laboratories (MFPL) Vienna. Subject of studies: „Physical interaction of Mesp1 and Brachyury with putative 5' enhancer elements of the brachyury gene in mouse embryonic stem cells“. Methods applied: ChIP, PCR, Western Blot, cell culture.

10/2012: Research internship in Kraft Lab, Max F. Perutz Laboratories (MFPL) Vienna. Subject of studies: „Cloning of Atg9-9xmyc-birA “. Methods applied: PCR, cloning, bacterial transformation.

06/2011-07/2011: Bachelor internship in Wiche Lab, Max F. Perutz Laboratories (MFPL) Vienna, under supervision of Eva Michailovska. Subject of studies: „Congenital myasthenic syndrome due to plectin deficiency: Deciphering plectin's role in acetylcholine receptor clustering and synaptic transmission at the neuromuscular junction“. Methods applied: Protein expression and purification, Western Blot, mouse dissection, immunofluorescence, cell culture.